

Galaxy-IGC workshop

August 3 -- 7, 2020, on-line



# Review: AGN observations

河野孝太郎

KOHNO, Kotaro



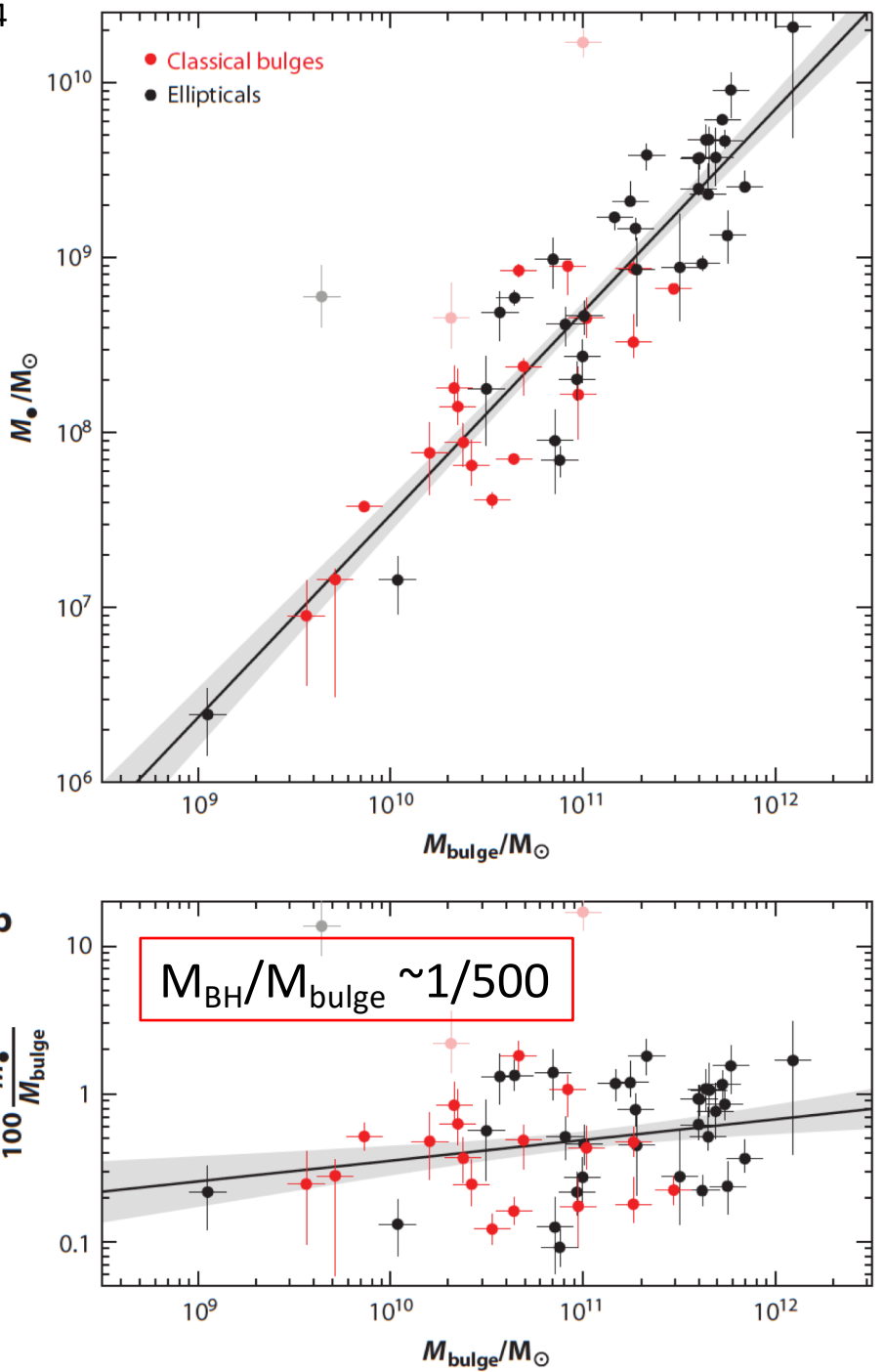
THE UNIVERSITY OF TOKYO

# Outline

- Introduction: “SMBH – galaxy connection”
- Quasars: What can be learned from?
  - Review of recent works
  - SMBH growth, metallicity, obscuration, dust and star-formation in host galaxies,  $M(BH)$ - $M(\text{host})$ ,  $M(\text{halo})$ , environments and (optically-dark) companion galaxies
- AGN feedback
  - Including basic stories for graduate students
  - Recent ALMA observations of outflows (and inflows)
  - cold outflows (ALMA) vs ultra-fast outflows (X-ray)
  - AGN feedback: negative? positive? or .. ??

# Active Galactic Nuclei (AGNs)

- Powered by mass accretion onto a super-massive black hole (SMBH)
  - $M(BH) = 10^6 - 10^{10} M_{\odot}$
- Huge amount of energy ( $L > 10^{12} L_{\odot}$ ) released from a very compact area (<0.1 pc)
- Often accompanied with powerful bi-directional jets and outflows → significant impact on the star-formation in the host galaxies → “co-evolution of galaxies and SMBH” has been suggested
- Found even in the very early Universe ( $z=7.5$ )



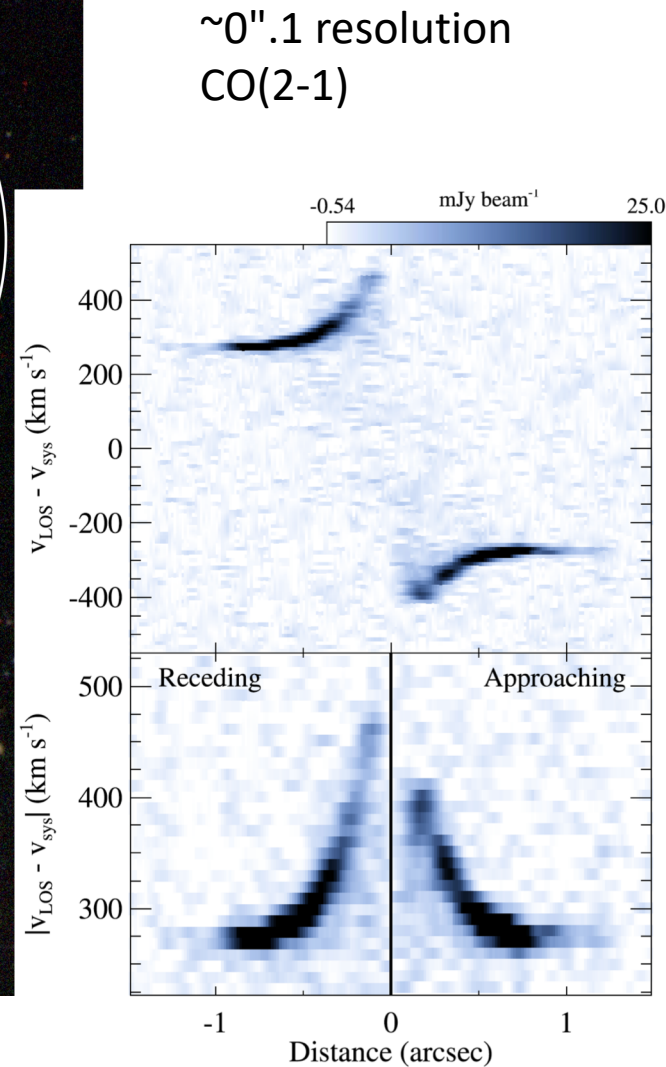
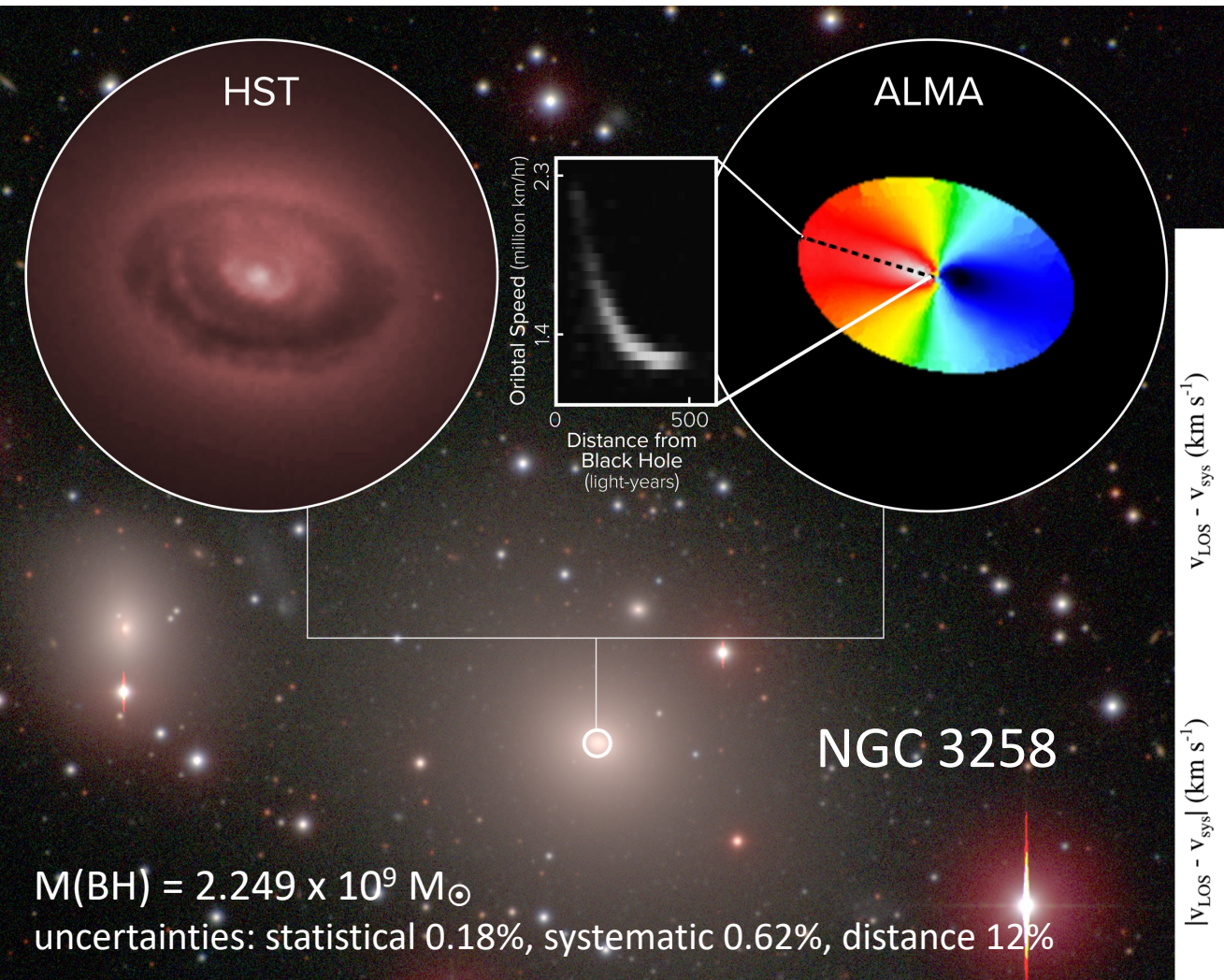
# Intimate connection between SMBHs and galaxies

- More massive SMBHs reside in more massive host galaxies
- The mass ratio: typically 0.5%
- Ranging from 0.1% to 1.8%
- Exceptions up to 14% - 17% (NGC 4486B and NGC 1277, respectively)

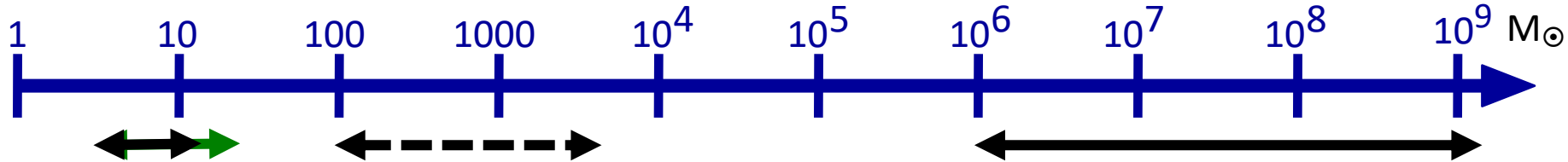
$$\frac{M_{\bullet}}{10^9 M_{\odot}} = (0.49^{+0.06}_{-0.05}) \left( \frac{M_{\text{bulge}}}{10^{11} M_{\odot}} \right)^{1.17 \pm 0.08}$$

★ Why do they know each other despite ~10 orders of magnitude difference in spatial scale..?

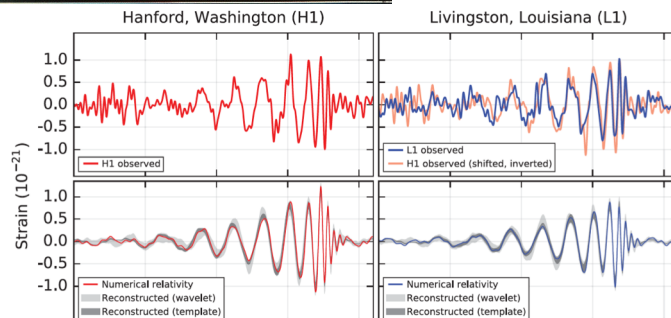
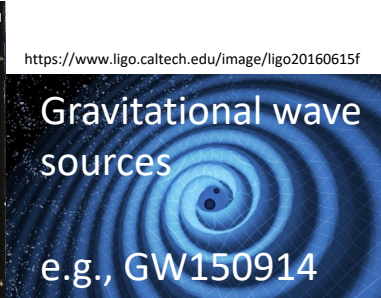
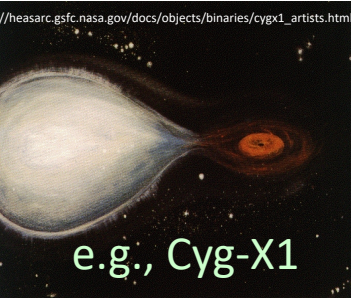
# ALMA offers a new method to accurately quantify the SMBH masses



# The mass range of black holes

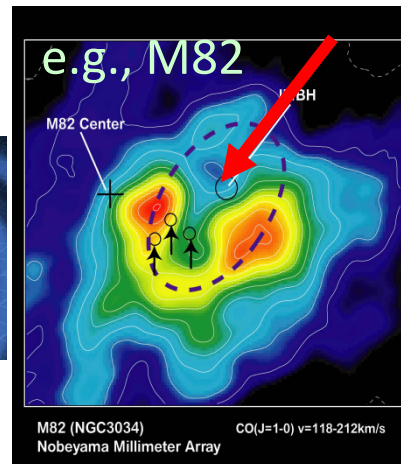


“stellar mass BH”  
From massive stars ( $>20\text{M}_\odot$ )



Abbott et al. 2016, PRL, 116, 061102

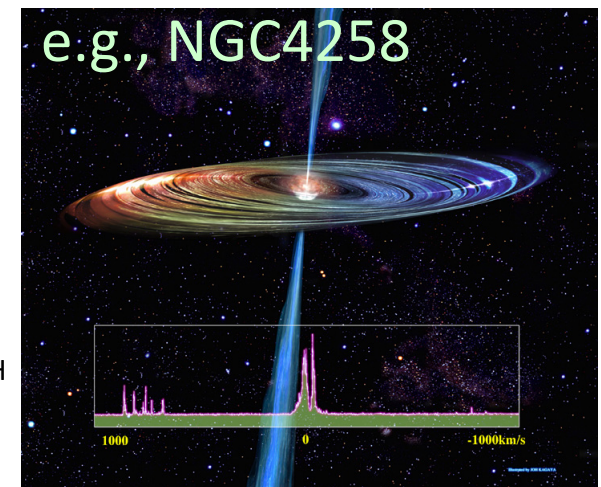
? Do “intermediate mass black holes exist?”



$36^{+5}_{-4} \text{ M}_\odot$   
 $29 \pm 4 \text{ M}_\odot$

Is this a stellar mass BH with super-Eddington accretion?

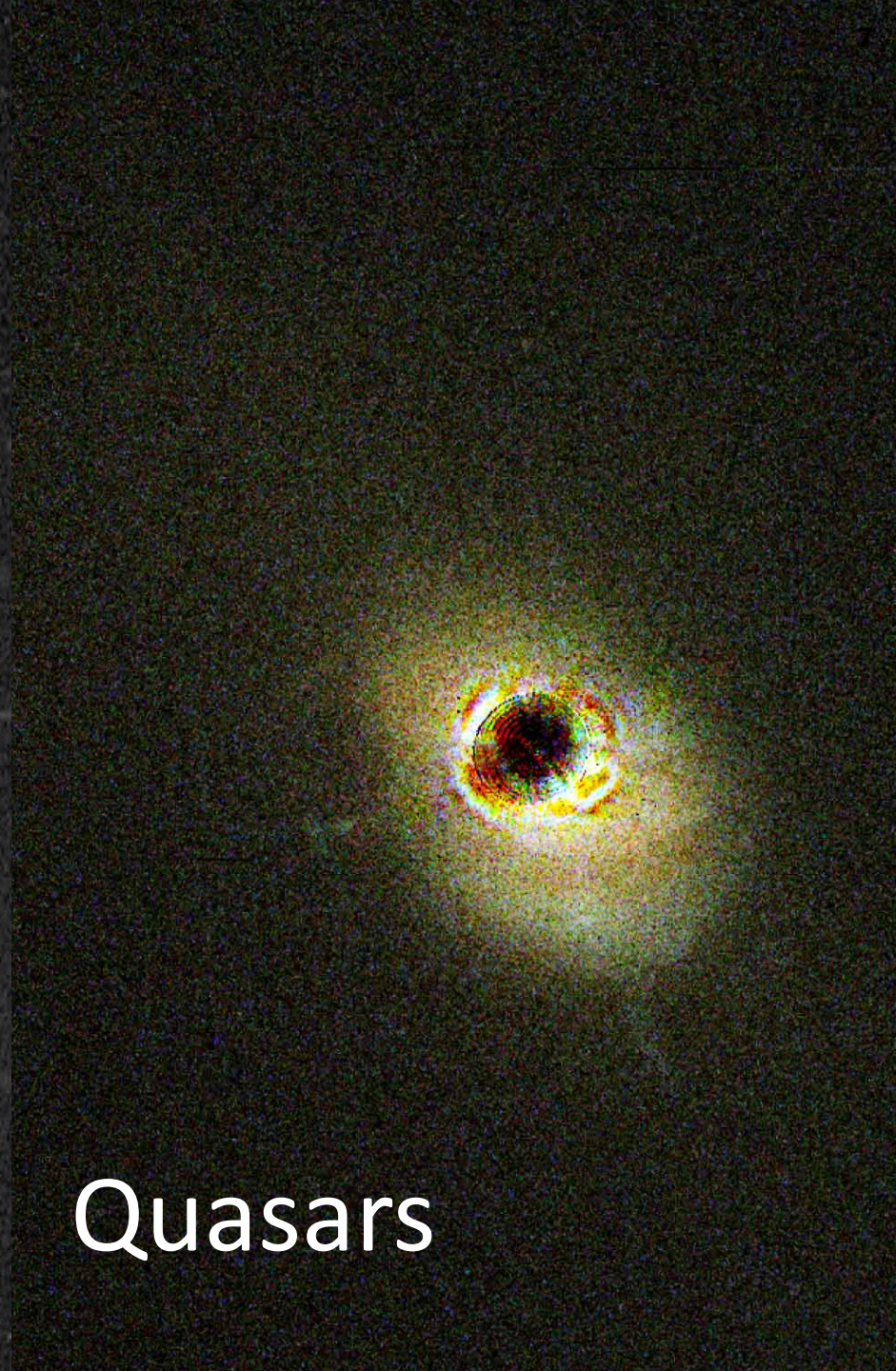
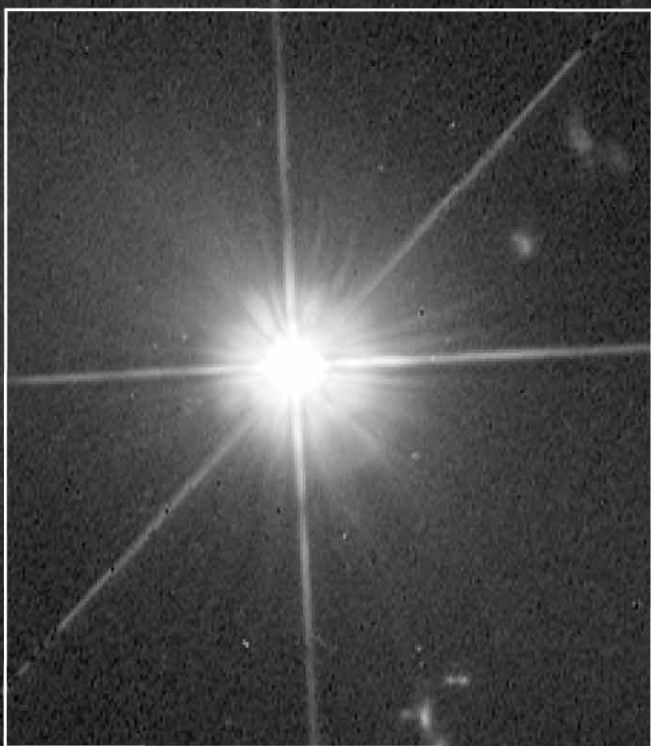
Not typical stellar mass BHs;  
What is the origin? → low metal stars? “first stars” ??



$$1\text{M}_\odot = 2.0 \times 10^{30} \text{ kg}$$

$$10^9 \text{ M}_\odot$$

- From stellar mass black holes ( $5 - 15 \text{ M}_\odot$ ) to
- Super massive black holes (a few million – billion  $\text{M}_\odot$ )



Quasars

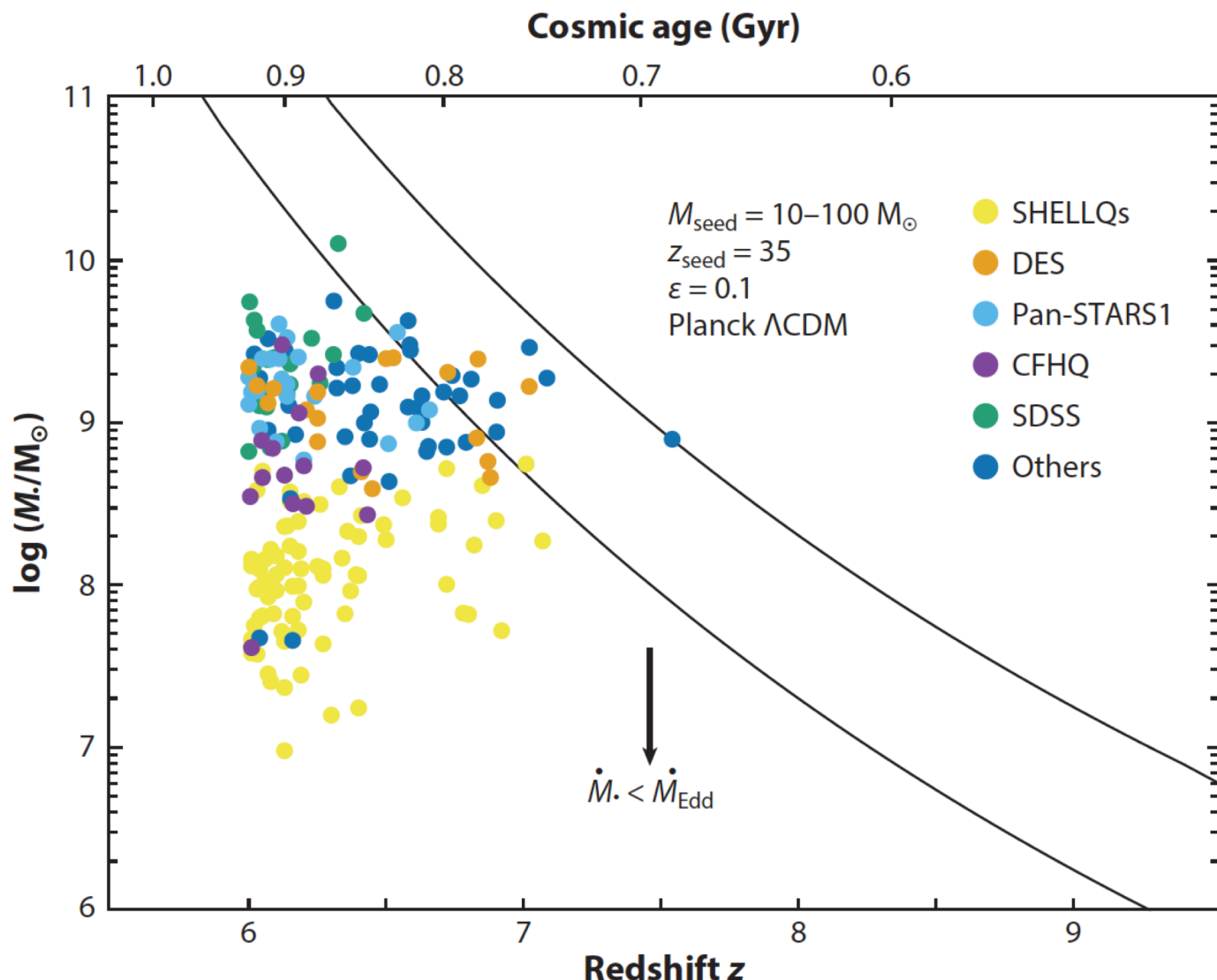
**Table 1** List of surveys utilized in the discoveries of high- $z$  quasars at redshift  $z \geq 6^{\mathrm{a}}$  Inayoshi et al. 2020, ARAA, **58**, 27

Name	Bands	Area (deg <sup>2</sup> )	Number of quasi-stellar objects	References
Subaru (including SHELLQs + Subaru SC)	Optical $g, r, i, z, y$	1,400	78	SHELLQS: Matsuoka et al. 2016, 2018a,b, 2019a;
	Optical $zB, zR$	7	2	Subaru SC: Kashikawa et al. 2015
Pan-STARRS1	Optical $g, r, i, z, y$	31,000	44	Chambers et al. 2016
DELS (including DECaLS, BASS, MzLS)	Optical $g, r, z$	14,000	27	Dey et al. 2019
DES (including DES SV, Yr1, and DR1)	Optical $g, r, i, z, Y$	5,000	18	DES Collab. et al. 2005
SDSS	Optical $u, g, r, i, z$	15,000	26	York et al. 2000
CFHQS (including other CFHTLS)	Optical $g, r, i, z$	500	15	Willott et al. 2007, 2010b
UKIDSS (including ULAS, UKIDSS-DXS, and UHS)	IR $z, Y, J, H, K$	7,000 <sup>b</sup>	64	Lawrence et al. 2007
VISTA (including VHS and VIKING)	IR $J, Ks$	20,000	62	VHS: McMahon et al. 2013
	IR $z, Y, J, H, K$	1,500	31	VIKING: Edge et al. 2013; Venemans et al. 2019
VST ATLAS	Optical $u, g, r, i$ , $z + \mathrm{IR}$	4,700	4	Shanks et al. 2015
FIRST + NDWFS + FLAMEX	21 cm + optical + IR	4	1	McGreer et al. 2006
WISE (including unWISE + AllWISE)	mid-IR	All sky	71	Wright et al. 2010
2MASS	IR $J, H, Ks$	All sky	26	Skrutskie et al. 2006

# SMBH masses of $z > 6$ quasars

- $\sim 200$   $z > 6$  quasars
  - 47  $z > 6.5$
  - 7  $z > 7$

As of July 2020



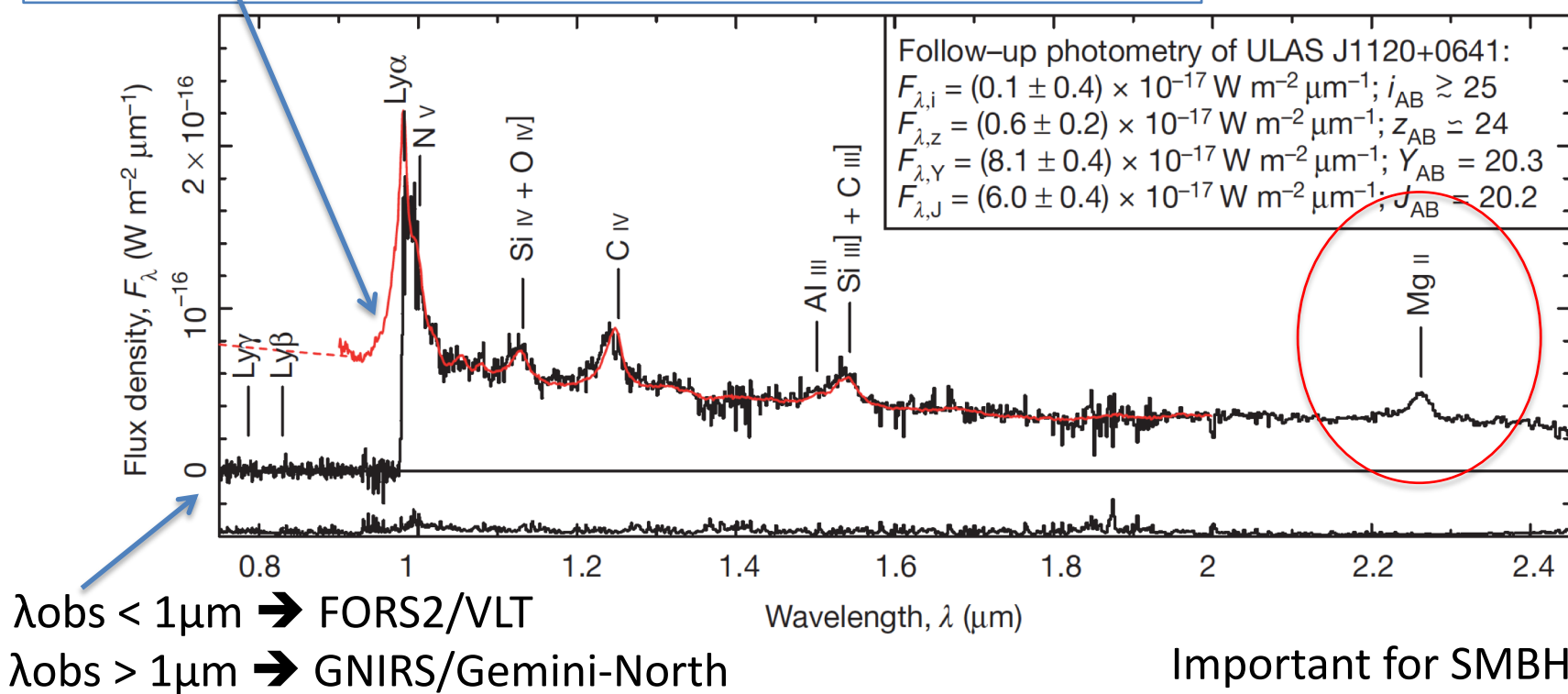
Inayoshi et al. 2020,  
ARA&A, 58, 27

# ULAS J1120+0641 @z=7.084 (2011)

- Combination of wide area infrared and optical imaging (UKIDSS + SDSS)
- $M(\text{BH}) = 2.0^{+1.5}_{-0.7} \times 10^9 M_\odot$  based on MgII line width
  - $L(0.3\mu\text{m}) = (1.3 \pm 0.1) \times 10^{40} \text{ W}/\mu\text{m}$
  - MgII line width =  $3800 \pm 200 \text{ km/s}$  (FWHM)

Composite spectrum of 169 SDSS quasars @ $z = 2.3 - 2.6$

Mortlock et al. 2011,  
Nature, 474, 616



# Seven quasars @ $z > 7$

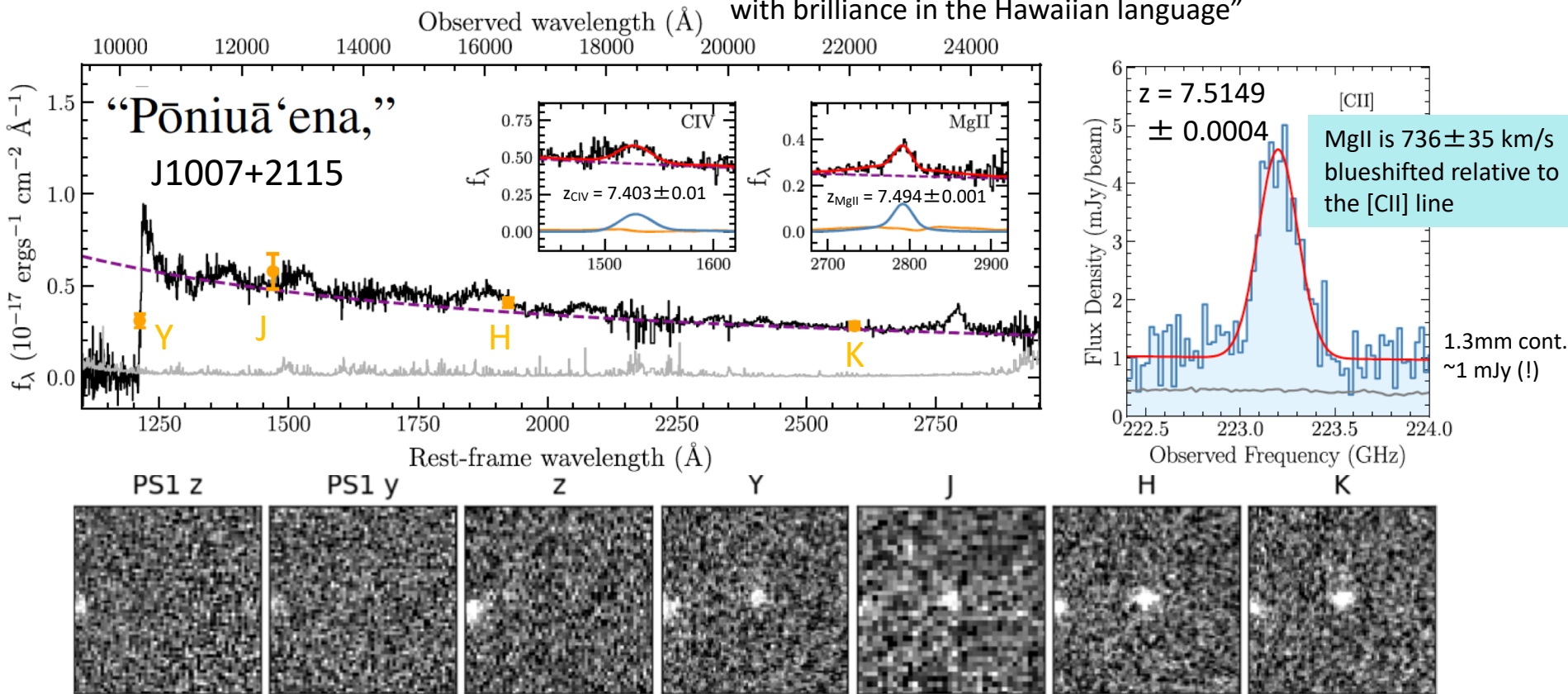
As of July 2020

Source name	Redshift	M1450 (mag)	M(BH) $M_\odot$	$L_{\text{bol}}/L_{\text{Edd}}$	$L(\text{IR})$ $L_\odot$	ref
ULAS J1342+0928	$z_{\text{[CII]}} = 7.5413 \pm 0.0007$	-26.76 $\pm 0.04$	$9.1^{+1.4}_{-1.3} \times 10^8$	1.1 $\pm 0.2$	$(0.5 - 1.4) \times 10^{12}$	Banados et al. 2018, Nature, 553, 473; Onoue et al. 2020, ApJ, 989, 105
J1007+2115 ``Poniua ena''	$z_{\text{[CII]}} = 7.5149 \pm 0.0004$	-26.66 $\pm 0.07$	$(1.5 \pm 0.2) \times 10^9$	1.06 $\pm 0.2$	$(4.7 \pm 0.1) \times 10^{12}$	Yang, J., et al. 2020, ApJL, 897, L14
ULAS J1120+0461	$z_{\text{[CII]}} = 7.085 \pm 0.0007$	-26.6 $\pm 0.1$	$2.0^{+1.5}_{-0.7} \times 10^9$	1.2 $+0.6_{-0.5}$	$(0.58 - 1.8) \times 10^{12}$	Mortlock et al. 2011, Nature, 474, 616; Venemans et al. 2012, ApJ, 751, L25
HSC J124353.93 + 010038.5	$z_{\text{MgII}} = 7.07 \pm 0.01$	-24.13 $\pm 0.08$	$(3.3 \pm 2.0) \times 10^8$	0.34 $\pm 0.20$	(ALMA data)	Matsuoka et al. 2019, ApJL, 872, L2
J0038-1527	$z_{(\text{fit})} = 7.021 \pm 0.005$	-27.10 $\pm 0.08$	$(1.33 \pm 0.25) \times 10^9$	1.25 $\pm 0.19$	N/A	Wang, F., et al. 2018, ApJL, 869, L9
J025216.64-050331.8	$z = 7.02$	-26.5 $\pm 0.09$	N/A	N/A	N/A	Yang, J., et al. 2019, AJ, 157, 236
HSC J235646.33 +001747.3	$z = 7.01$	-25.31 $\pm 0.04$	N/A	N/A	N/A	Matsuoka et al. 2019, ApJ, 883, 183

# 1.5 Billion solar mass BH at $z = 7.515^{12}$

THE ASTROPHYSICAL JOURNAL LETTERS, 897:L14 (7pp), 2020 July 1

"Unseen spinning source of creation, surrounded with brilliance in the Hawaiian language" Yang et al.



Selection:  $\sim 20,000 \text{ deg}^2$

$z, y, J$  (21mag,  $5\sigma$ )

UKIRT Hemisphere Survey

ALLWISE+unWISE

$$L_{[\text{CII}]} = (1.5 \pm 0.2) \times 10^9 L_\odot$$

$$\text{SFR}_{[\text{CII}]} = 80 - 520 M_\odot/\text{yr}$$

$$L_{\text{TIR}(8-1000\mu\text{m})} = (4.7 \pm 0.1) \times 10^{12} L_\odot$$

$$T_{\text{dust}} = 47\text{K}, \beta = 1.6 \text{ w/ CMB}$$

$$\text{SFR}_{\text{TIR}} = 700 M_\odot/\text{yr}$$

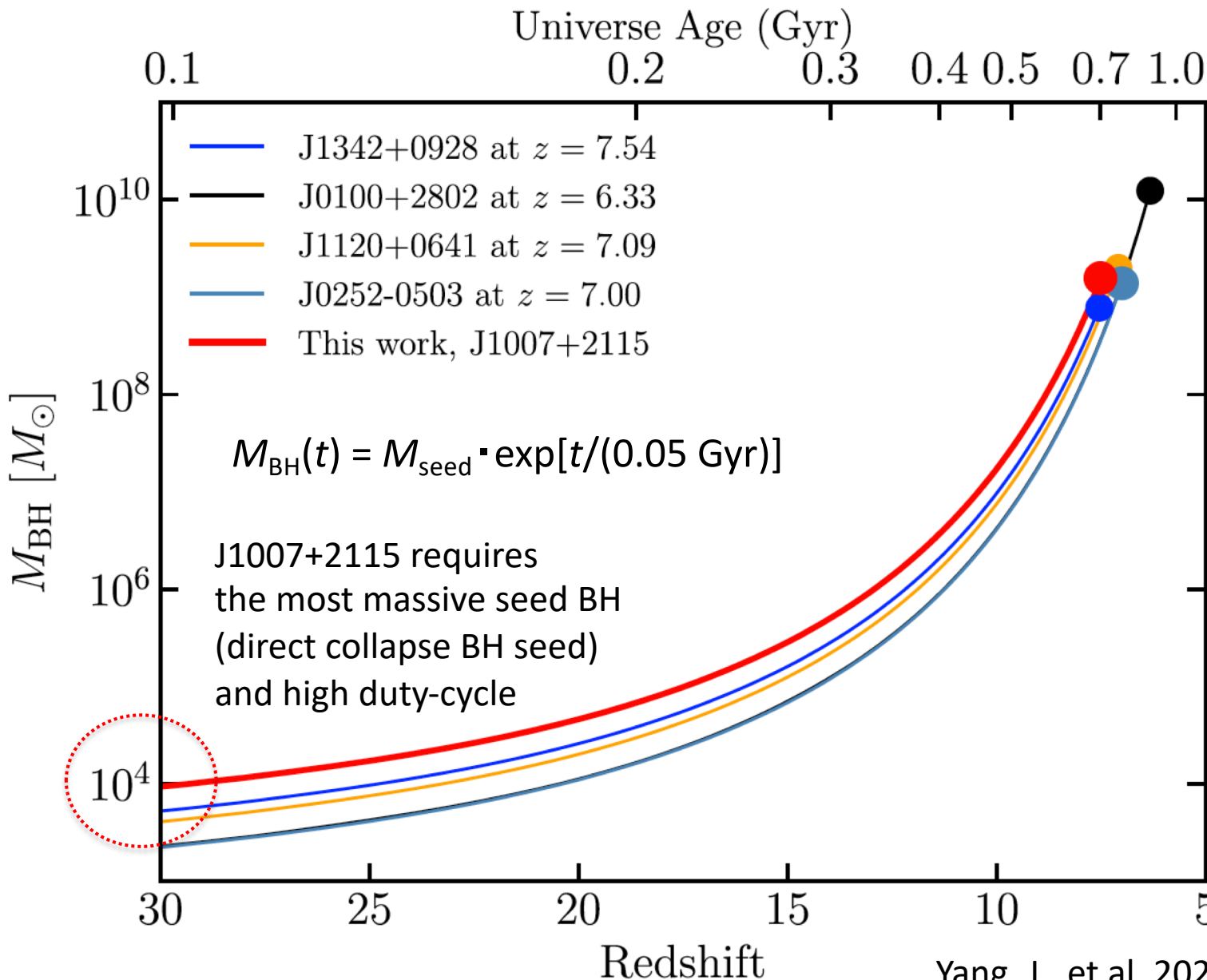
$$L_{\text{bol}} = (1.9 \pm 0.1) \times 10^{47} \text{ erg/sec}$$

$$M(\text{BH}) = (1.5 \pm 0.2) \times 10^9 M_\odot$$

$$L_{\text{bol}}/L_{\text{Edd}} = 1.06 \pm 0.2$$

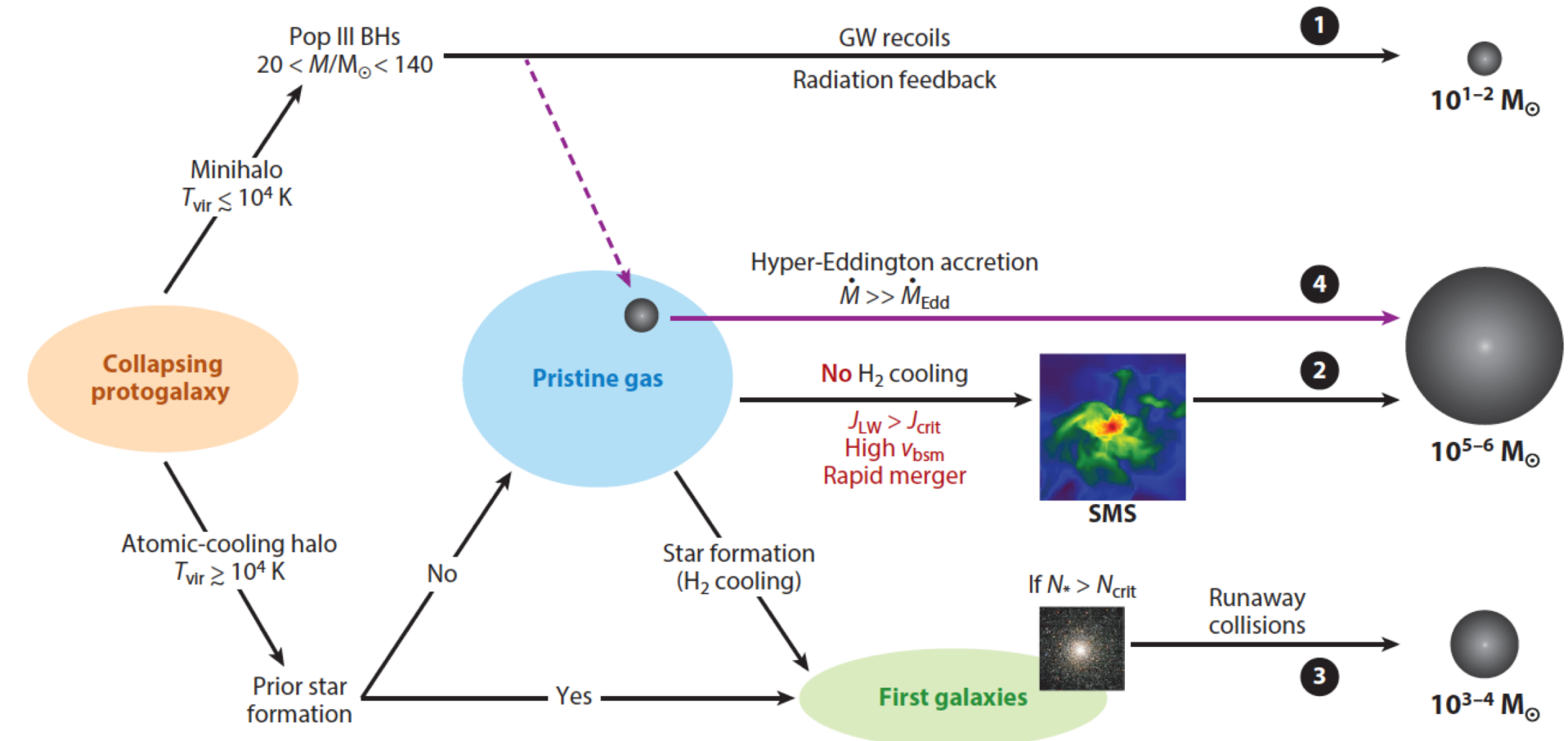
KK comment: This kind of sources must be detected in deep (sub)mm continuum survey!

# Black hole growth curves



# Seed BH formation models

→ Sugimura-san's review



# Eddington ratios of high-z quasars

- Tend to be (super-)Eddington

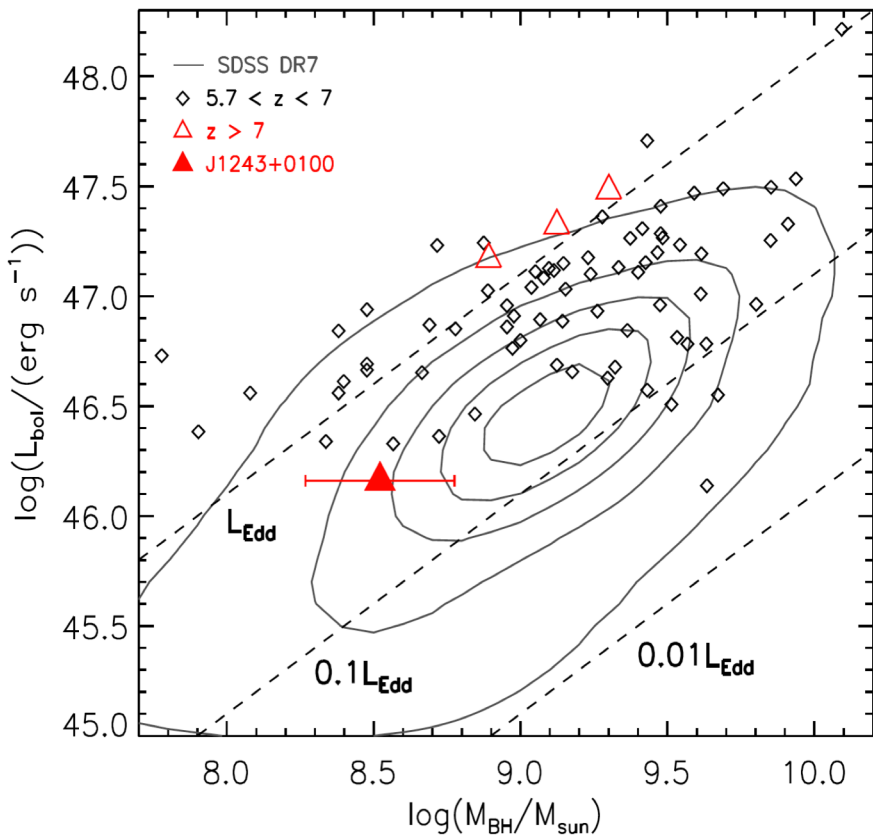


Lensing??

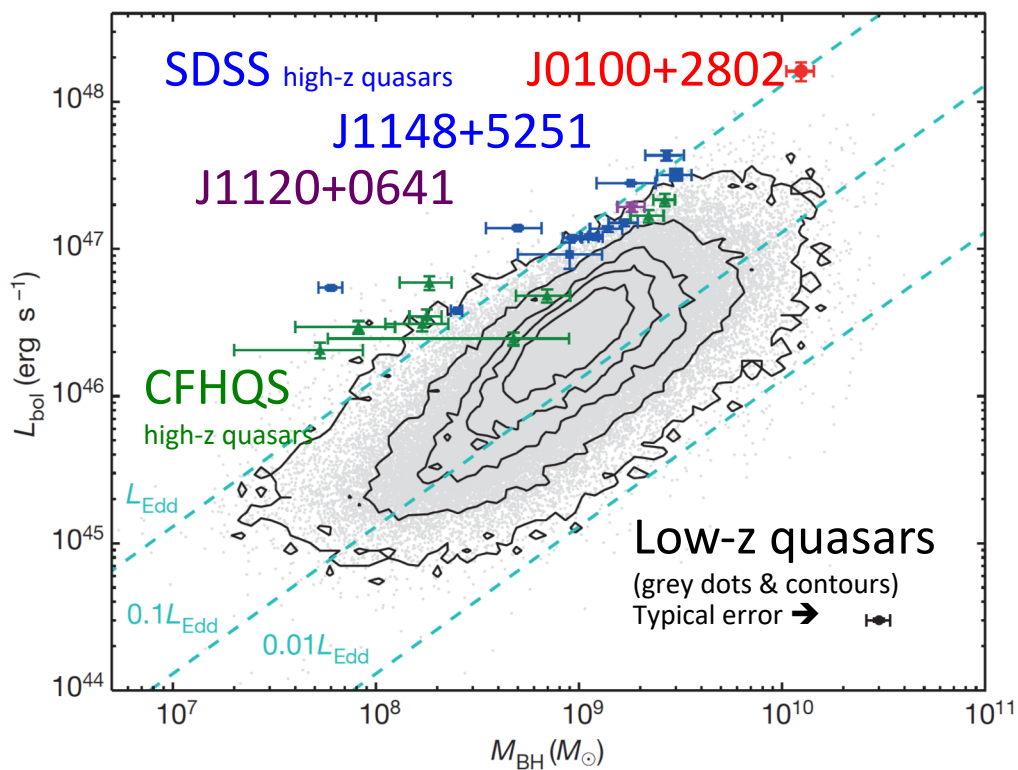
Fan, X., et al. 2019, ApJL, 870, L11

Fujimoto, S., et al. 2020, ApJ, 891, 64

Wu et al. 2015, Nature, 518, 512

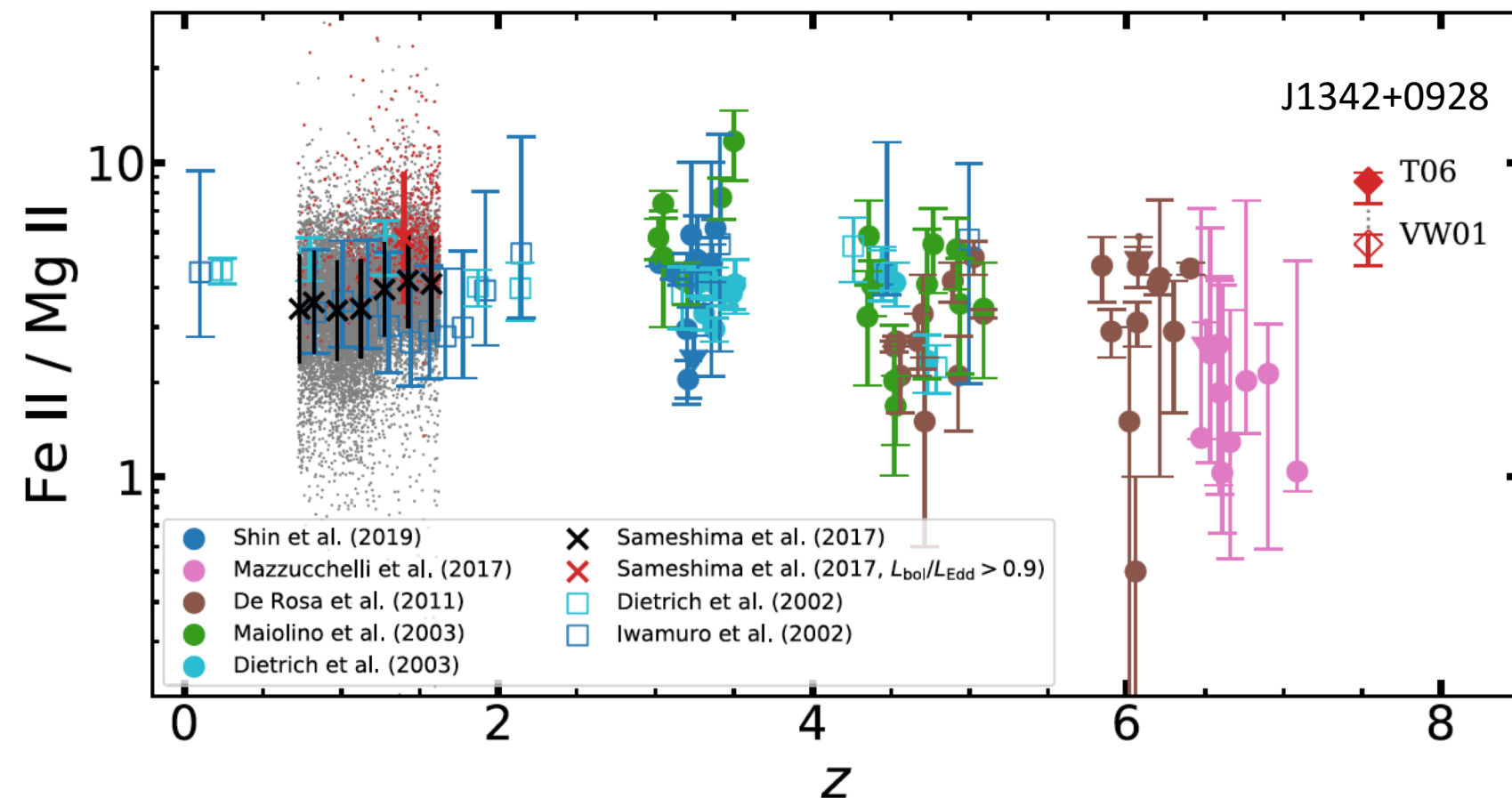


Matsuoka et al. 2019, ApJL 872, L2



# Metal enriched BLR gas

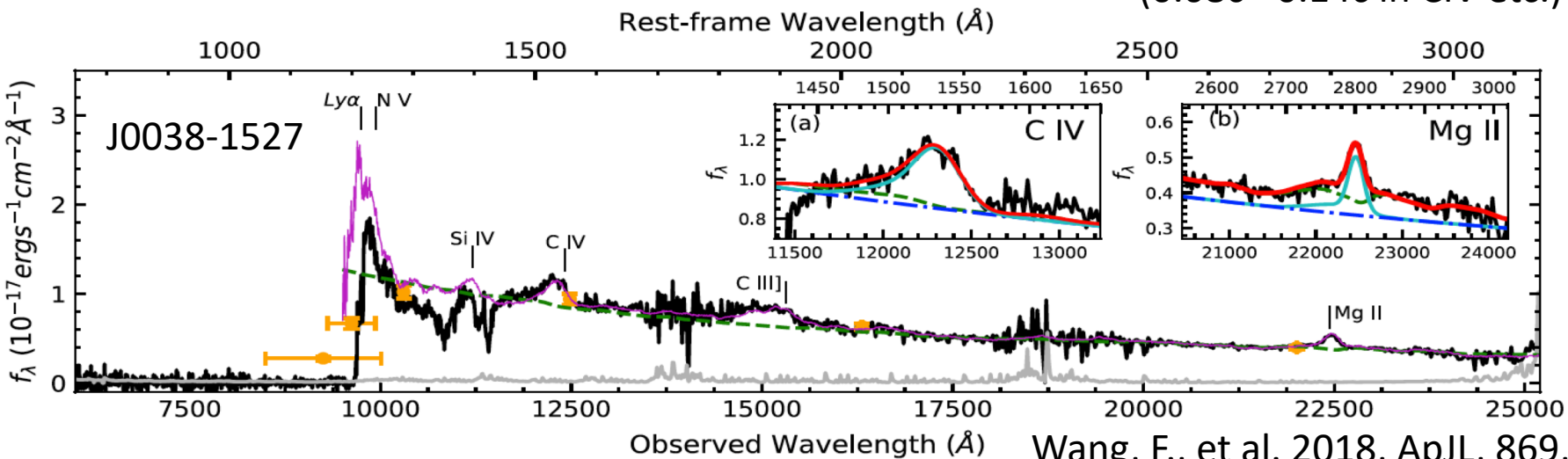
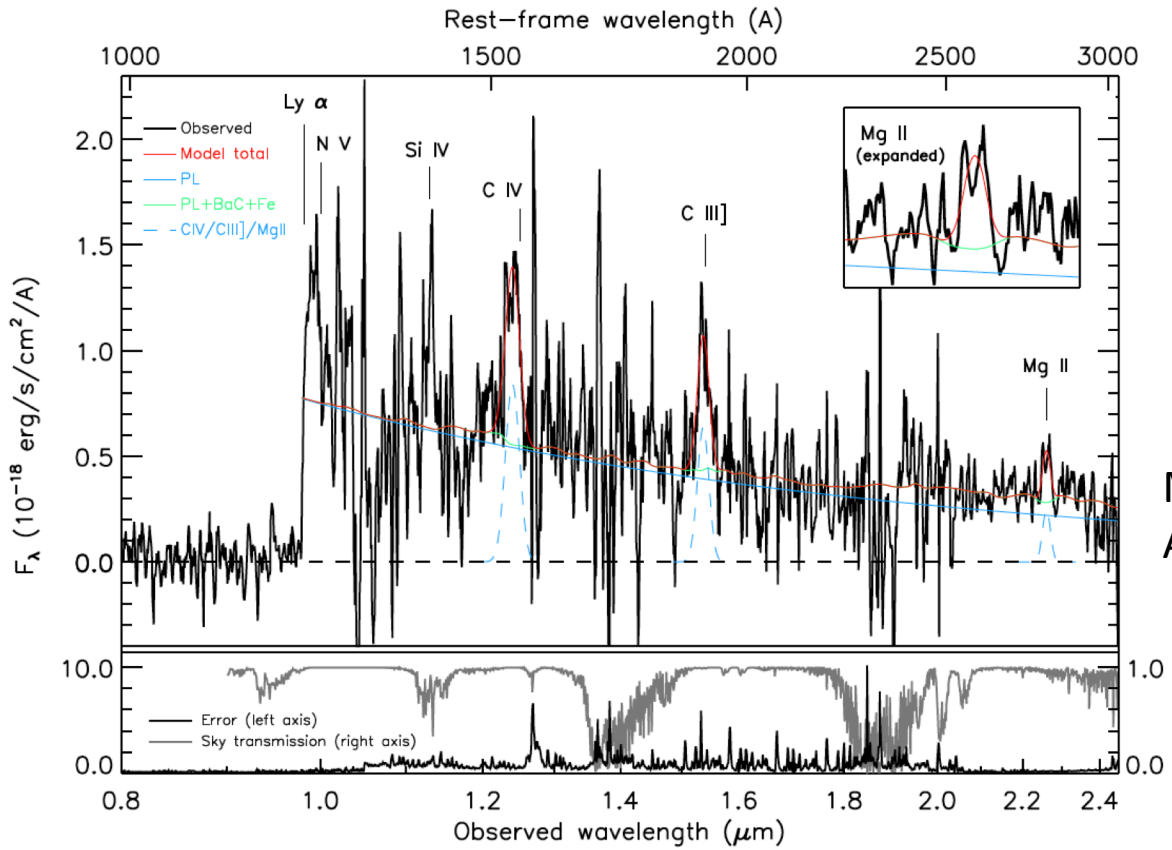
- No redshift evolution in the broad-line region metallicity up to  $z = 7.54$ !



# BAL-like rest-UV spectra @z>7 quasars

Matsuoka et al. 2019,  
ApJL, 872, L2

Relativistic outflows  
(0.08c - 0.14c in CIV etc.)



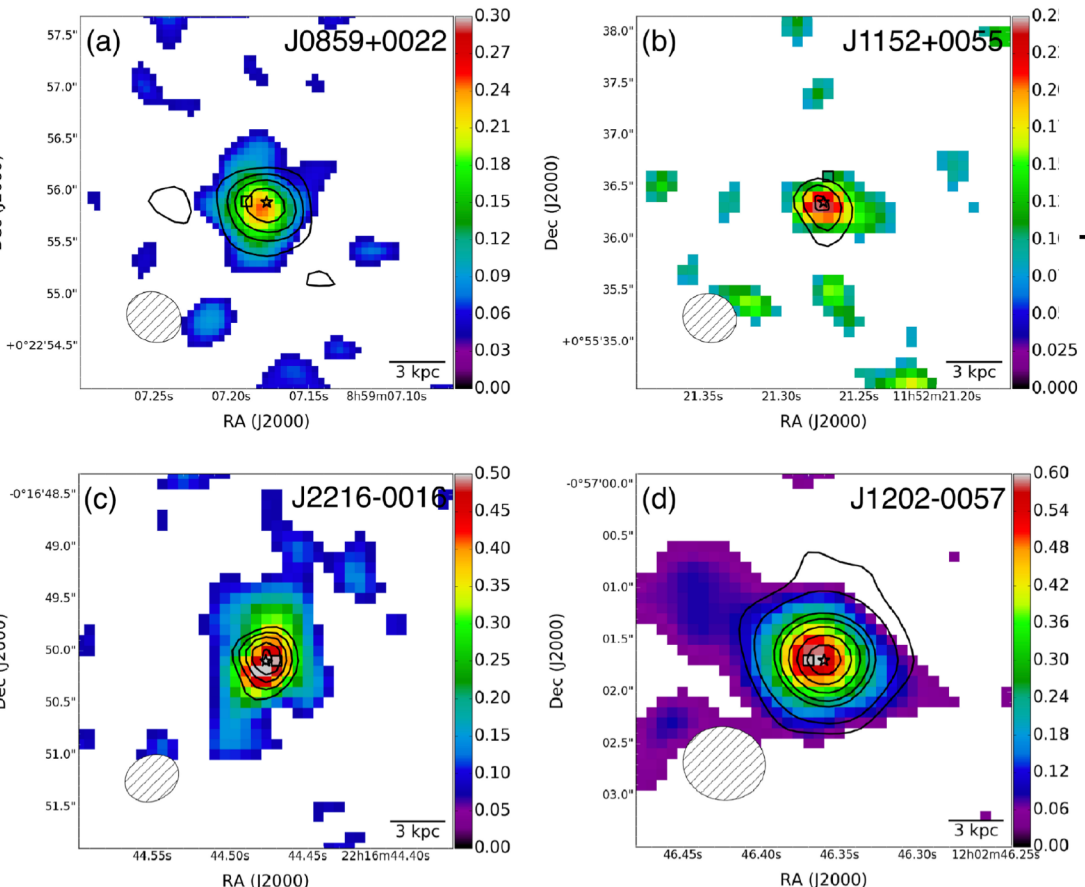
Wang, F., et al. 2018, ApJL, 869, L9

# Quasar host galaxies (unobscured SMBHs)<sup>18</sup>

## at $z > 6-7$ are already dust-rich

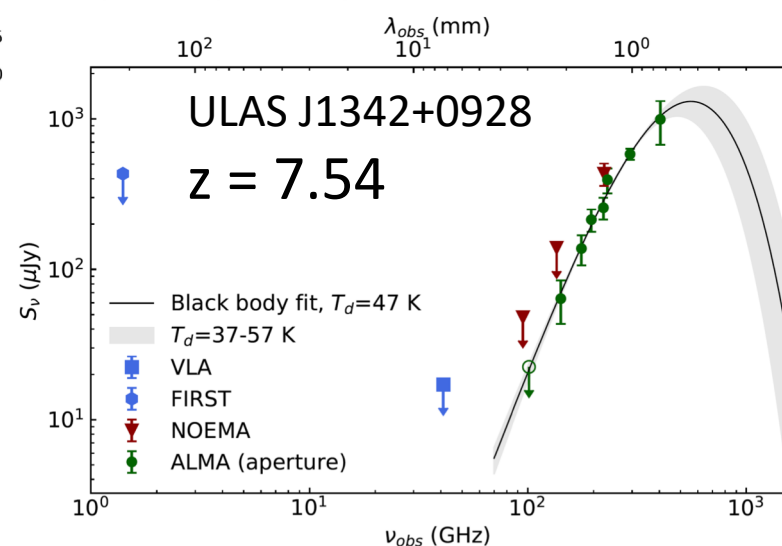
Contours: 1 mm cont.

Pseudo color: [CII]158um



$$L(\text{IR}) = (1-2) \times 10^{12} L_{\odot}$$

$$M(\text{dust}) = (2-8) \times 10^7 M_{\odot}$$



ALMA-SHELLQs

Izumi, T., et al., PASJ, 2018, 70, 36

Novak, M., et al., ApJ, 2019,

ApJ, 881, 63

# Highly obscured growth of $z > 7$ quasars?

THE ASTROPHYSICAL JOURNAL LETTERS, 884:L19 (9pp), 2019 October 10

© 2019. The American Astronomical Society. All rights reserved.

<https://doi.org/10.3847/2041-8213/ab42e3>



## Evidence for Low Radiative Efficiency or Highly Obscured Growth of $z > 7$ Quasars

Frederick B. Davies<sup>1</sup> , Joseph F. Hennawi<sup>1,2</sup> , and Anna-Christina Eilers<sup>2,3</sup>

<sup>1</sup> Department of Physics, University of California, Santa Barbara, CA 93106-9530, USA

<sup>2</sup> Max Planck Institut für Astronomie, Königstuhl 17, D-69117 Heidelberg, Germany

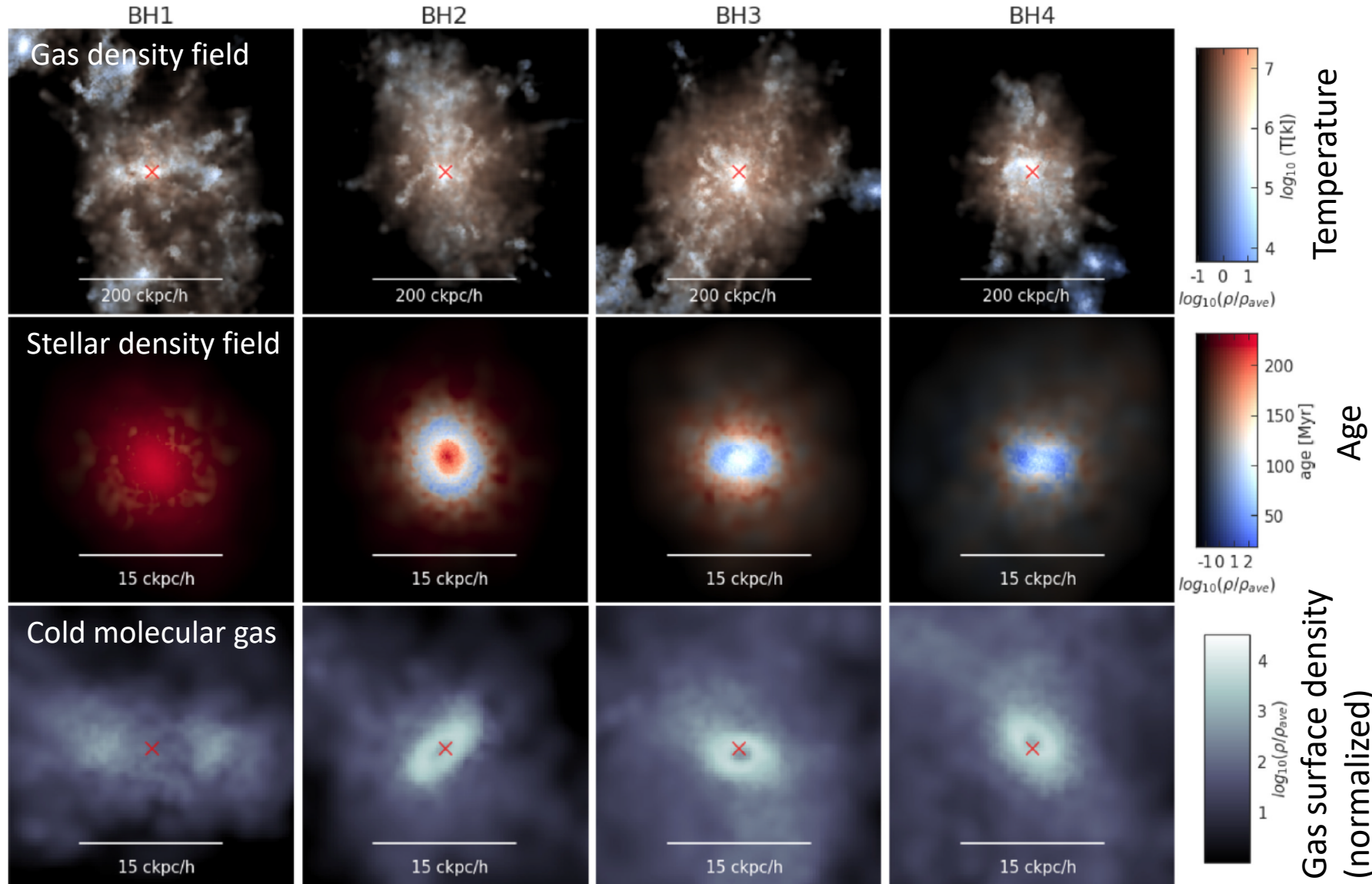
Received 2019 June 25; revised 2019 September 3; accepted 2019 September 9; published 2019 October 7

### Abstract

The supermassive black holes (SMBHs) observed at the centers of all massive galaxies are believed to have grown via luminous accretion during quasar phases in the distant past. The fraction of inflowing rest mass energy emitted as light, the radiative efficiency, has been inferred to be 10%, in agreement with expectations from thin disk accretion models. But the existence of billion solar-mass SMBHs powering quasars at  $z > 7$  challenges this picture: provided they respect the Eddington limit, there is not enough time to grow  $z > 7$  SMBHs from stellar remnant seeds unless the radiative efficiency is below 10%. Here we show that one can constrain the radiative efficiencies of the most distant quasars known using foreground neutral intergalactic gas as a cosmological-scale ionizing photon counter. From the Ly $\alpha$  absorption profiles of ULAS J1120+0641 ( $z = 7.09$ ) and ULAS J1342+0928 ( $z = 7.54$ ), we determine posterior median radiative efficiencies of 0.08% and 0.1%, respectively, and the combination of the two measurements rules out the canonical 10% efficiency at 99.8% credibility after marginalizing over the unknown obscured fraction. This low radiative efficiency implies rapid mass accretion for the earliest SMBHs, greatly easing the tension between the age of the universe and the SMBH masses. However, our measured efficiency may instead reflect nearly complete obscuration by dusty gas in the quasar host galaxies over the vast majority of their SMBH growth. Assuming 10% efficiency during unobscured phases, we find that the obscured fraction would be  $>82\%$  at 95% credibility, and imply a  $25.7^{+49.6}_{-16.5}$  times larger obscured than unobscured luminous quasar population at  $z > 7$ .

Unified Astronomy Thesaurus concepts: [Quasars \(1319\)](#); [Supermassive black holes \(1663\)](#); [Reionization \(1383\)](#)

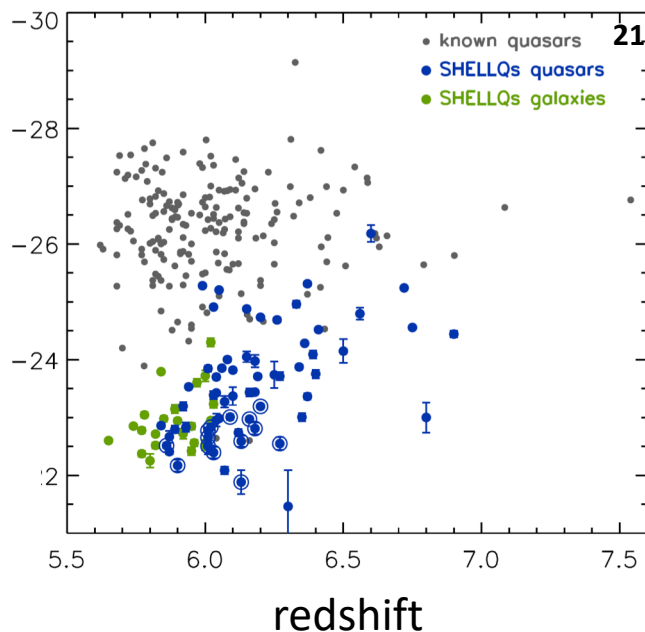
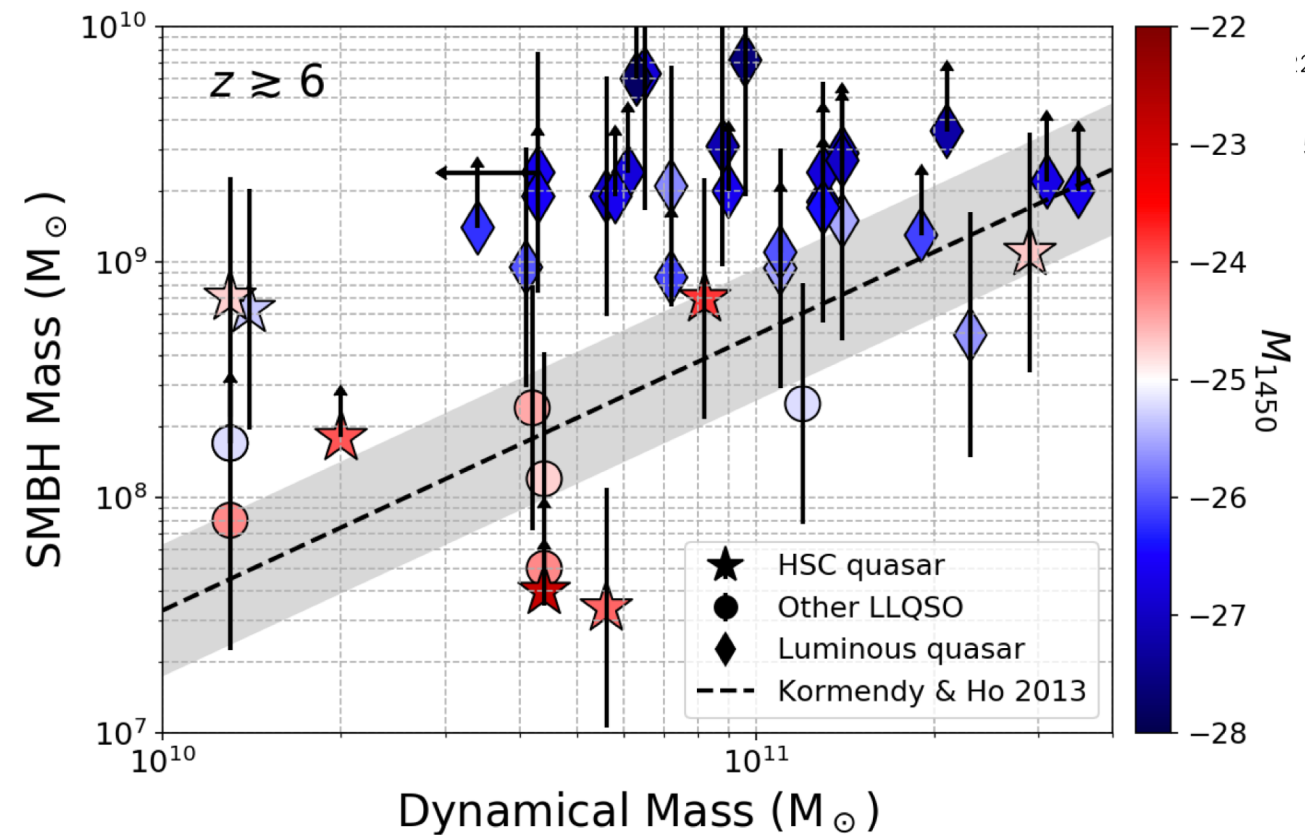
# Simulated host environments of quasars at $z = 7^{20}$



Gas rich; host-scale gas can contribute  
to the nuclear obscuration. “Obscured growth”

Ni et al. 2020, MNRAS, 495, 2135

# Does M(SMBH)-M(host) relation already exist at $z > 6-7$ ??

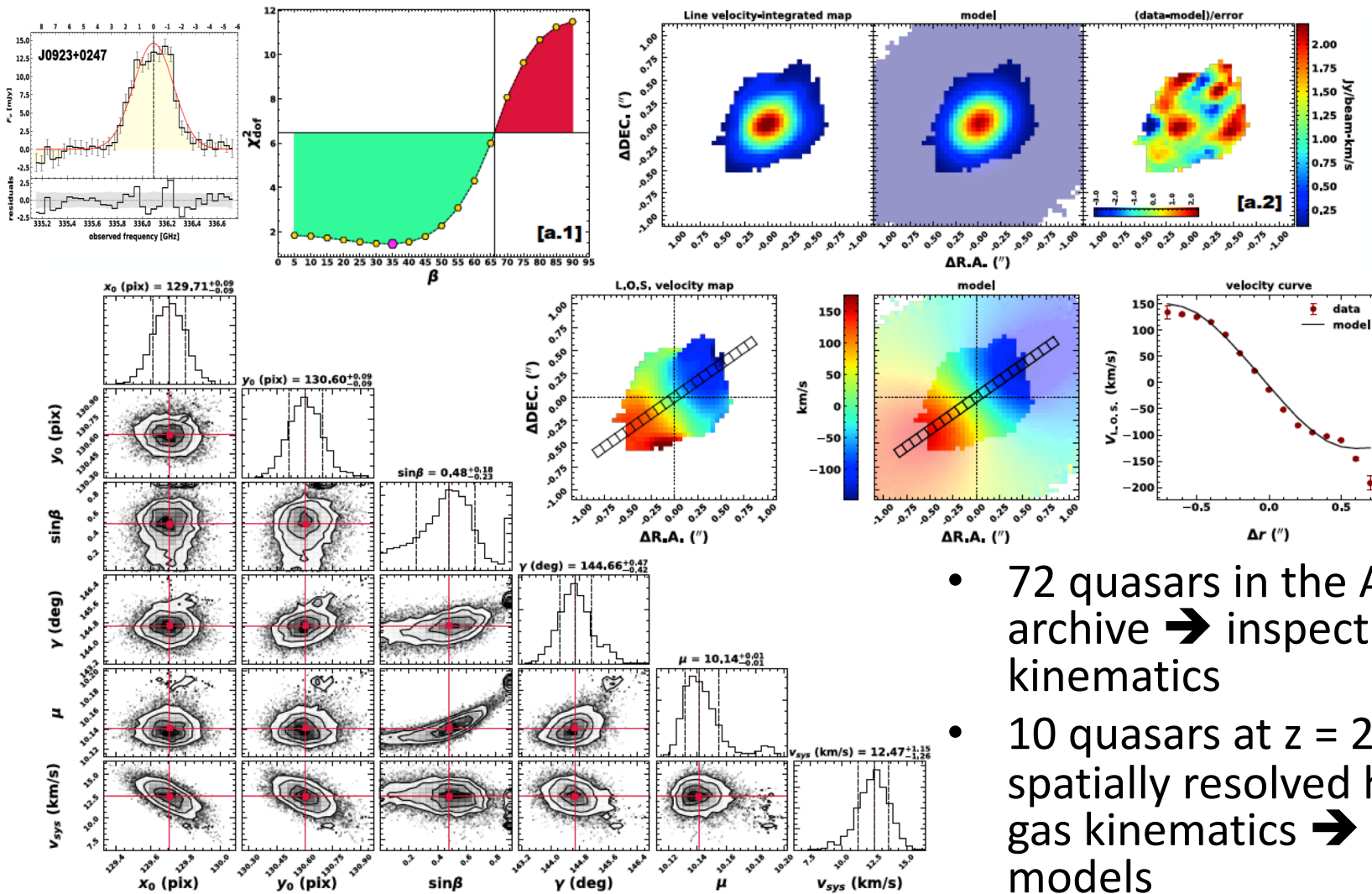


Matsuoka, Y., et al.  
2018, ApJS, 237, 5

Izumi, T., Onoue, M.,  
Matsuoka, Y., KK, et al.  
2019, PASJ, 71, 111

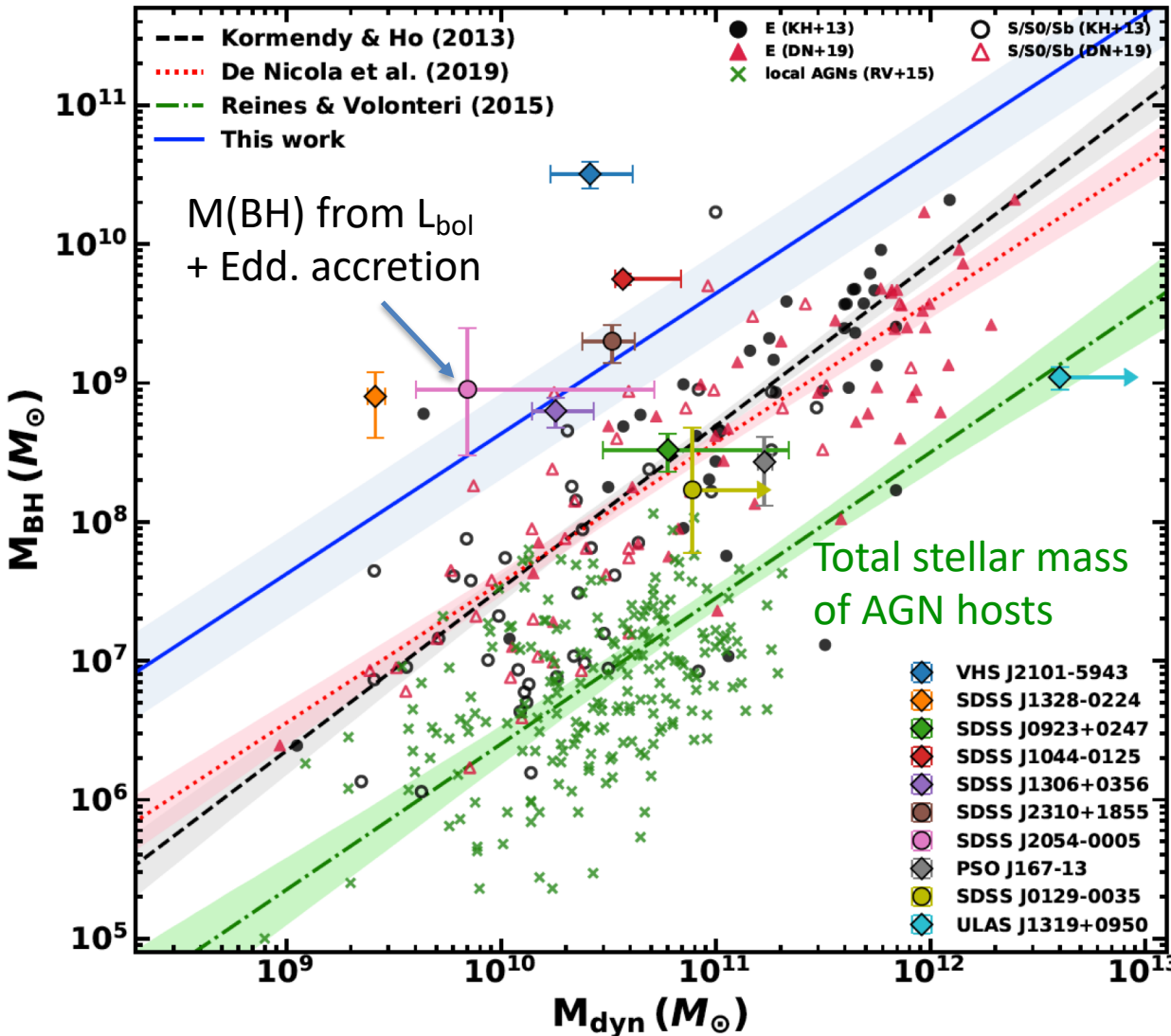
- ALMA [CII]158um observations of low-luminosity quasars uncovered by Subaru/HSC surveys (SHELLQs) → less biased view of the M(SMBH)-M(host) relation at  $z > 6-7$

# Further refinement of M(SMBH)-M(host) relation by high resolution ALMA [CII] or CO



- 72 quasars in the ALMA archive → inspection of kinematics
- 10 quasars at  $z = 2 - 7$  with spatially resolved high S/N gas kinematics → dynamical models

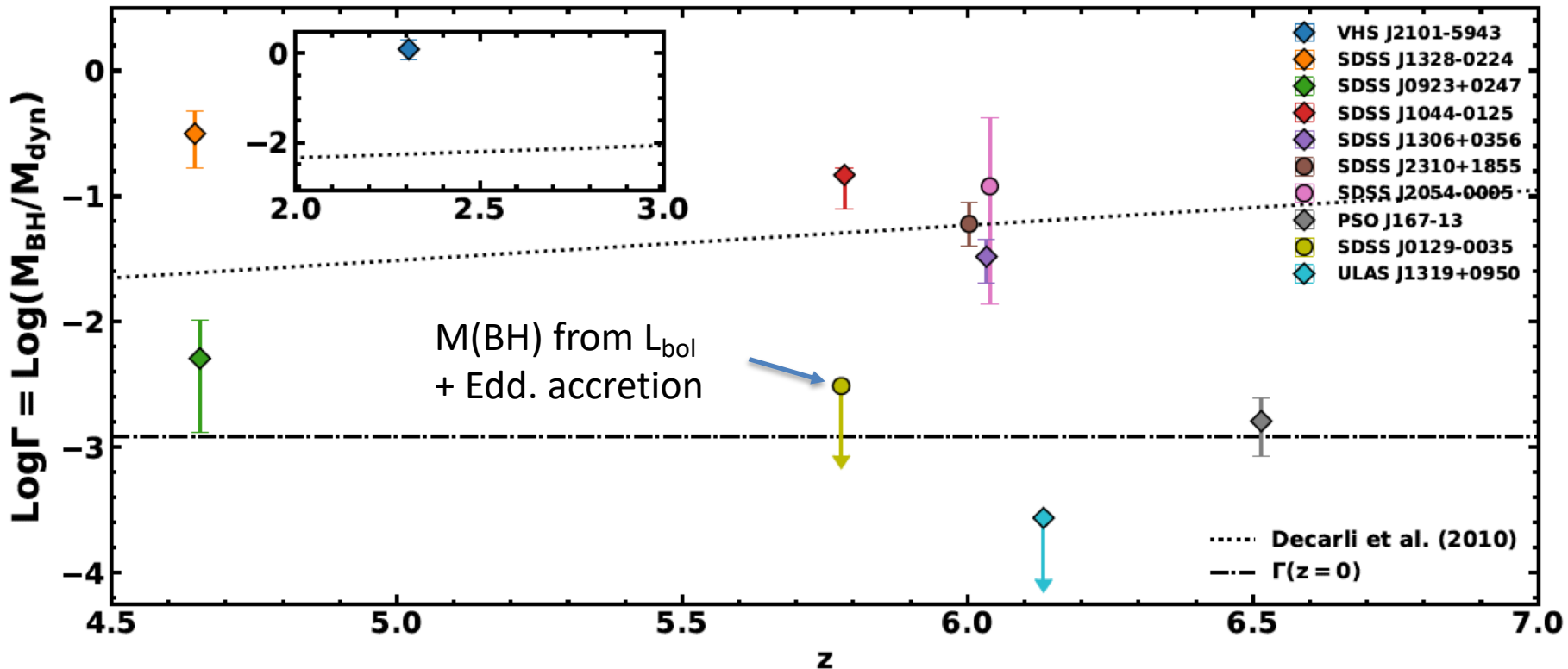
# Further refinement of M(SMBH)-M(host) relation by high resolution ALMA [CII] or CO



- 6 quasars: above the local relation
- 4 quasars @z=4-6: consistent with the local relation
- Inappropriate/incorrect treatment of the beam smearing effect can result in the significant deviation of the M(BH)/M(dyn) ratio !!

Pensabene et al. 2020,  
A&A, 637, A84

# Redshift evolution of $M(\text{BH})/M(\text{dyn})$ of quasars at $z = 2$ to 7 (!?)



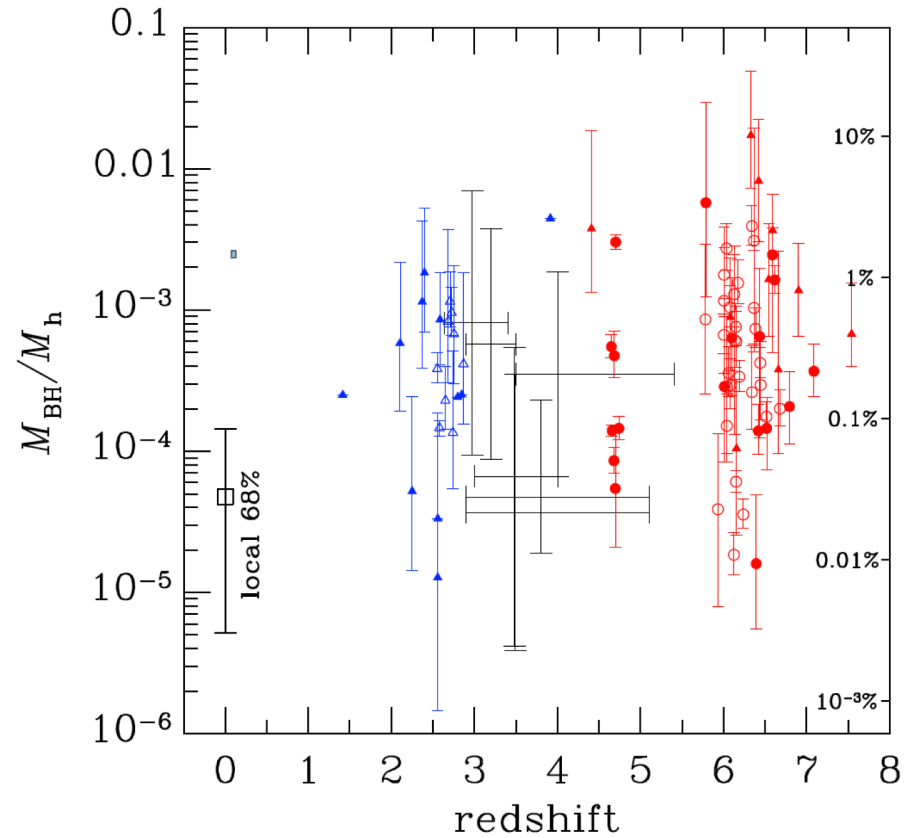
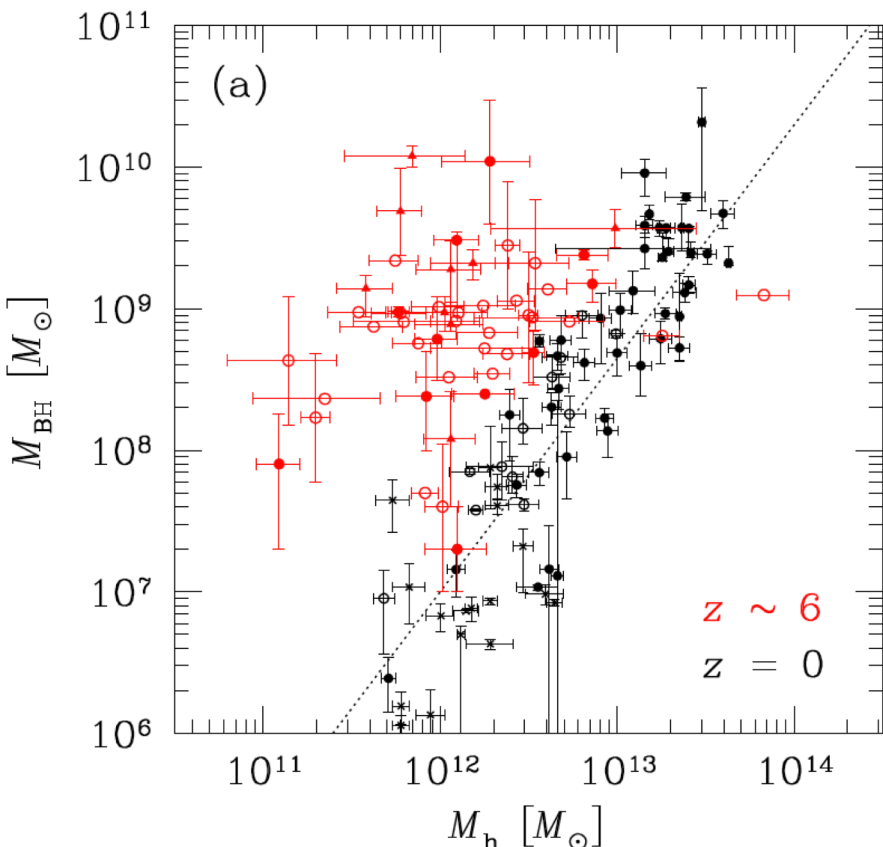
- $\text{Log } \Gamma(z) = (0.28 \pm 0.06)z - (2.91 \pm 0.06)$
- A possible decreasing of  $\Gamma$  at  $z > 6$ !? Need more sample.

# Constraining the formation process via M(halo)-M(SMBH) relation

Shimasaku & Izumi 2019, ApJL, 872, L29

- Relation between  $M(BH)$  and the mass of hosting dark halos  $M(halo)$  → constraining the SMBH growth efficiency in halos
  - Both stellar and SMBHs grow at similarly high pace, or grow low pace
  - The former predicts a higher  $M(BH)$ - $M(halo)$  relation
- $M(halo)$  from ALMA [CII] rotation velocity  $V_{\text{rot}}$ 
  - Assuming that the circular velocity of the hosting dark matter halo,  $V_{\text{circ}}$ , is equal to  $V_{\text{rot}}$
  - Calibrated with  $z \sim 3$  quasars with clustering-based  $M(halo)$  estimates

# Constraining the formation process via M(halo)-M(SMBH) relation



- A vast majority of  $z \sim 6$  SMBHs are more massive than expected from the local M(BH)-M(halo) relation
  - The median mass ratio  $M(\text{BH})/M(\text{halo}) = 6 \times 10^{-4}$ , i.e., 0.4% of the baryons in halos are locked up in SMBHs.

Shimasaku & Izumi 2019, ApJL, 872, L29

# Do quasars live in a biased environment?

- Some studies say no, while some works tell yes.
  - No significant over-density of LAEs around  $z \sim 6$  quasars
    - Ohta et al. 2018, ApJ, 856, 109
    - Mazzucchelli et al. 2017, ApJ, 834, 83
    - Banados et al. 2013, ApJ, 773, 178
  - Detections of [CII]- and FIR-bright companion galaxies around luminous  $z \sim 6$  quasars
    - Decarli et al. 2017, Nature, 545, 457
    - Willott et al. 2017, ApJ, 850, 108
    - Trakhtenbrot et al. 2017, ApJ, 836, 8
    - Neeleman et al. 2019, ApJ, 882, 10
- See also  
Kashikawa et al. 2007, ApJ, 663, 765  
(LAEs around  $z = 4.8$  quasar)  
Kikuta et al. 2017, ApJ, 841, 128  
(LAEs around 2 quasars @ $z \sim 4.9$ )  
Uchiyama et al. 2019, ApJ, 870, 45
- 4 of 27 quasars at  $z > 6$   
[CII] companion galaxies  
projected separation  $< 60$  kpc  
line-of-sight vel. shift  $< 450$  km/s  
quasars at  $z = 6.5$   
a close [CII] companion galaxy  
projected separation  $\sim 5$  kpc (!)  
line-of-sight vel. shift  $\sim 300$  km/s

# ALMA reveals [CII] companions around z~6 quasars

28

Neeleman et al. 2019, ApJ, 882, 10

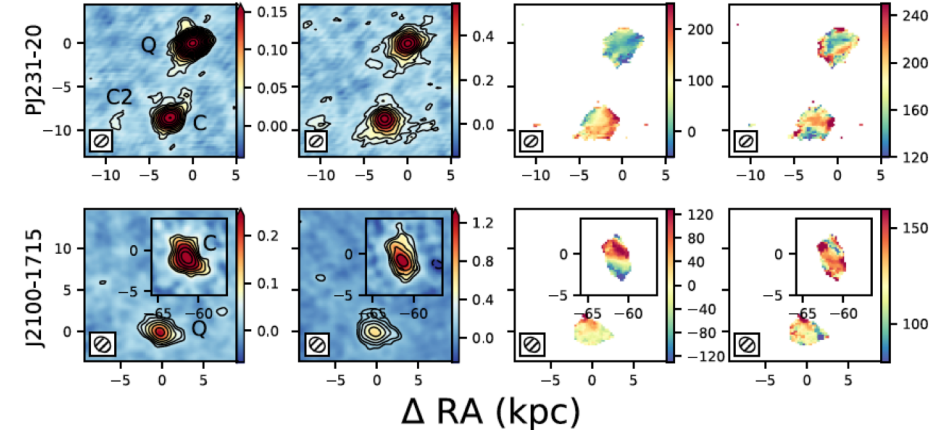
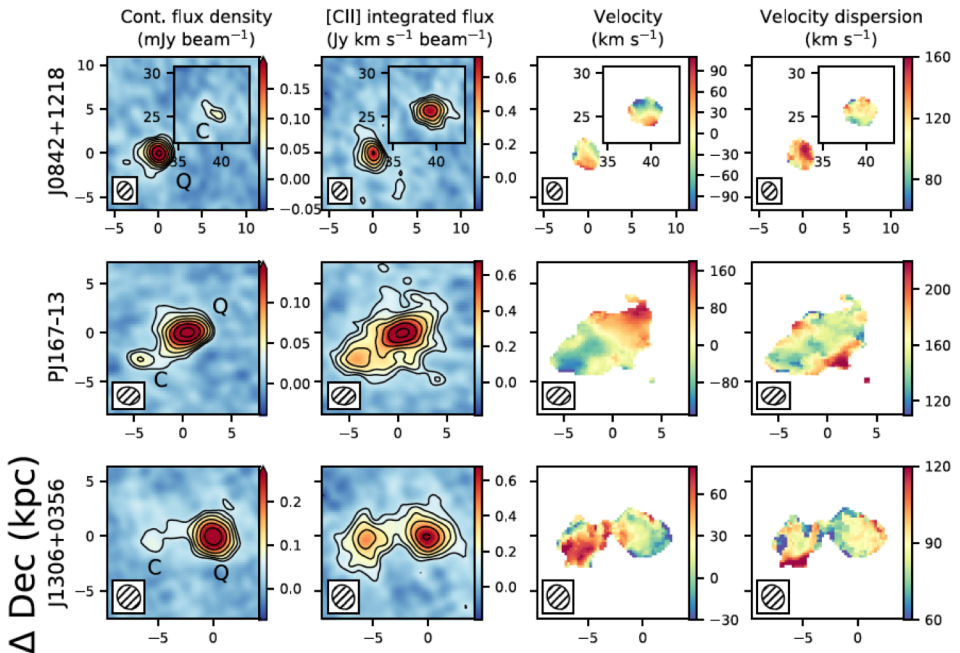
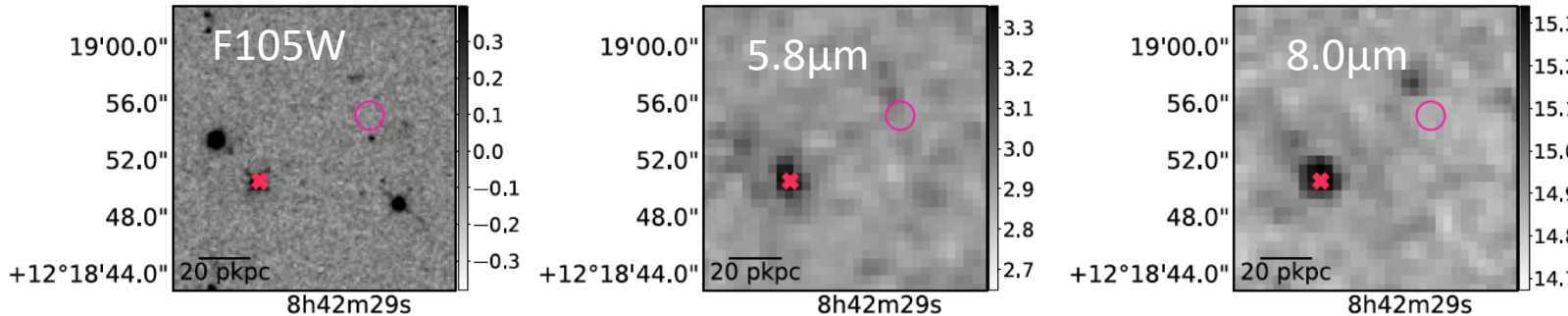


**Table 3**  
Derived Far-infrared Properties of the Quasar Host and Companion Galaxies

Name <sup>a</sup>	Impact Parameter <sup>b</sup>		$L_{\text{[C II]}}^{\text{c}}$ ( $10^9 L_{\odot}$ )	$L_{\text{TIR}}^{\text{d}}$ ( $10^{11} L_{\odot}$ )	$\text{SFR}_{\text{[C II]}}^{\text{e}}$ ( $M_{\odot} \text{ yr}^{-1}$ )	$\text{SFR}_{\text{TIR}}^{\text{f}}$ ( $M_{\odot} \text{ yr}^{-1}$ )	$M_{\text{dyn,obs}}^{\text{g}}$ ( $10^{10} M_{\odot}$ )	$M_{\text{dyn,mod}}^{\text{h}}$ ( $10^{10} M_{\odot}$ )
J0842+1218Q			$1.35 \pm 0.14$	$5.1\text{--}23$	$71\text{--}450$	$77\text{--}350$	$1.5\text{--}4.8$	$>1.3$
J0842+1218C	8.2	47	$1.73 \pm 0.23$	$1.6\text{--}7.5$	$95\text{--}600$	$24\text{--}110$	$0.8\text{--}2.5$	$>2.3$
J0842+1218C2	5.4	31	$0.39 \pm 0.09$	...	$17\text{--}100$	...	$<4$	... <sup>i</sup>
PJ167-13Q			$3.53 \pm 0.15$	$5.6\text{--}26$	$220\text{--}1400$	$84\text{--}380$	$4.1\text{--}13$	$3.5 \pm 0.4$
PJ167-13C	0.92	5.0	$1.32 \pm 0.10$	$1.3\text{--}5.8$	$69\text{--}440$	$19\text{--}86$	$2.4\text{--}7.4$	$>1.8$
J1306+0356Q			$1.71 \pm 0.14$	$6.5\text{--}30$	$94\text{--}590$	$97\text{--}440$	$0.8\text{--}2.4$	$>0.6$
J1306+0356C	0.95	5.4	$0.82 \pm 0.10$	$2.1\text{--}9.7$	$39\text{--}250$	$32\text{--}140$	$0.4\text{--}1.1$	$>0.3$
PJ231-20Q			$6.13 \pm 0.31$	$32\text{--}150$	$420\text{--}2700$	$480\text{--}2200$	$2.0\text{--}6.2$	$>2.0$
PJ231-20C	1.7	9.1	$3.37 \pm 0.28$	$10\text{--}46$	$210\text{--}1300$	$150\text{--}690$	$2.7\text{--}8.4$	$>5.4$
PJ231-20C2	2.5	14	$0.28 \pm 0.08$	$1.5\text{--}7.0$	$11\text{--}70$	$23\text{--}100$	$2.0\text{--}3.1$	... <sup>i</sup>
J2100-1715Q			$2.17 \pm 0.21$	$6.3\text{--}29$	$120\text{--}790$	$94\text{--}430$	$1.3\text{--}4.1$	$>1.1$
J2100-1715C	10.8	61	$3.99 \pm 0.50$	$16\text{--}73$	$260\text{--}1600$	$240\text{--}1100$	$4.1\text{--}14$	$4.2 \pm 1.0$

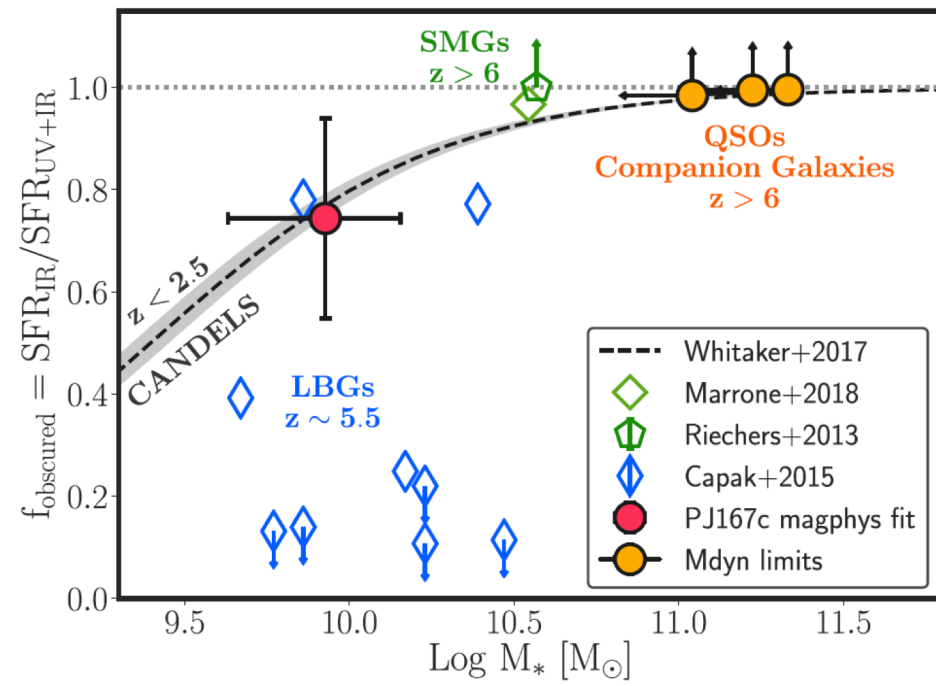
# Physical properties of companion galaxies to z~6 quasars<sup>29</sup>

Dec. (J2000)

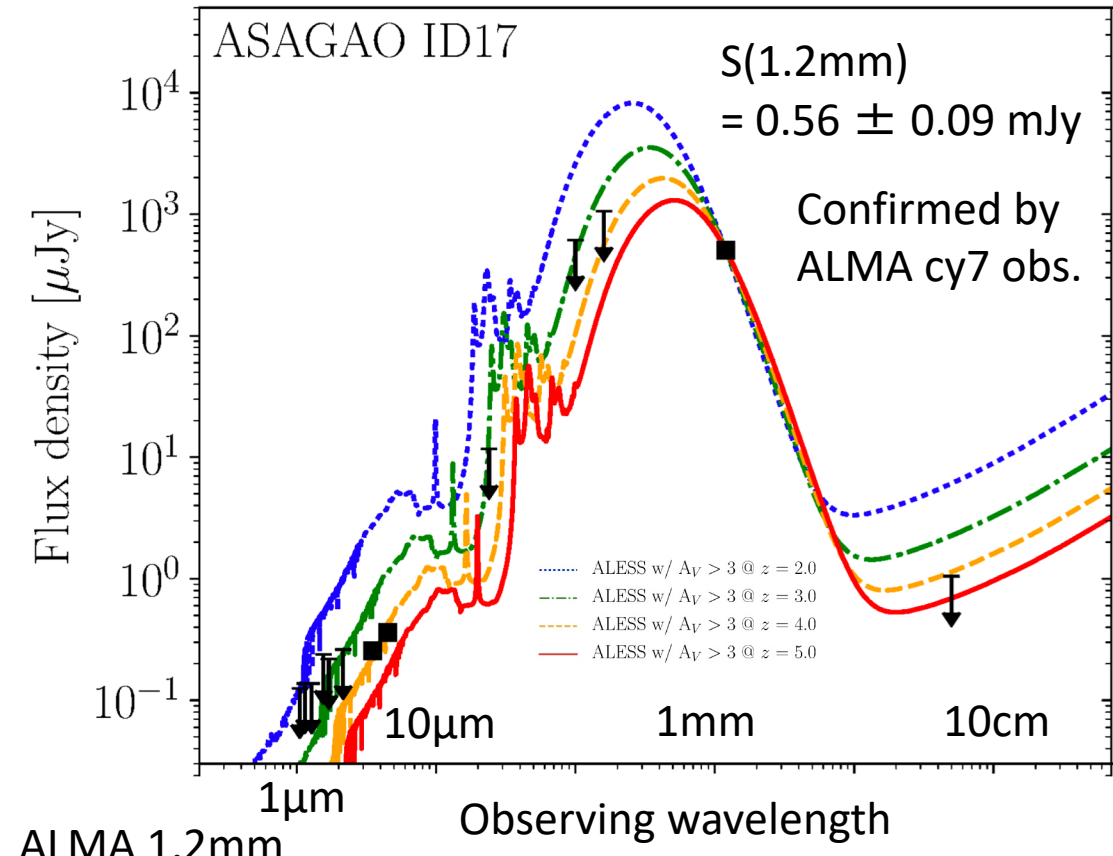


Name	SFR <sub>UV</sub> ( $M_{\odot} \text{ yr}^{-1}$ )	SFR <sub>IR</sub> ( $M_{\odot} \text{ yr}^{-1}$ )	SFR <sub>[C II]</sub> ( $M_{\odot} \text{ yr}^{-1}$ )	$f_{\text{obscured}} =$ SFR <sub>IR</sub> /SFR <sub>UV+IR</sub>	$M_{\text{dyn}}$ ( $\times 10^{10} M_{\odot}$ )	$M_{*}$ ( $\times 10^{10} M_{\odot}$ )
SDSS J0842+1218c	<2	$124 \pm 54$	$260 \pm 40$	>0.98	$12 \pm 5$	<11
PSO J167.6415–13.4960c	$11 \pm 3$	$32 \pm 4$	$182 \pm 16$	$0.74 \pm 0.20$	...	$0.84^{+0.64}_{-0.40}$
PSO J231.6576–20.8335c	<3	$709 \pm 157$	$730 \pm 100$	>0.99	$22 \pm 8$	<16.8
CFHQS J2100–1715c	<3	$573 \pm 73$	$360 \pm 70$	>0.99	$27 \pm 13$	<21.5

- Some companion galaxies do not show significant emission in the optical/near-IR
- Highly dust-enshrouded galaxies w/  $M_{\text{star}} < 10^{10} \text{ Msun}$
- Still consistent with residing on the galaxy main sequence @z~6

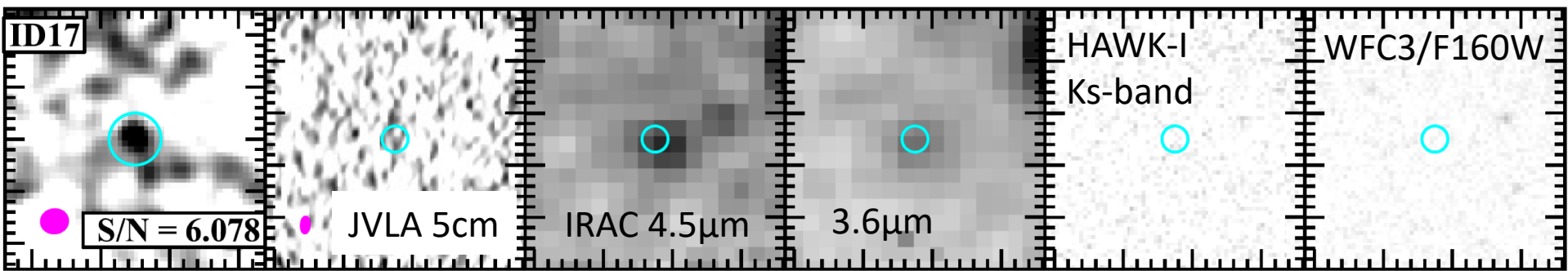


A heavily obscured and/or high-redshift dusty starburst galaxy, which is invisible in WFC3 & HAWK-I in a blind deep survey using ALMA



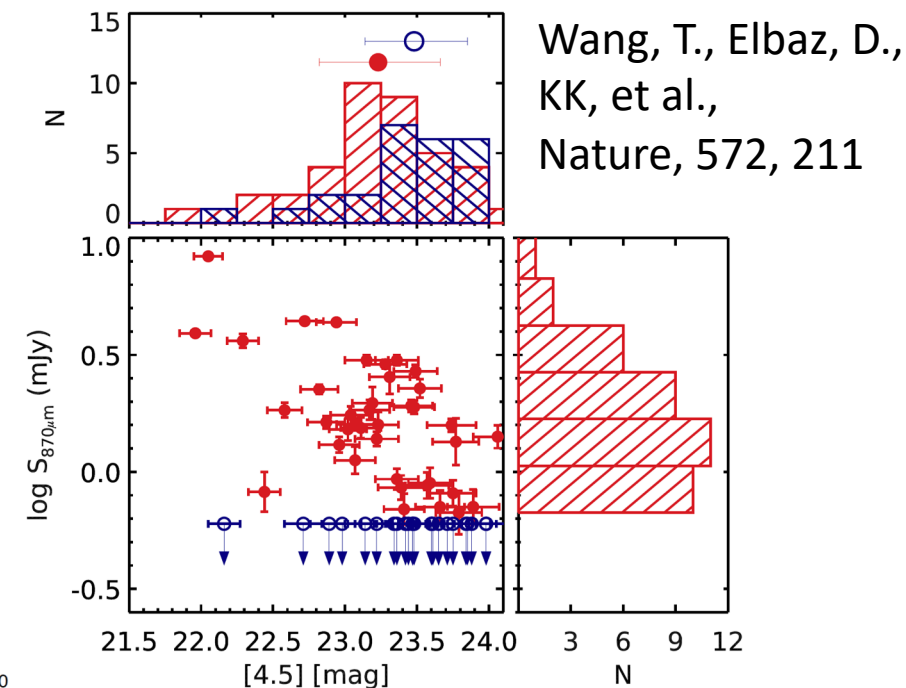
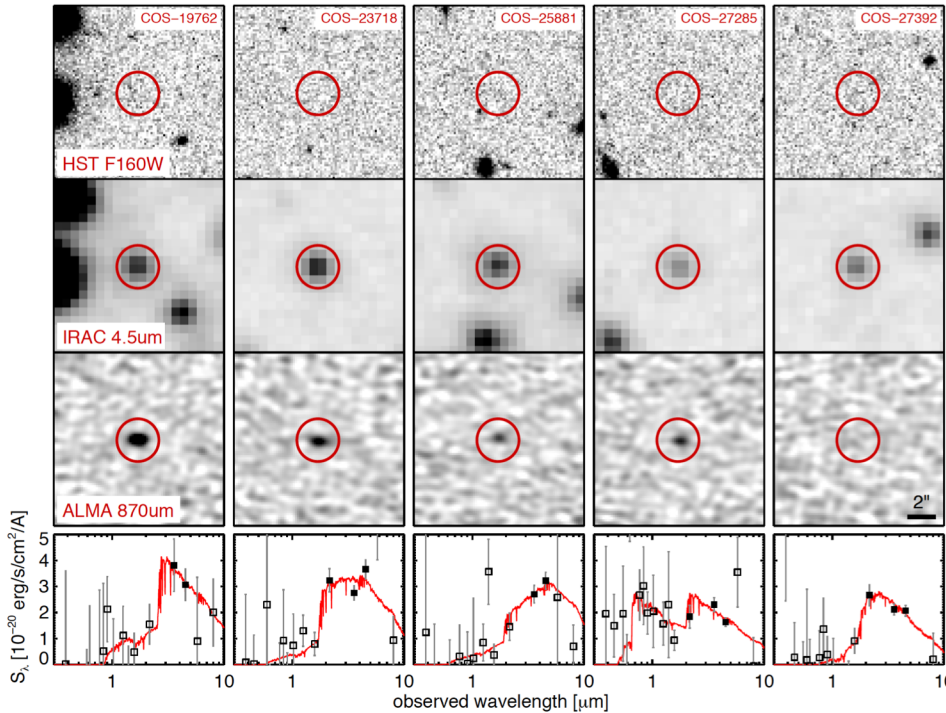
- GOODS-S
- “NIR-dark faint (sub)mm galaxies”
- IRAC counterpart only
  - “H-dropouts” (Wang, T. et al., 2016; 2019)
- similar to “GN10” but >10x fainter

Yamaguchi, Y., KK, et al.,  
2019, ApJ, 878, 73

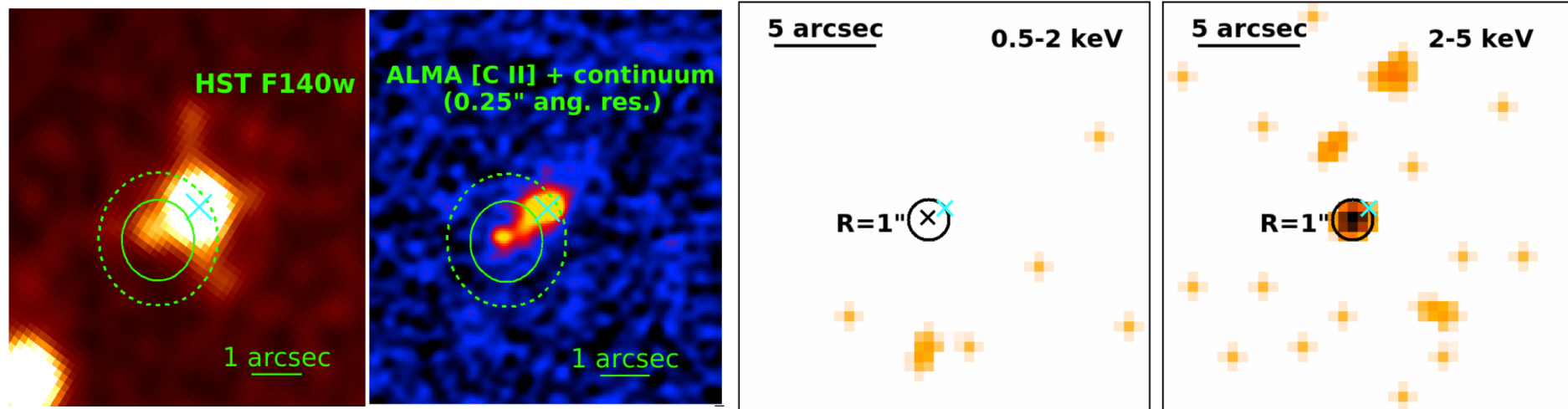


# HST-dark/Near-infrared-dark faint dusty submm galaxies: what are they?

- **$z > 6-8$  galaxies??**
  - some of them must be !?
- **massive galaxies in their forming phase @ $z > 3-6$** 
  - recent indication of H-band-drop-out population



# Do [CII]-bright companion galaxies host highly-obscured growing SMBHs?



- 59 ks Chandra obs. Of PSO167-13 @ $z=6.515$  → detection of a heavily-obscured ( $N_H > 2 \times 10^{24} \text{ cm}^{-2}$  at 68% confidence level) growing SMBH!? (Vito et al. 2019, A&A, 628, L6)
  - Regardless of which of the two galaxies is associated with the X-ray, this source is the first heavily obscured quasar candidate at  $z > 6$ .
- 140 ks Chandra observations of J231.6576-20.8335 at  $z = 6.59$  → no detection from the companion (Connor et al. 2020, ApJ, in press); see also Connor et al. 2019, ApJ, 887, 171

## Cycle 28 Approved Programs

Phase II ID	FirstName	LastName	Institution	Country	Type	Resources	Title
16225	Seth	Redfield	Wesleyan University	USA	SNAP	84	A SNAP Survey of the Local Interstellar Medium: New NUV Observations of Stars with Archived FUV Observations
16246	Mitchell	Revalski	Space Telescope Science Institute	USA	GO	14	Are Narrow Line Region Outflows an Effective Mode of AGN Feedback?
16198	Adam	Leslie	The Johns Hopkins University	USA	GO	32	From M87 to Coma, A Single Step Measurement of the Hubble Constant and a Reservoir of New SNe Ia
16217	Liliana	Rivera Sandoval	Texas Tech University	USA	GO	9	Identifying Double White Dwarf Binaries in Globular Clusters
16218	Liliana	Rivera Sandoval	Texas Tech University	USA	GO	10	Confirming the first double degenerates in globular clusters
16321	Liliana	Rivera Sandoval	Texas Tech University	USA	AR		A search for variable stars and compact binaries in globular clusters with HST
16261	Carsten	Bauer	University of South Carolina	USA	GO	22	Probing the Evolution of the Galaxy Population at High Redshift
<b>Project title</b>							
1619	Confirmation of a black hole at z=10.154						
1623	<b>PI name</b>						
1614	Drouart, Guillaume						
1631	<b>Proposal abstract</b>						
1623	With this proposal, we propose to unambiguously confirm the most distant black hole to date, located at z=10.15! We rely on a successful selection technique that already confirmed a z=5.55 source out of four candidates from our pilot study in the GAMA09 field (Drouart et al, accepted). We now have a short window of opportunity to publicize with a high impact publication, as well as a press release, a new distance record for black hole, breaking the symbolic z=10 limit.						
16271	Daniel	Schaerer	Observatoire de Geneve	CHE	GO	30	A new window on the UV SED of star-forming galaxies: direct measurements of ionizing spectra in the Lyman continuum
16233	Christian	Schneider	Universitat Hamburg, Hamburger Sternwarte	DEU	GO	17	Jets and disk scattering - Spatially resolved optical and FUV observations of AA Tau
16148	Peter	Senchyna	University of Arizona	USA	AR		Painting the first empirical picture of massive stars below the metallicity of the SMC with ULLYSES
16184	Nicholas	Seymour	Curtin University	AUS	GO	5	Lyman-alpha Observations of a z=10.15 Powerful Radio Galaxy
16149	Anowar	Shajib	University of California - Los Angeles	USA	AR		Systematics in H_0 from lensing: a comprehensive study of internal structure in elliptical galaxies

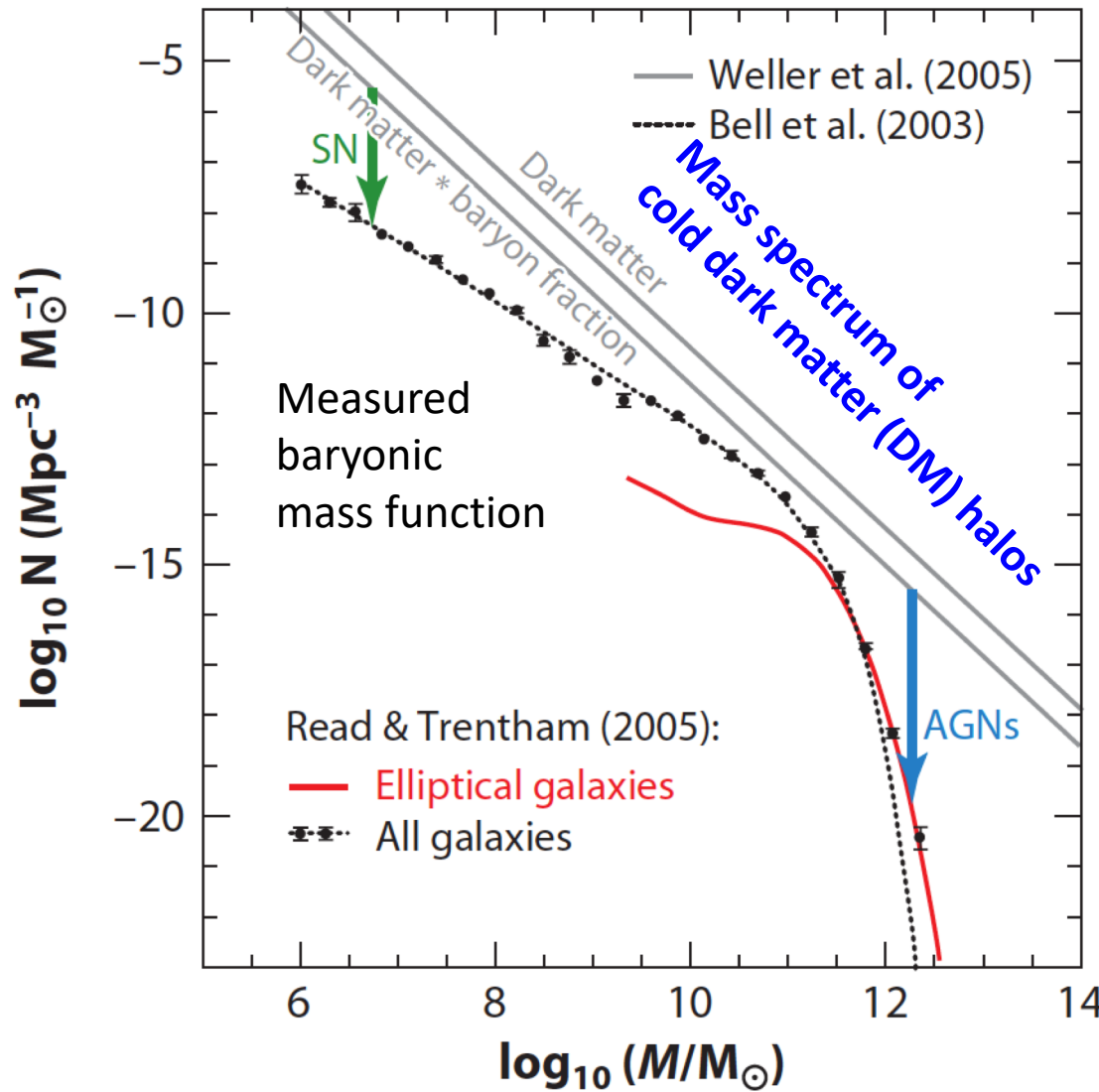
# Summary 1: quasars at $z > 6$

- >200 quasars above  $z > 6$ , including 7 quasars above  $z > 7$ , thanks to the wide field optical/near-infrared/mid-infrared surveys including HSC/Subaru
  - 1.5 Billion  $M_{\odot}$  SMBH at  $z = 7.515 \rightarrow$  need  $10^4 M_{\odot}$  seed at  $z = 30$  with high duty cycle at Edd. rate
- No redshift evolution of BLR metallicity up to  $z = 7.54$
- Prevalence of BAL features among  $z \sim 7$  quasars?
- Most of  $z \sim 6-7$  quasars are associated with dust-enshrouded starburst with intense [CII] 158  $\mu\text{m}$  emission
  - Indications for highly obscured growth of SMBHs at  $z > 7? \rightarrow$  search for obscured growing SMBHs by mm/submm spectroscopy surveys
- $M(\text{BH}) - M(\text{host})$  &  $M(\text{BH}) - M(\text{halo})$  relations
- Do quasars live in a biased environment?
  - No significant enhancement in LAEs, LBGs; some massive halos but not most massive
  - Instead, optically invisible but [CII]-bright companion galaxies exist

An artistic rendering of a supermassive black hole at the center of a galaxy. A bright, white and yellow accretion disk surrounds the black hole, showing intense radial motion. A powerful, multi-colored outflow, primarily blue with hints of red and white, jets upwards and to the left from the top of the disk. The background is a dark, star-filled space.

AGN feedback (outflows)

# Necessity of negative feedbacks



- SN feedback: make SF efficiency smaller in low-mass end
- AGN feedback: make high-mass cut-off of baryonic mass function

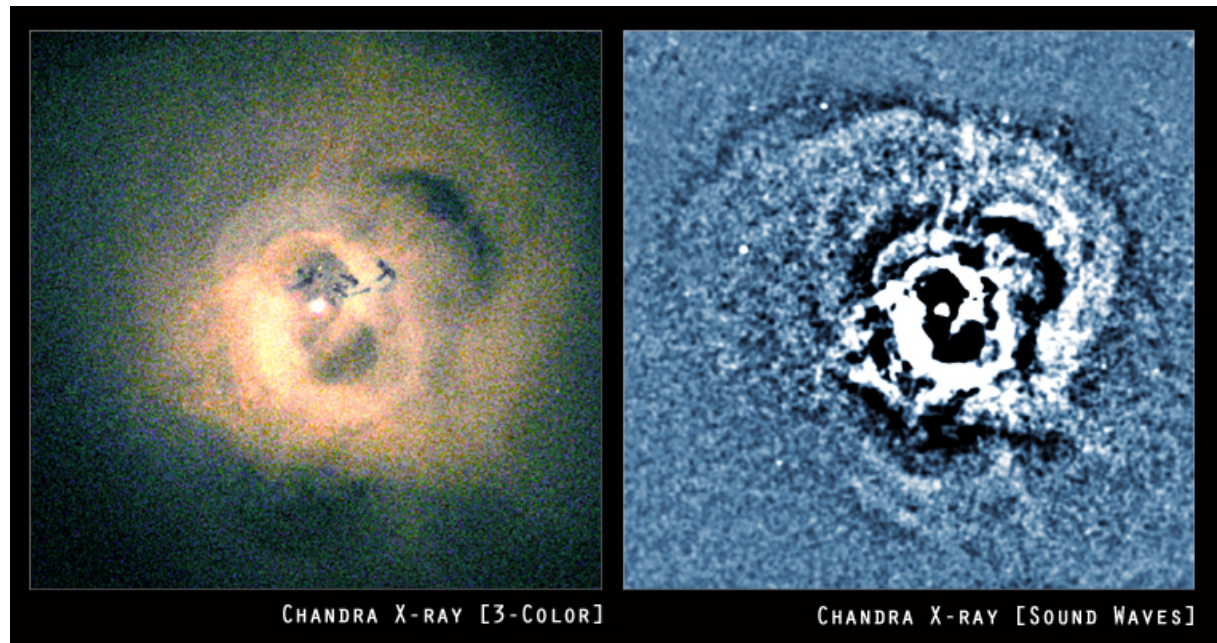
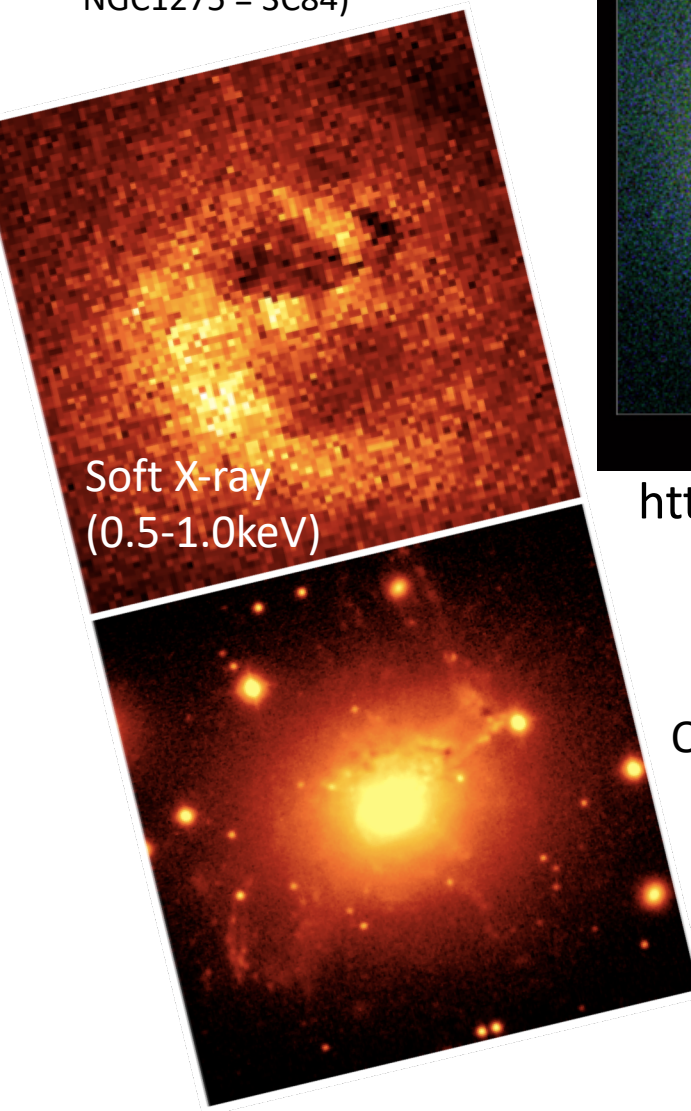
Read & Trentham 2005,  
Philisophical Transactions of  
The Royal Society A, 363, p. 2693

Kormendy & Ho, 2013,  
ARA&A, 51, 511

# Evidence for AGN feedback in cluster scales

## Perseus cluster

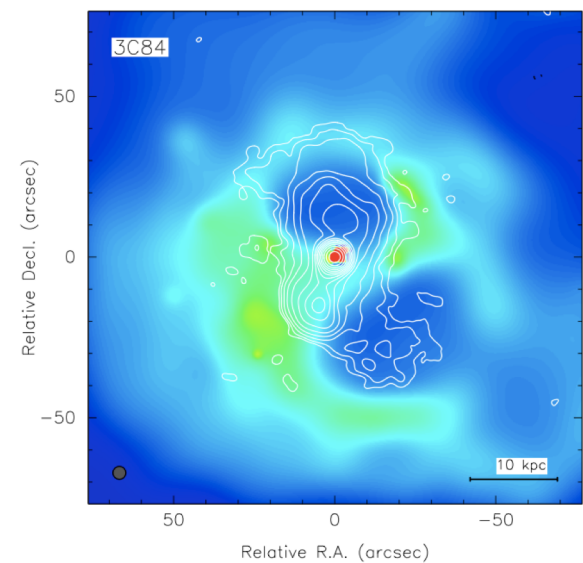
(the central cD galaxy  
NGC1275 = 3C84)



<http://chandra.harvard.edu/photo/2012/phoenix/media/>

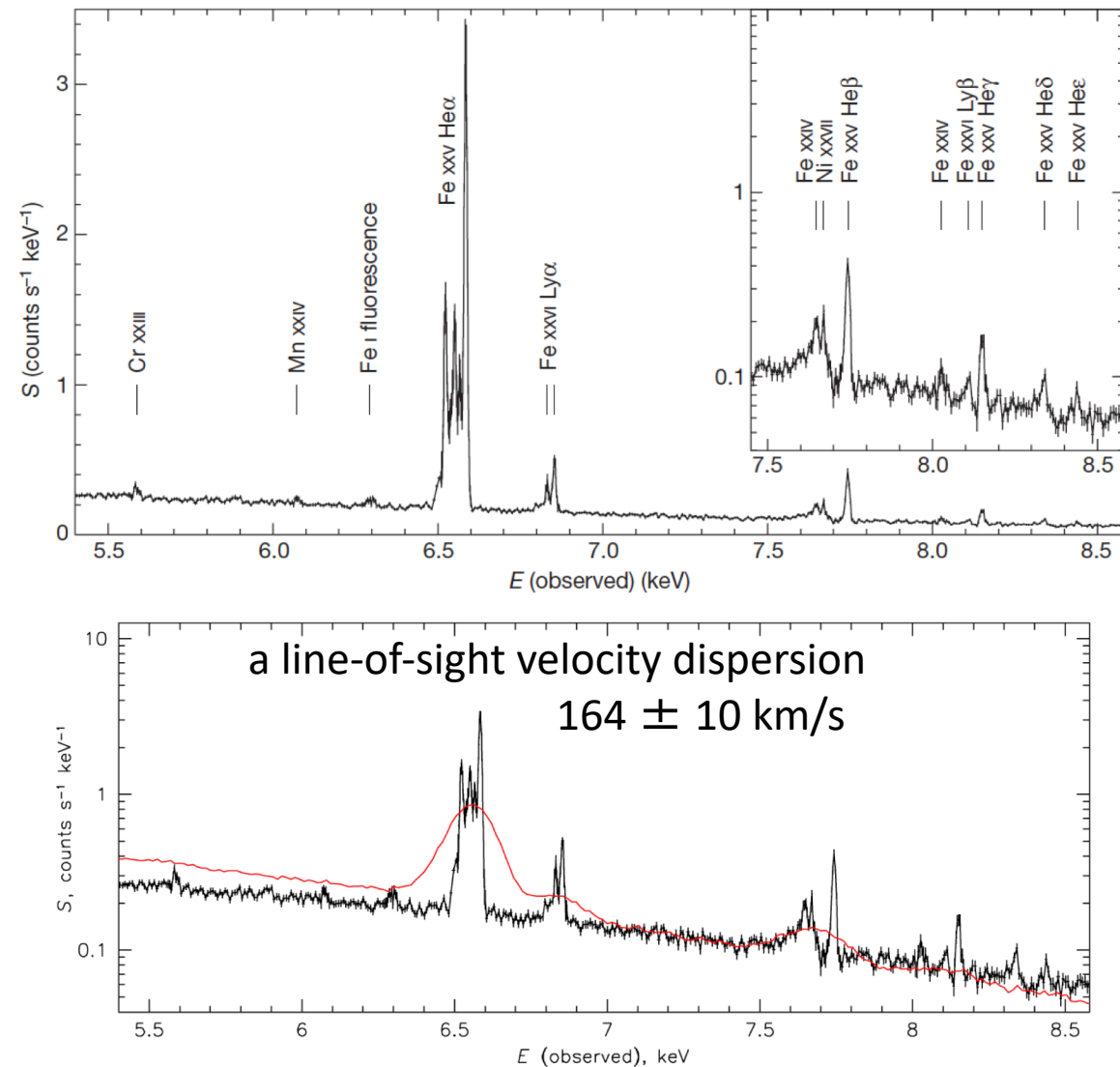
Fabian et al. 2000,  
MNRAS, 331, 369

contour: 1.4GHz



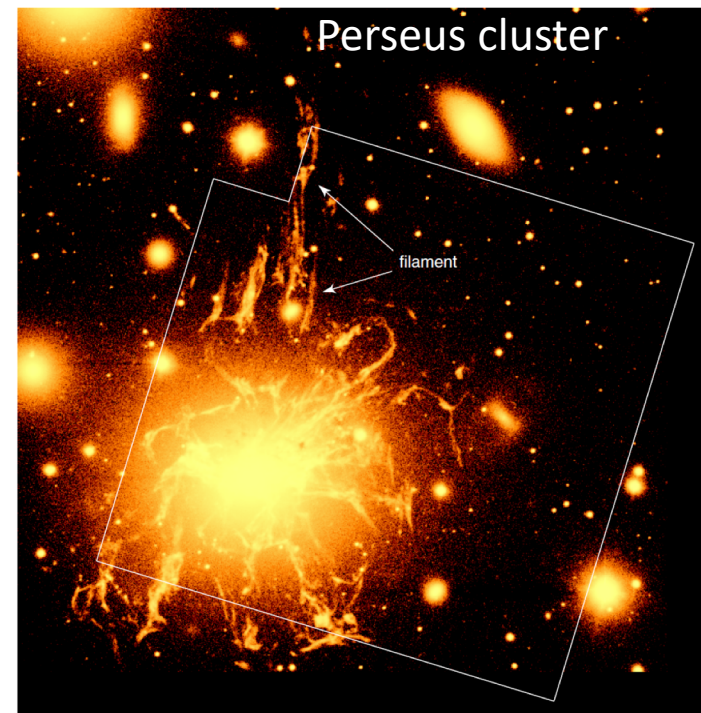
# Hitomi measurement of AGN feedback

The Hitomi collaboration, 2016, Nature, 535, 117



Extended Data Figure 1 | SXS spectrum of the full field overlaid with a CCD spectrum of the same region. The CCD is the Suzaku X-ray imaging spectrometer (XIS) (red line); the difference in the continuum slope is due to differences in the effective areas of the instruments.

Turbulent pressure support in the gas is four per cent of the thermodynamic pressure; that turbulence in the intracluster medium is difficult to generate and/or easy to damp!



Extended Data Figure 7 | The SXS field overlaid on the cold gas nebulosity surrounding NGC 1275. The image shows H $\alpha$  emission<sup>34</sup>. The radial velocity along the long northern filament measured from

CO data<sup>21</sup> decreases, south to north (within the SXS field of view), from about +50 km s<sup>-1</sup> to -65 km s<sup>-1</sup>. This is similar to the trend seen in the SXS velocity map (Extended Data Fig. 6).

# Molecular outflows and key physical quantities

A physical process extracting molecular medium (= direct ingredient of stars) from galaxies → a direct example of negative feedback of activities (AGN and starbursts)

- Mass outflow rate  $dM/dt$        $\Leftrightarrow$  to be compared with SFRs
  - Kinetic luminosity       $\Leftrightarrow$  to be compared with AGN luminosity  
(a few  $\times$  0.1% ~ 1% are expected in theory)
  - Momentum flux       $\Leftrightarrow$  momentum driven by AGN photon:  
to be compared with  $dP_{\text{AGN}}/dt = L_{\text{AGN}}/c$
- $$L_{\text{kin}} = 1/2 \times \frac{dM}{dt} \times \left( \frac{V_{\text{out}}}{\cos(\alpha)} \right)^2$$
- $$\frac{dP_{\text{out}}}{dt} = \frac{dM}{dt} \times \frac{V_{\text{out}}}{\cos(\alpha)}$$
- $\alpha$ : angle between line of sight and outflow axis

# Two modes of AGN feedback: quasar mode vs radio mode

- Quasar mode
  - Radiation feedback
    - Via radiation-driven (fast) wind
  - High accretion rate AGNs (High Eddington ratio)
  - Triggered by major merger → it is accompanied with starbursts; short duration → episodic; therefore has limited roles on quenching cluster-scale gas cooling.
- Radio mode
  - Direct heating of ISM via AGN jets
  - Low accretion rate AGNs
  - Caused by steady gas flow without major mergers → it is expected to have significant impact on quenching cluster-scale gas cooling. (cosmologically important)

# Two types of conservation: energy vs momentum conservation

- Although energy is conserved globally, the wind can in principle radiate away the thermal energy generated when it shocks with the surrounding interstellar medium.
- On the other hand, momentum cannot be radiated away.
- In the limit in which the shocked wind energy is rapidly radiated away → “**momentum conserving**” outflow.
- If radiative losses are negligible → outflow is “**energy conserving**”
  - real outflows may be somewhat intermediate between these two limits. Nevertheless, the degree to which AGN outflows conserve energy has very significant implications.
  - In particular, the momentum flux of the material swept up in energy-conserving outflows increases with time owing to work done by hot shocked gas. (an analogous in SNRs)

# An analogous phenomenon operates in supernova remnants (SNRs)

- I: Free expansion phase
  - During the 1<sup>st</sup> phase of the SNR evolution the surrounding ISM has no influence on the expansion of the shock wave, i.e., the pressure of interstellar gas is negligible.

$$E_{\text{SN}} = \frac{1}{2} M_e v_e^2 \quad \rightarrow \quad v_e = \left( \frac{2E_{\text{SN}}}{M_e} \right)^{1/2}$$

- The accumulated mass of the ISM compressed between the forward shock and the contact discontinuity equals the ejected mass of stellar material, and it will start to affect the expansion of the SNR. → the end of free expansion phase.

- The corresponding radius of the SNR, “the sweep-up radius”  $R_{\text{SW}}$  is defined by

$$M_e = \frac{4\pi}{3} R_{\text{SW}}^3 \rho_0 \quad \rightarrow \quad R_{\text{SW}} = \left( \frac{3M_e}{4\pi\rho_0} \right)^{1/3}$$

where  $\rho_0$  is the initial density of the interstellar medium. This radius is reached at the sweep-up time  $t_{\text{SW}} = R_{\text{SW}}/v_e$ .

# An analogous phenomenon operates in supernova remnants (SNRs)

- II: Sedov-Taylor phase (energy-conserving)
  - After the passage of the reverse shock, the interior of the SNR is so hot that energy losses by radiation are very small (all atoms are ionized, no recombination). The following pressure-driven expansion phase can therefore be regarded as adiabatic, the cooling of the gas is only due to the expansion.
  - The momentum of the remnant at the end of the Sedov-Taylor phase can exceed the momentum of the explosion ejecta by a factor of  $\sim 50$  (e.g., Cioffi, McKee, & Bertschinger 1988). Such momentum boosts have a large effect on the efficiency of stellar feedback in galaxies (e.g., Hopkins, Quataert & Murray 2012).

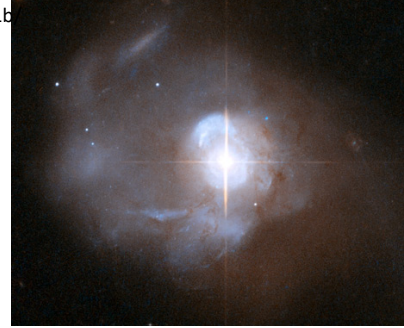
# An analogous phenomenon operates in supernova remnants (SNRs)

- III: (Radiative) cooling phase or snow plough phase
  - As the SNR expands and cools adiabatically it will reach a critical temperature ( $\sim 10^6$  K). At this temperature the ionized atoms start to capture free electrons and they can lose their excitation energy by radiation.
  - Due to the efficient radiative cooling the thermal pressure in the post-shock region decreases and the expansion slows down. → the snow plough phase (since more and more ISM is accumulated until the swept-up mass is much larger than the ejected stellar material.)
- IV: dispersing SNRs
  - Finally the shell breaks up into individual clumps, probably due to a Rayleigh-Taylor instabilities (hot thin gas is pushing cool dense gas) and the SNR disperses into the ISM as the expansion velocity decreases to values typical of the interstellar gas. 「宇宙流体力学」坂下・池内 1996 (培風館)

# Stellar wind

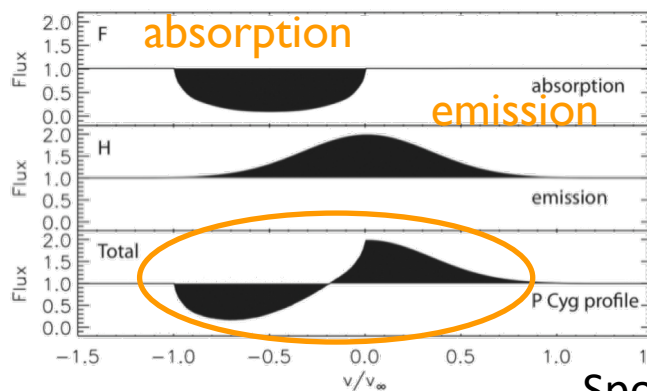
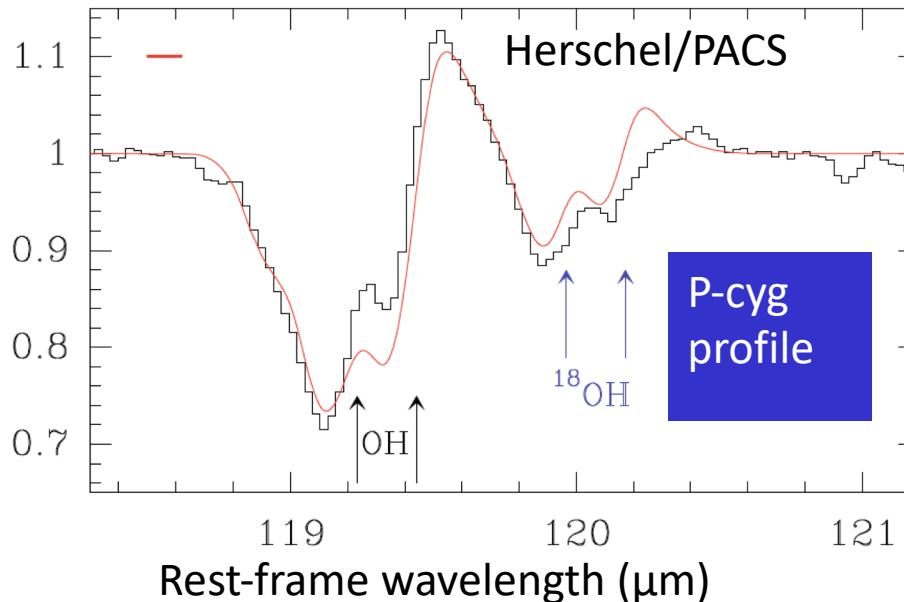
- Energy-driven wind
  - Driven by internal energy of stellar wind
  - $R(t) \propto t^{(3/5)}$
  - Examples: stellar wind from O, B stars
- Momentum-driven wind
  - Driven by ram pressure  $\rho V^2$
  - $R(t) \propto t^{(1/2)}$
  - Examples: Evolved winds with decreased pressure by radiative cooling; e.g., expanding shells seen in Wolf-Rayet stars (such as NGC 6888, NGC 2359, S308)
  - Another example: bipolar stellar wind in proto-stars

# Detection of molecular outflows in the local quasar Mrk 231

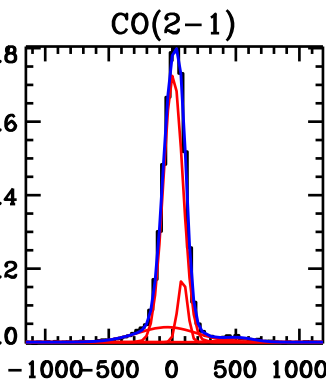
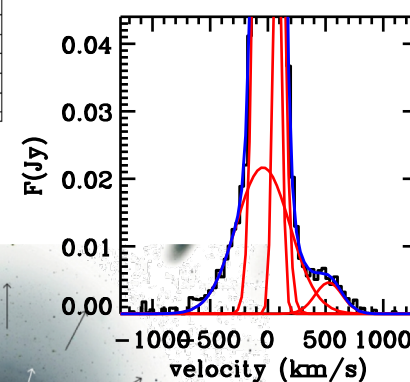
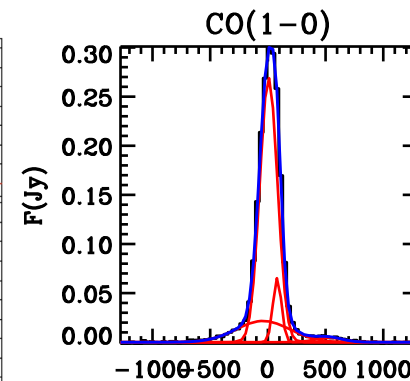


Relative intensity  
(normalized to the continuum level)

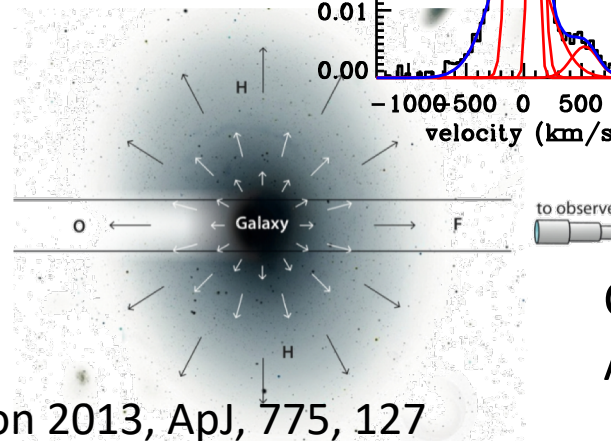
Fischer et al. 2010, A&A, 518, L41



Spoon 2013, ApJ, 775, 127



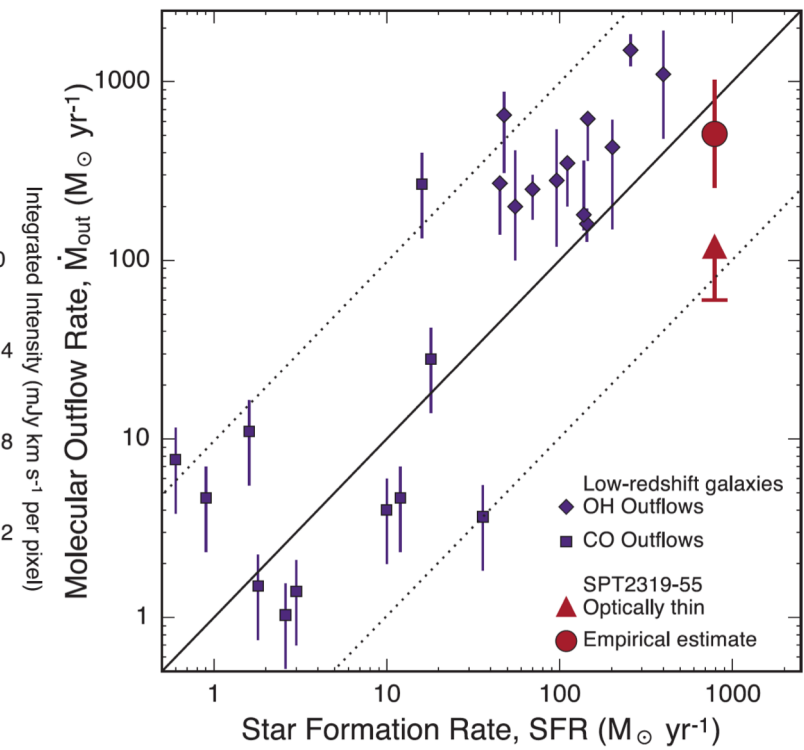
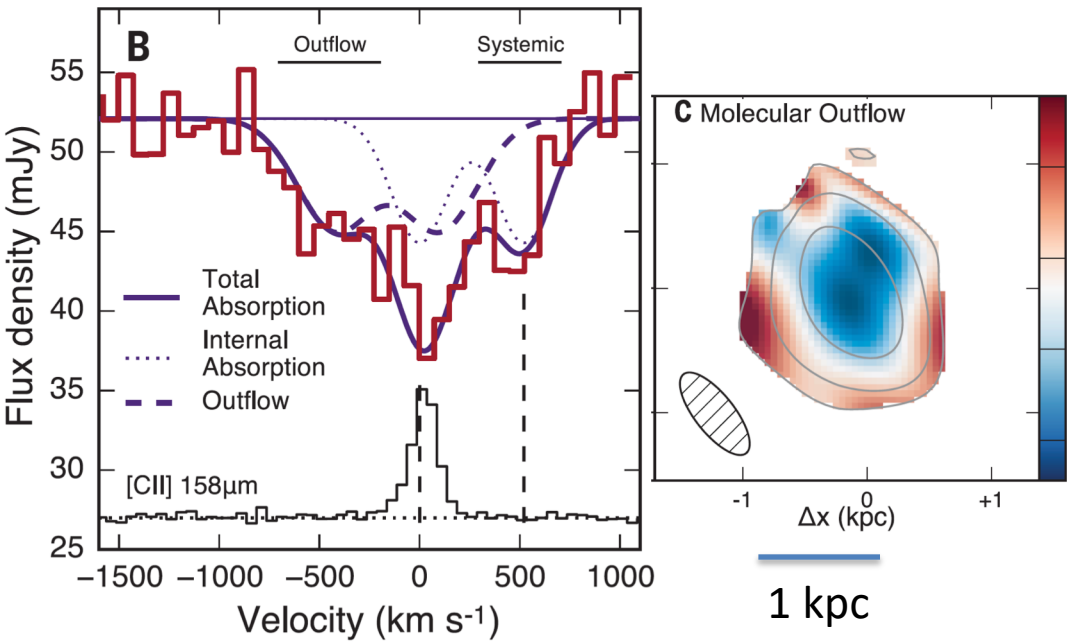
IRAM 30m



Cicone et al. 2012,  
A&A, 543, 99

# ALMA depicts OH outflow @z=5.293

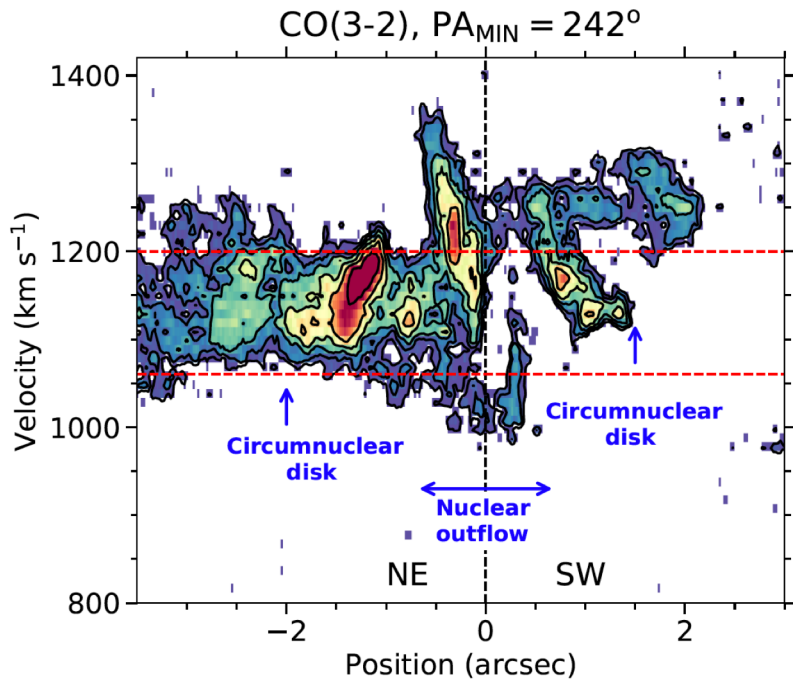
- massive (a few  $100 M_{\odot}/\text{yr}$ ), fast ( $\sim 800 \text{ km/s}$ ) molecular outflows toward SPT 2319-55 @z=5.293, a gravitationally lensed, bright thermal dust emission



# More molecular outflows in local AGNs captured and resolved by ALMA

NGC 3227 (Sy1)

CO(2-1), CO(3-2), 0''.09–0''.2 (7–15 pc)

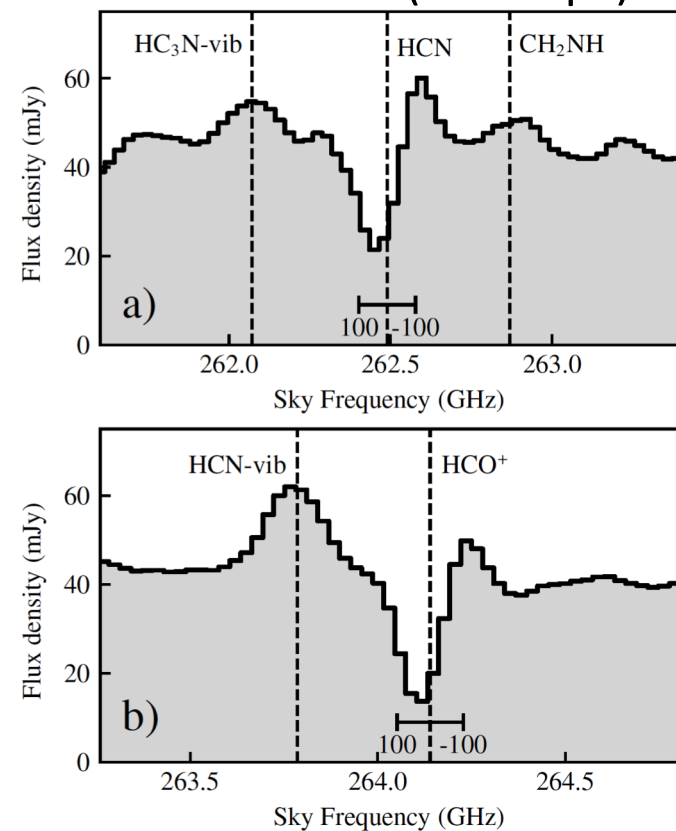


$dM/dt = 5 \text{ M}_{\odot}/\text{yr}$  (North),  $0.6 \text{ M}_{\odot}/\text{yr}$  (South)

Alonso-Herrero, A., et al. 2019, A&A, 628, A65

IC860 (heavily obscured)

0''.03 – 0''.09 (9 – 26 pc)



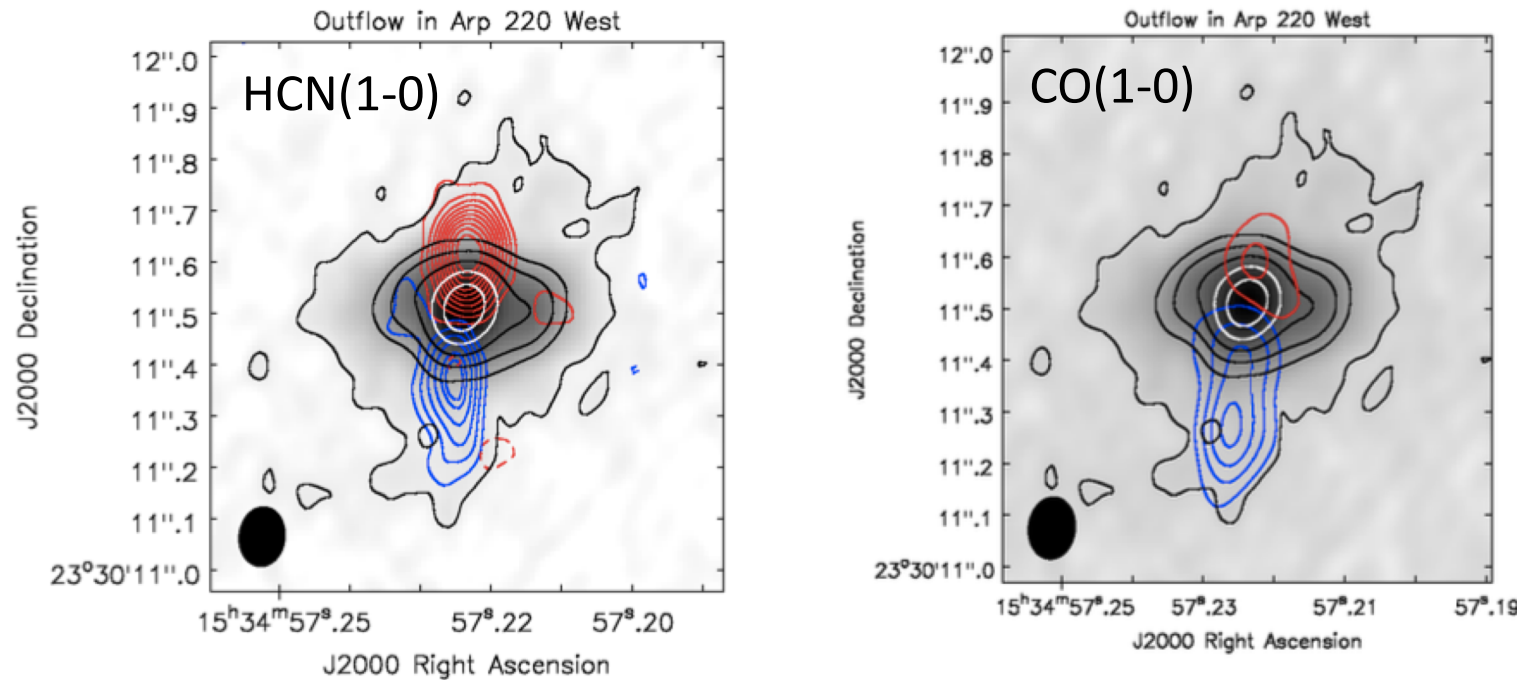
inverse P-Cyg of HCN and HCO<sup>+</sup>  
→ inflow ( $v \sim 50 \text{ km/s}$ )

Aalto, S., et al., 2019, A&A, 627, A147

# Dense molecular outflow in Arp220W

Cycle 3, ~11 km baselines

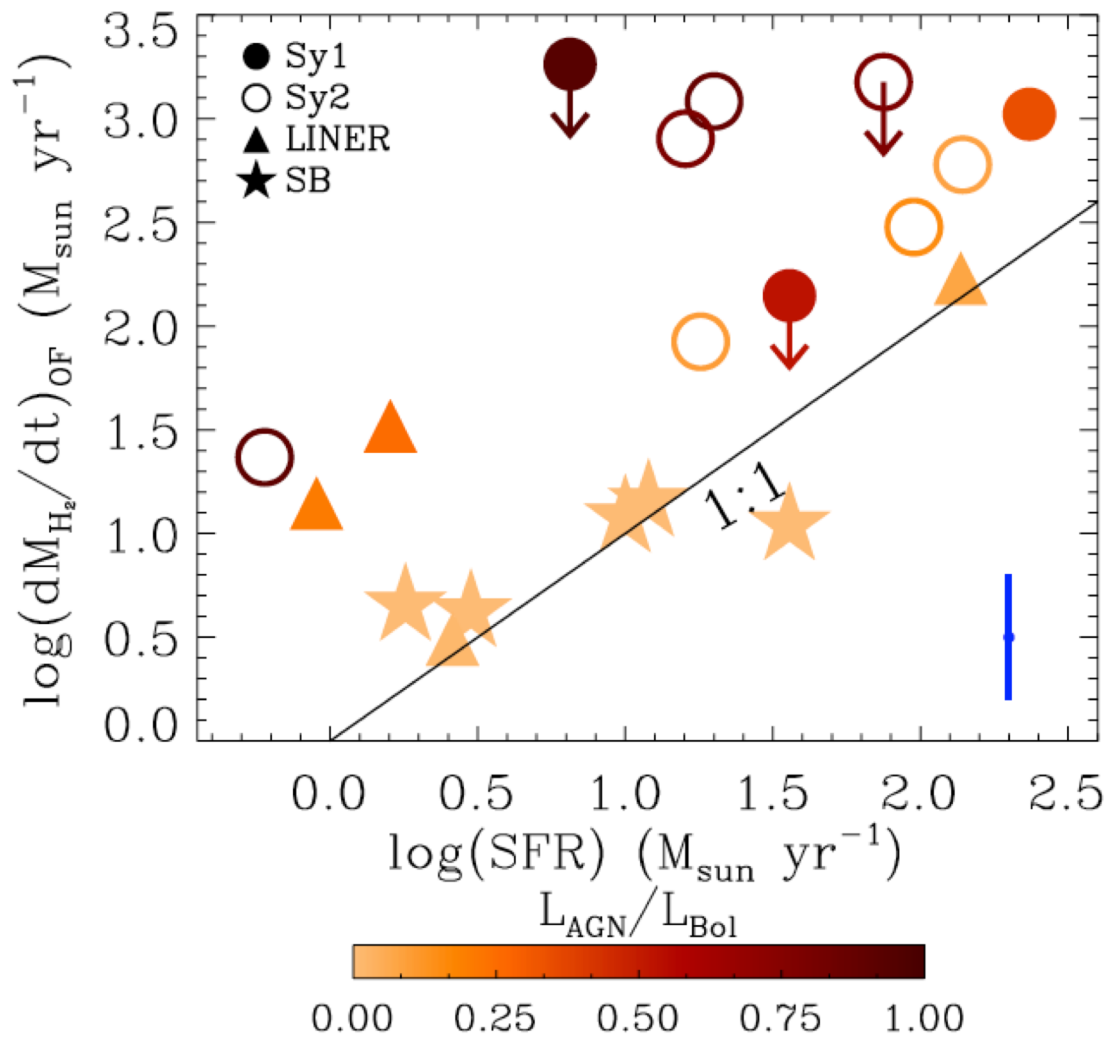
Barcos-Muñoz, Aalto, et al. 2018, ApJ, 853, L28



- ALMA reveals *extremely dense and fast* (840 km/s) outflow;  $dM/dt \sim 100 M_{\odot}/\text{yr}$
- The HCN 1-0 emission of the flow is very luminous with  $T_B(\text{HCN}) > T_B(\text{CO})!$
- Collimated flow *also seen in 3mm dust emission – opaque dust* (Sakamoto et al. 2017).
- Flow is *compact & collimated* with extension 120 pc and dynamical time scale of  $10^5$  yr.
- Energetics of flow can accommodate starburst or AGN as driving force – however collimated nature of flow may qualitatively strengthen the argument for AGN driving.

# Properties of molecular outflows

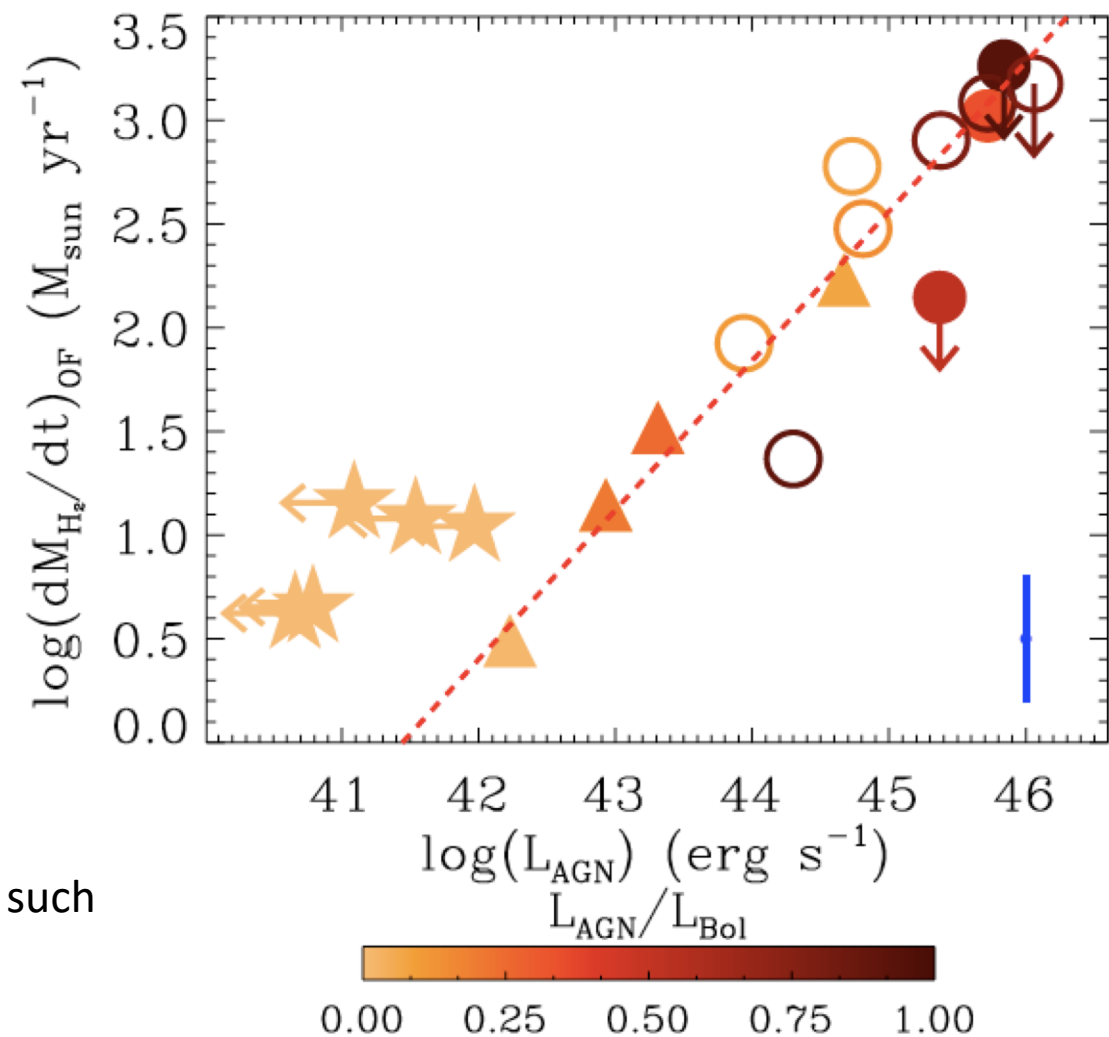
- Molecular outflows detected in AGN host galaxies are very massive
  - several  $100 M_{\odot}/\text{yr}$
- Star-forming galaxies show  $dM_{\text{out}}/dt \sim \text{SFR}$
- consistent to a model prediction
  - e.g., Murray et al. 2005, ApJ, 618, 569



Cicone et al. 2014, A&A, 562, A21

# Molecular outflow vs AGN luminosity

- Clear correlation between mass loss rate of molecular gas and AGN luminosity
- → these massive molecular outflows are driven by AGNs



Question: then, what kind of physical processes driven by AGNs can launch such massive molecular outflows?

# Kinetic power of the molecular outflows

- Theoretical models of AGN feedback and cosmological simulations predict **a coupling efficiency** between AGN-driven outflows and AGN power of  **$\sim 5\%$** , for AGN accreting close to the Eddington limit

– which is likely the case for, at least, the most luminous AGNs in the sample

- This is also the  $P_{\text{kin}}/L_{\text{AGN}}$  fraction needed to explain the  $M_{\text{BH}}-\sigma$  relation in local galaxies

– King 2010; Zubovas &  
King 2012; Lapi et al. 2005

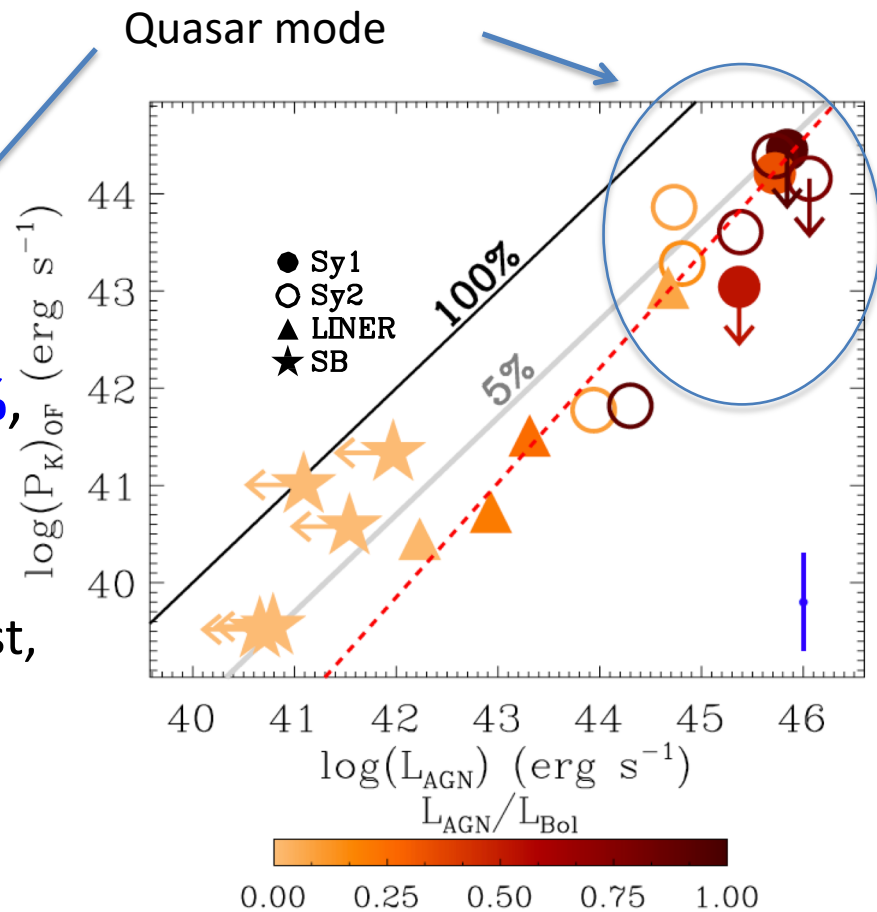


**Fig. 12.** Correlation between the kinetic power of the outflow and the AGN bolometric luminosity. Symbols and colour-coding as in Fig. 8. The grey line represents the theoretical expectation of models of AGN feedback, for which  $P_{\text{K,OF}} = 5\% L_{\text{AGN}}$ . The red dashed line represents the linear fit to our data, excluding the upper limits. The error bar shown at the bottom-right of the plot corresponds to an average error of  $\pm 0.5$  dex.

# Momentum rate of the molecular outflows

- In models in which the outflow is generated by a nuclear AGN-driven wind, the momentum rate transferred by the AGN photons to the surrounding medium is given by the average number of scattering by each photon.
- Some of these models predict, for AGNs accreting close to the Eddington limit, **momentum fluxes** of  $\sim 20 L_{\text{AGN}}/c$  (e.g., Zubovas & King 2012; Faucher-Giguere & Quataert 2012)
- Most of our sources (except the “pure” starbursts) do follow the relation  $\sim 20 L_{\text{AGN}}/c$

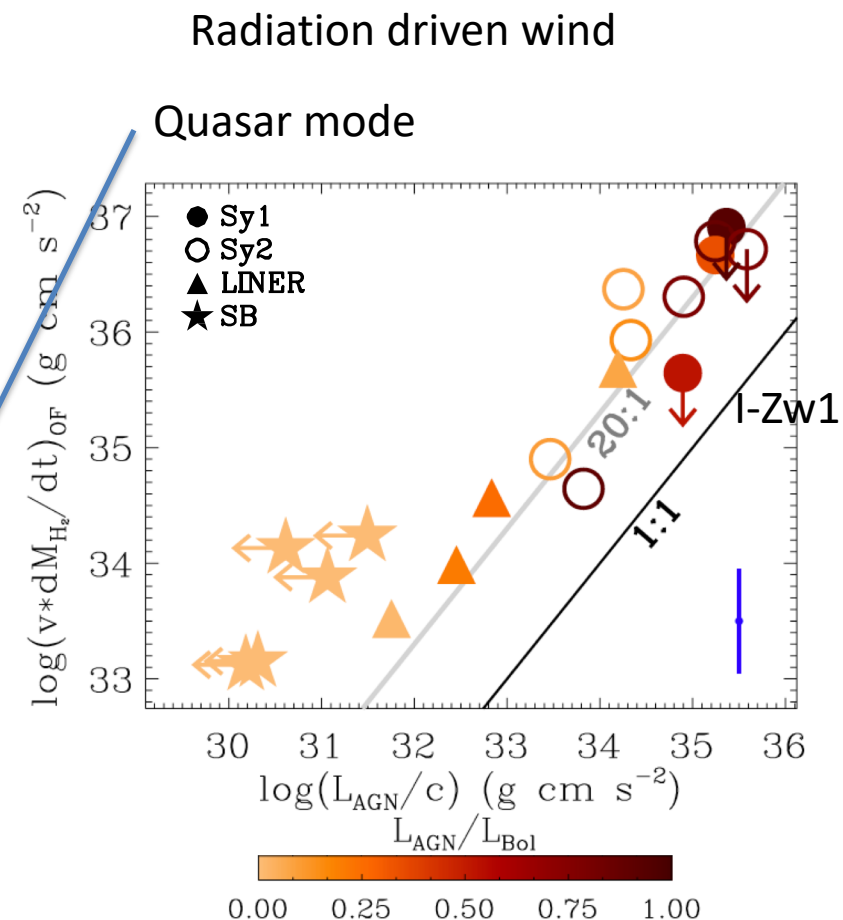


**Fig. 14.** Outflow momentum rate ( $v \dot{M}_{\text{H}_2,\text{OF}}$ ) versus photon momentum output of the AGN ( $L_{\text{AGN}}/c$ ). Symbols and colour-coding as in Fig. 8. The grey line shows the prediction of models of AGN feedback, i.e.  $\dot{M}_{\text{H}_2,\text{OF}} v \sim 20 L_{\text{AGN}}/c$ . The error bar shown at the bottom-right of the plot corresponds to an average error of  $\pm 0.45$  dex.

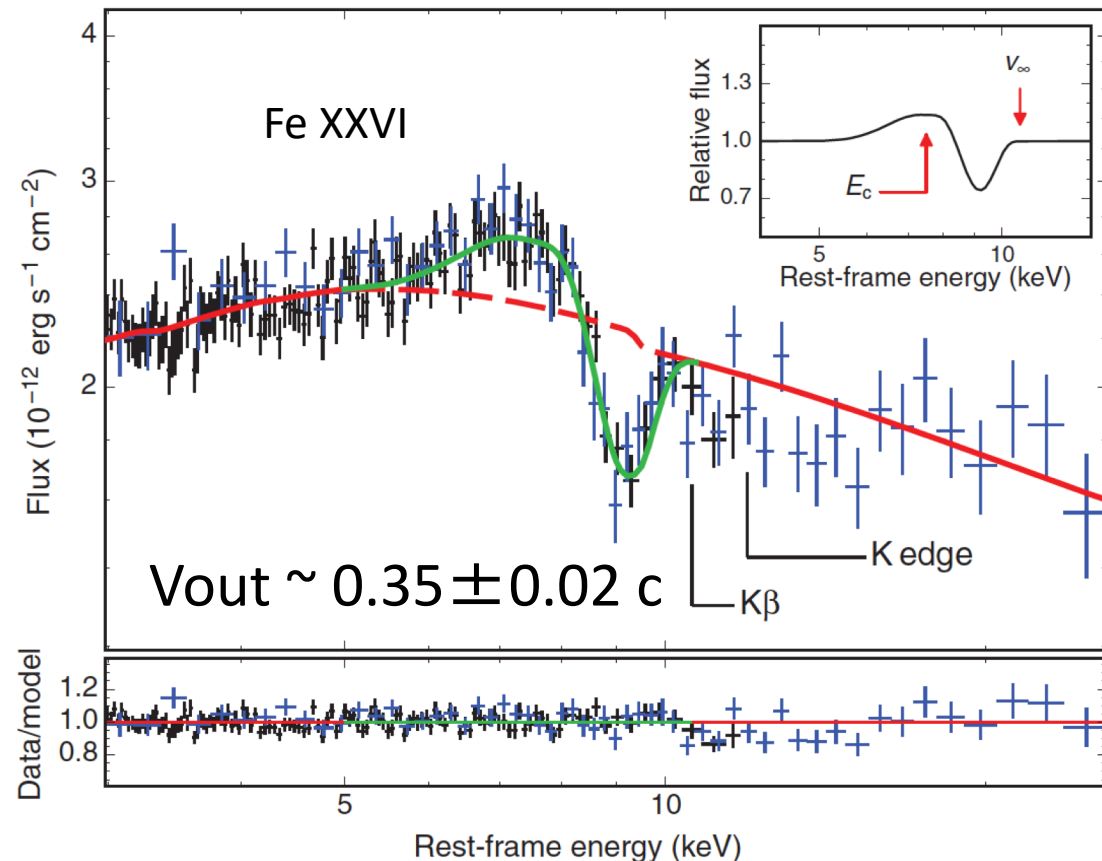
# Further reading (for assignments)

- Veilleux et al. 2020, A&A Review, vol. 28, 2  
“Cool outflows in galaxies and their implications”
- Fluetsch, A., et al. 2019, MNRAS, 483, 4586 for recent compilation of cold molecular outflows

Ionized fast outflows (UFOs)  
vs  
cold molecular outflows

# A highly ionized X-ray ultra-fast outflow (UFO) showing a P-Cyg profile

**Fig. 3. Fit with a P-Cygni line model.** Adopting the same baseline continuum of Fig. 2 (red curve), we fitted the emission and absorption residuals characterizing the Fe-K band by means of a self-consistent P-Cygni profile from a spherically symmetric outflow (green curve). The results are shown for the merged Obs. 3 and Obs. 4, which are separated by only 3 days and are virtually indistinguishable at 2 to 30 keV (Fig. 1). The two NuSTAR modules were combined into a single spectrum (plotted in blue;  $\pm 1$  SD error bars) for display purposes only. The inset contains a graphical explanation of the key parameters of this model: the characteristic energy  $E_c$ , corresponding to the onset of the absorption component, and the wind terminal velocity  $v_\infty = 0.35 \pm 0.02 c$ , which can be regarded as a measure of the actual outflowing speed of the gas. The bottom panel shows the ratio between the data and the best-fit model. The residual structures above 10 keV are due to the K $\beta$  and K edge absorption features from Fe XXVI. These are not included in the P-Cygni model but are detected with high significance (table S2) and remove any ambiguity in the identification of the ionic species.



The nearby ( $z=0.184$ ) radio-quiet quasar PDS 456

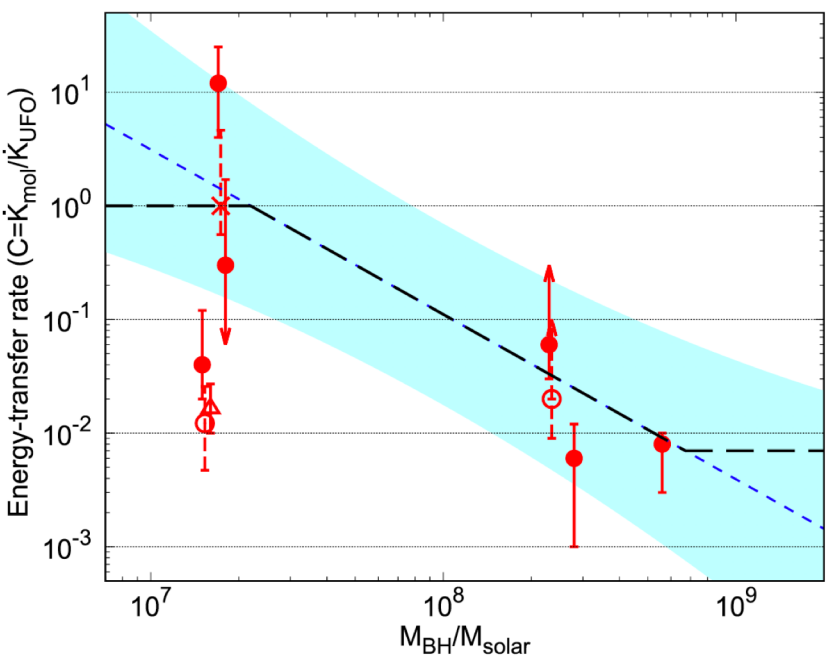
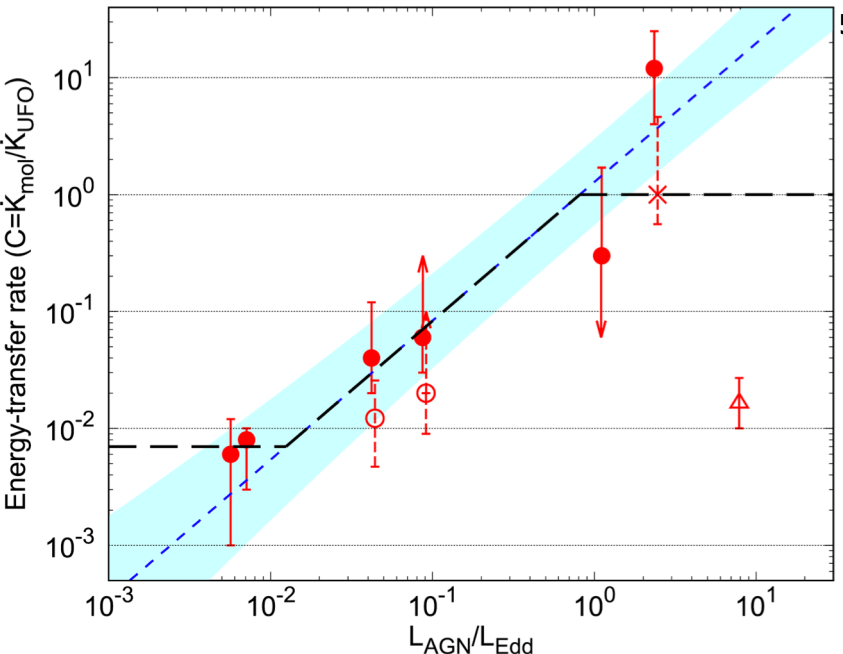
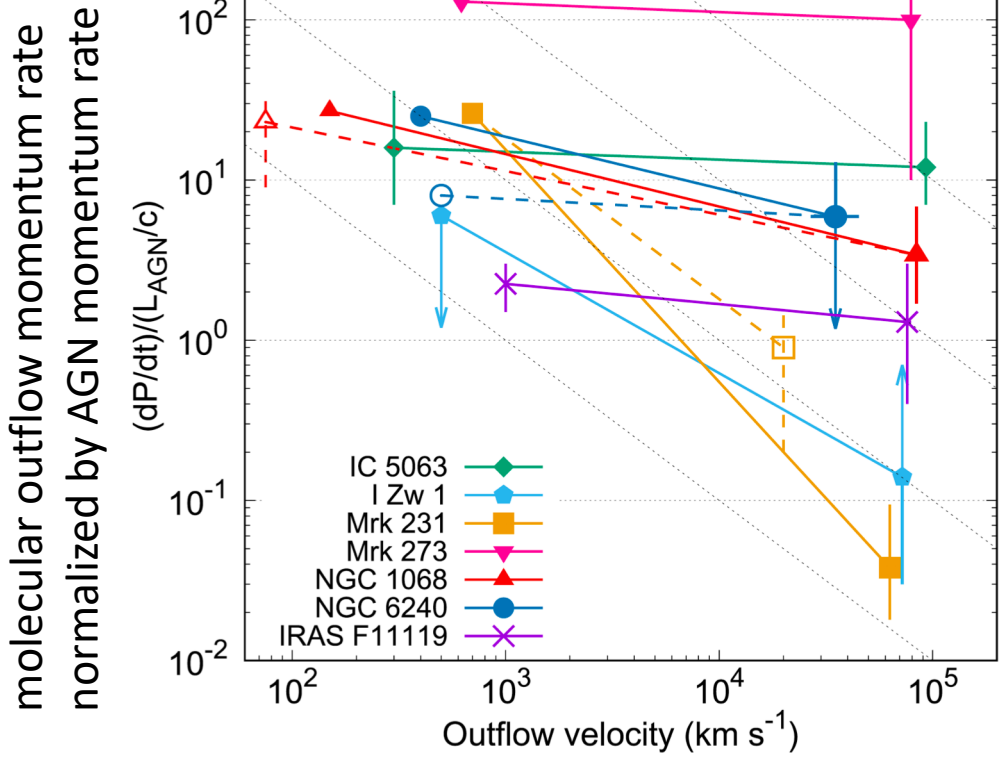
$L(\text{bol}) = 2 \times 10^{47} \text{ erg/sec}$  or  $5 \times 10^{13} L_\odot \sim L(\text{Edd})$  for  $M_{\text{BH}} = 10^9 M_\odot$

Nardini et al. 2015, Science, 347, 860

# Cold molecular outflow vs highly ionized outflow (UFOs)

- 8 of 14 AGNs with molecular outflow detections have good X-ray spectra (XMM and Suzaku)  
→ 6 of 8 have UFO lines
- energy transfer rate (**kinetic energy ratio of molecular outflows to UFOs**)
  - broad range:  $7 \times 10^{-3}$  to 1
  - negative correlation with BH mass → AGN feedback is more efficient in the lower BHs
  - theory: cooling timescale of outflowing gas becomes longer than the flow timescale when the BH mass is smaller

# Cold molecular outflow vs highly ionized outflow (UFOs)

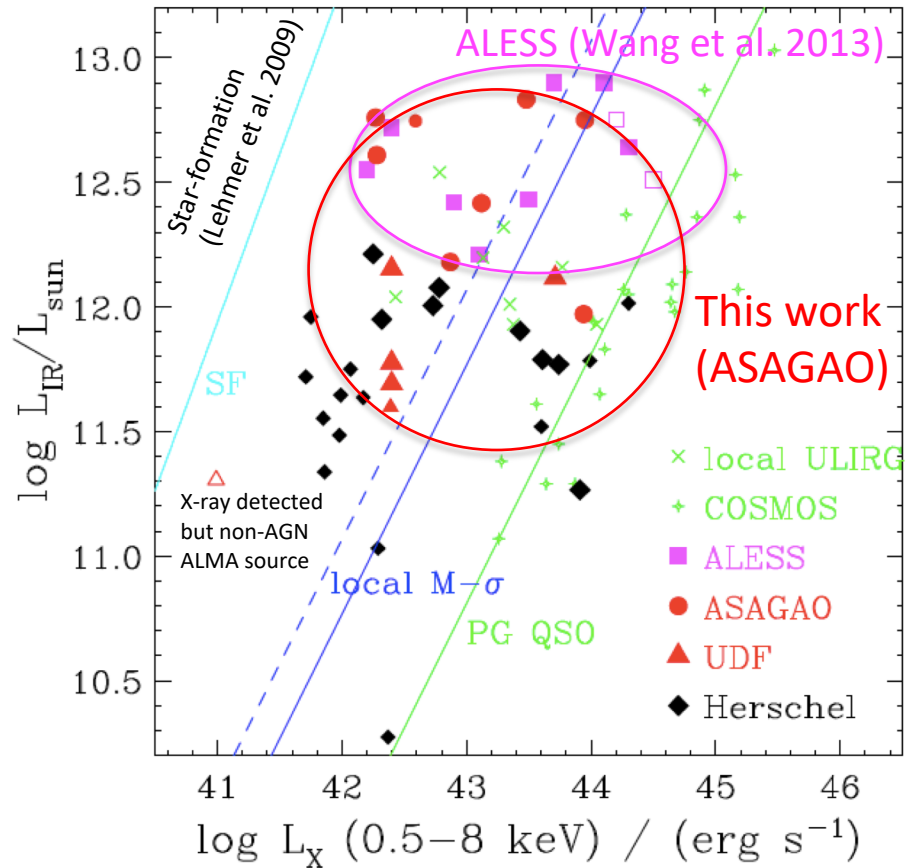
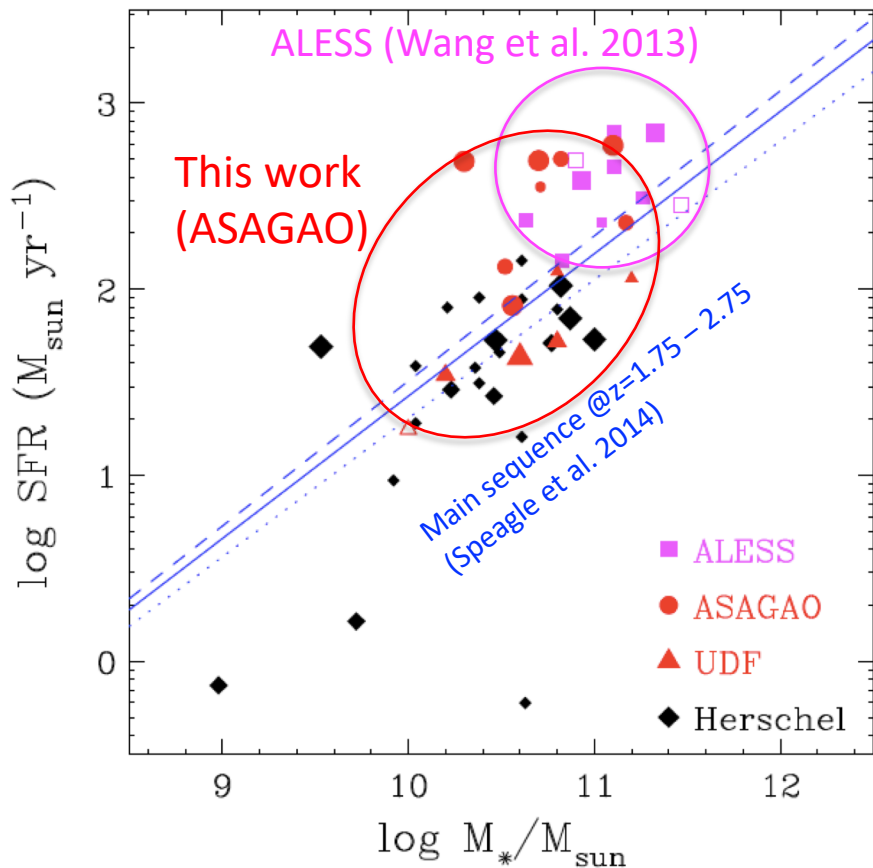


So, are you happy with the many detections of molecular outflows?

AGN feedback:  
negative, positive, or nothing?

# X-ray AGNs in ASAGAO (+ UDF) sources at $z = 1.5 - 3$

Ueda, Y., Hatsukade, B., KK, et al., 2018, ApJ, 853, id. 24



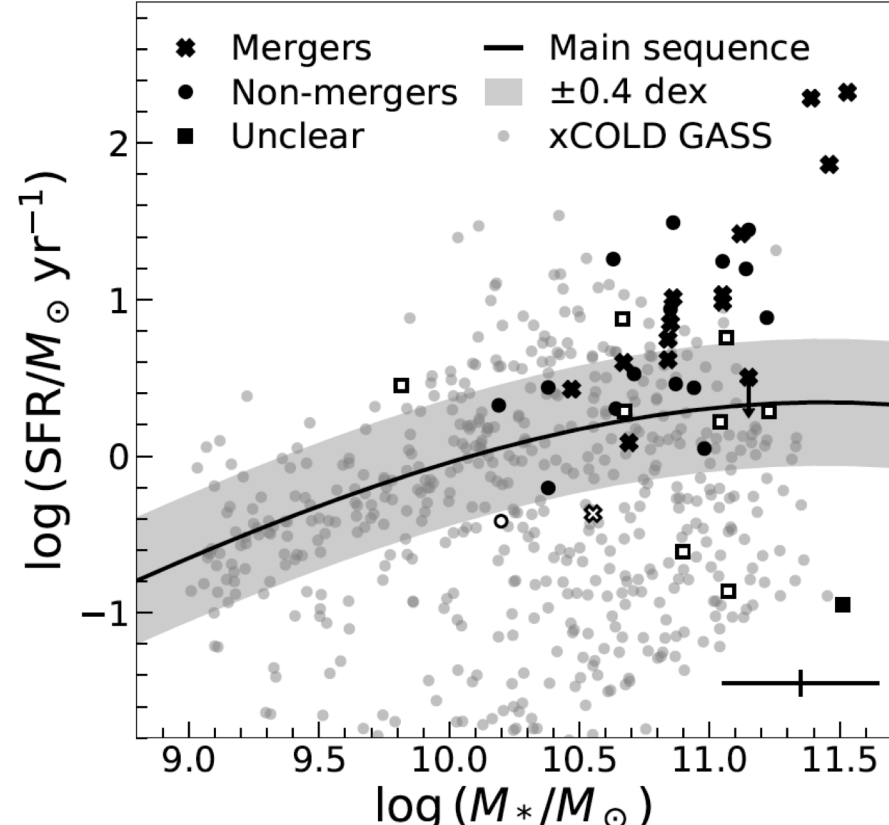
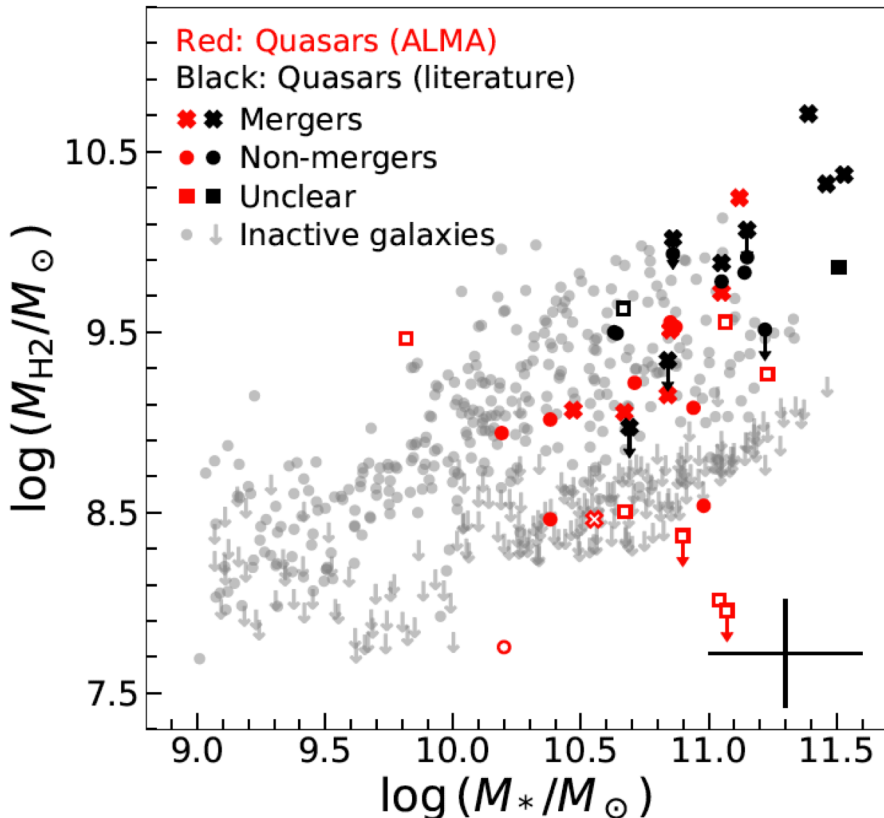
- Elevated AGN fraction at  $z = 1.5 - 3$  ULIRG-class ASAGAO sources, up to  $90^{+8}_{-19}\%$  (!) using Chandra 7Ms data
  - At X-ray flux limits of  $\sim 5 \times 10^{-17} \text{ erg cm}^{-2} \text{ s}^{-1}$  @ 0.5 – 7 keV band
  - Host growth first → an AGN-dominant phase follows later?

see also  
 Yang, G., et al.,  
 2017, ApJ, 842, 72

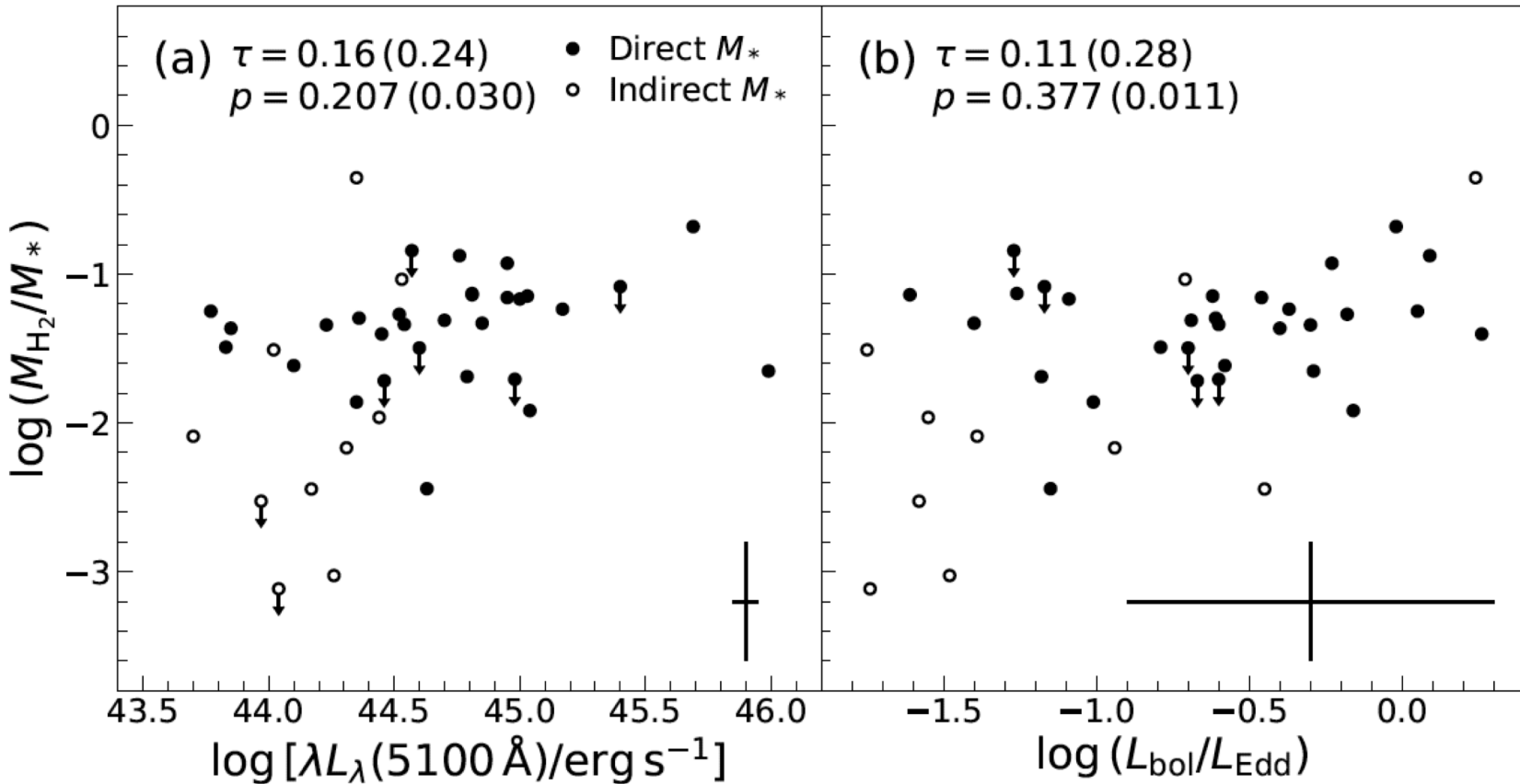
# Does AGN feedback quench star formation in quasar host galaxies?

- CO(2-1) observations of 40 Palomar-Green quasars at  $z < 0.3$  (including literature)
  - The largest and most sensitive CO survey of local quasars to date

No significant difference from star-forming galaxies; rather, star formation is enhanced

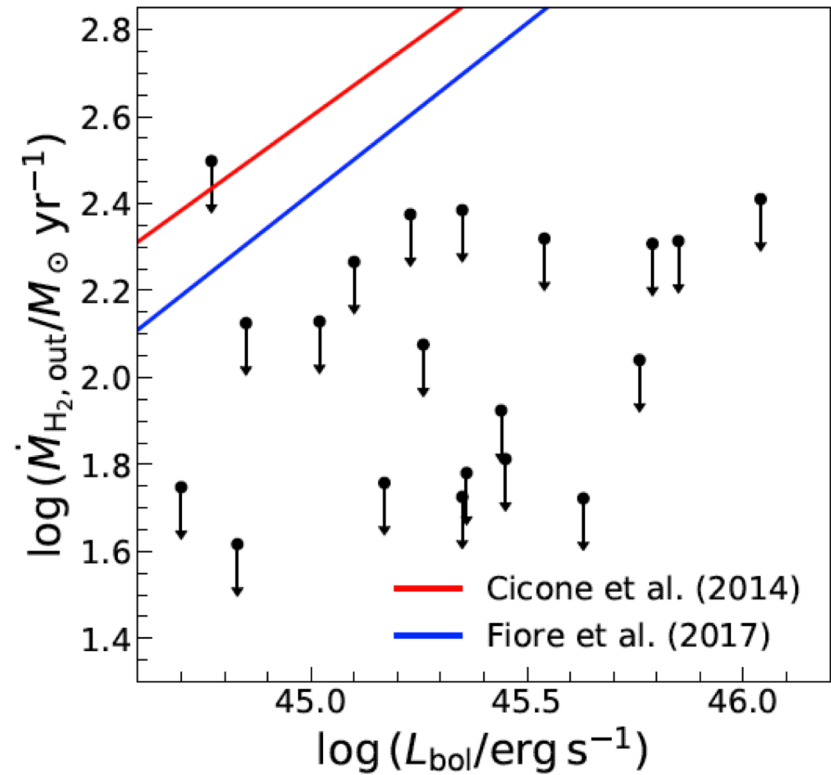
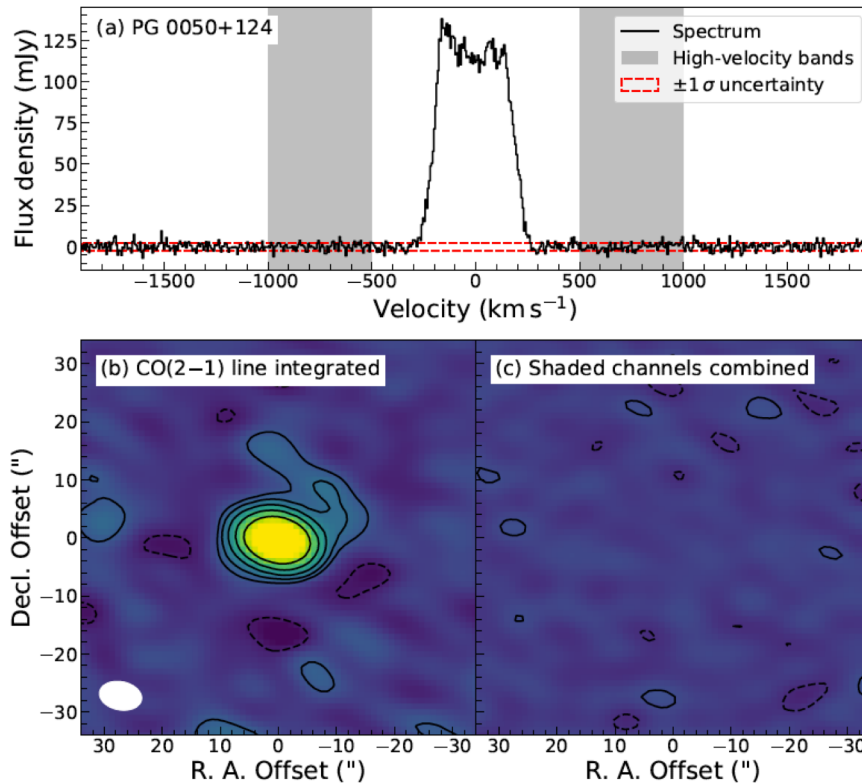


# AGN power and Eddington ratio: no impact<sup>62</sup> on molecular gas fraction in quasar hosts



- The dependence of molecular gas fraction ( $M_{H_2}/M_{\text{star}}$ ) on AGN power and Eddington ratio
    - Open circles: indirect  $M(\text{star})$  using  $M(\text{BH})-M(\text{star})$

# CO outflows (seen as high velocity wings in the spectrum) are NOT ubiquitous in quasar host galaxies



- Local quasars, while abundant in molecular gas, do NOT drive strong molecular outflows.
- Using  $\alpha_{\text{CO}} = 0.8 \text{ Msun (K km/s pc}^2)^{-1}$

Shangguan, J., et al. 2020,  
ApJ, in press (arXiv: 2007.11286)

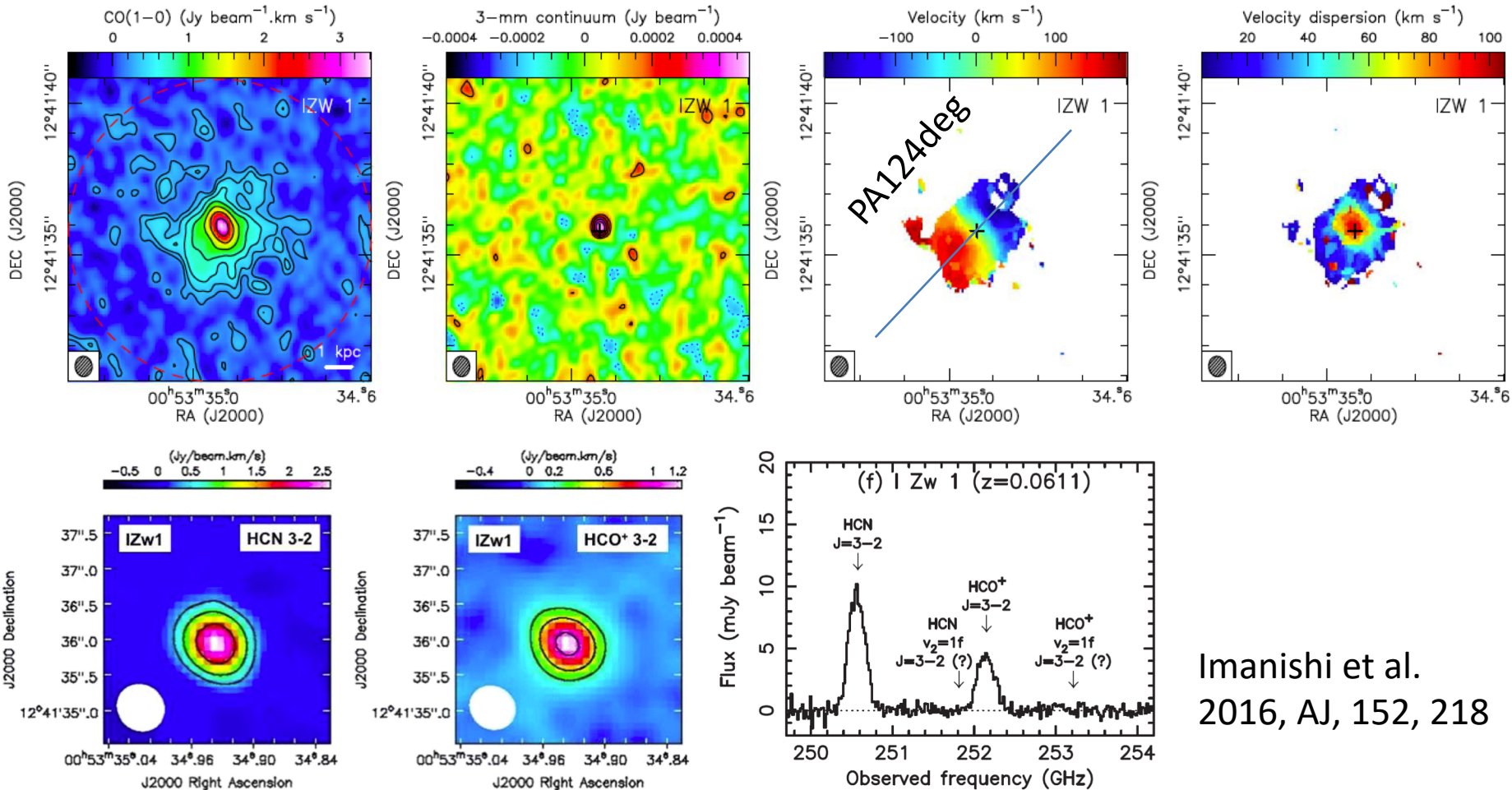
# Scant evidence that “quasar-mode” feedback exerts any impact on the content or kinematics of the cold molecular gas in the quasar host galaxies

- Molecular gas masses of low-redshift quasar host galaxies are consistent with those of galaxies on the star-forming main sequence.
  - Only 20% of the quasar host are gas-poor ( $M_{\text{H}_2}/M_{\text{star}} < 0.01$ )
- Despite the coexistence of abundant molecular gas and powerful quasar activity, no obvious high-velocity CO emission from molecular gas outflows is detected
  - below the empirical relation between molecular mass outflow rate and AGN luminosity
- CO luminosity ( $L'_{\text{CO}}$ ) correlates significantly with AGN luminosity. AGN luminosity is correlated with  $L'_{\text{CO}}$  and  $M(\text{BH})$ , strongly suggesting that AGN fueling is coupled to the cold gas reservoir of the host galaxy.
- The molecular gas mass fraction ( $M_{\text{H}_2}/M_{\text{star}}$ ) does not significantly depend on AGN power or Eddington ratio.
- Quasar host galaxies tend to have an enhanced SFE similar to starburst galaxies, but the SFE show no correlation with AGN luminosity or Eddington ratio

# IZw1 CO(1-0), HCN(3-2), HCO<sup>+</sup>(3-2) 0.6" imaging

- very ordered circular rotation!

Tan, Q.-H., KK et al. 2019, ApJ, 887, 24



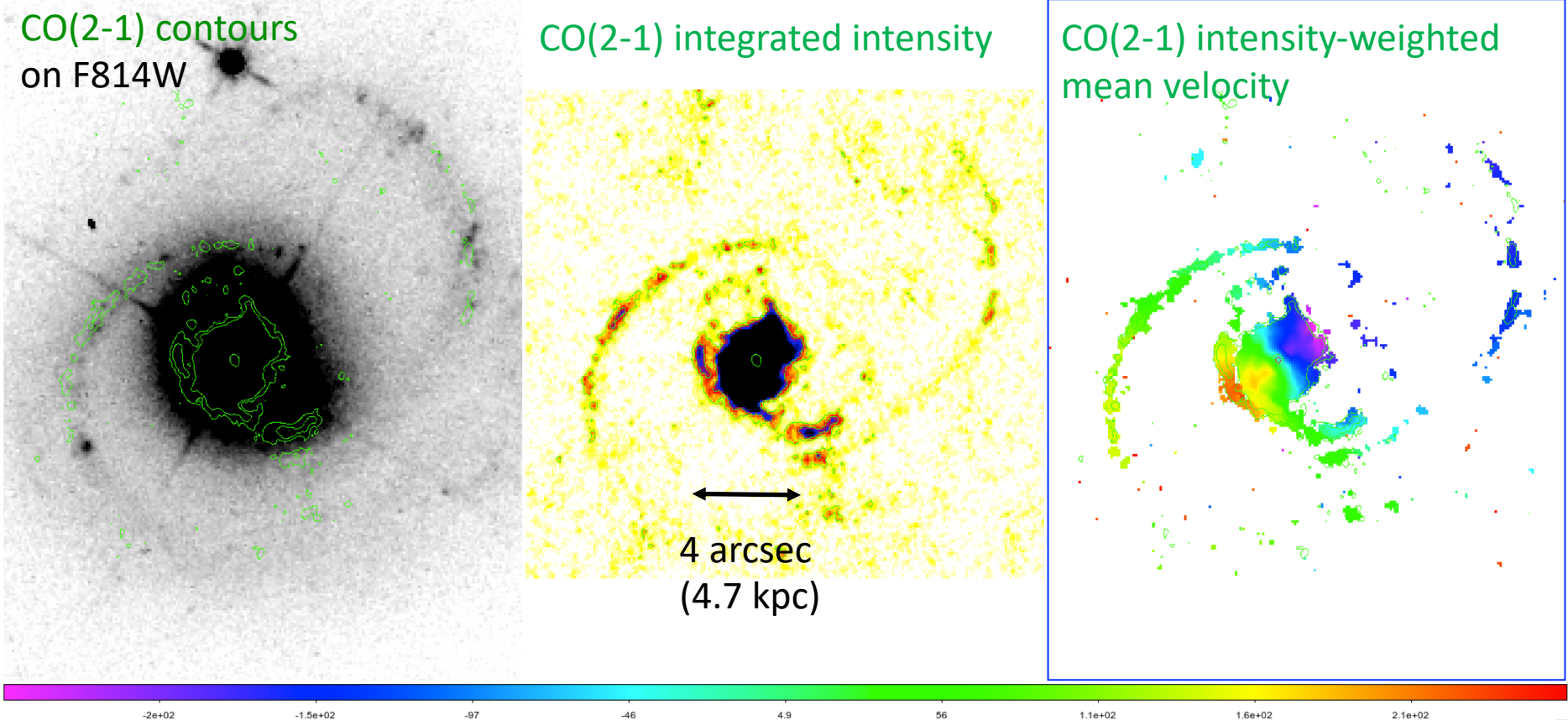
Imanishi et al.  
2016, AJ, 152, 218

# IZw1 CO(2-1) 0''.3 imaging (360 pc)

2018.1.00699.S

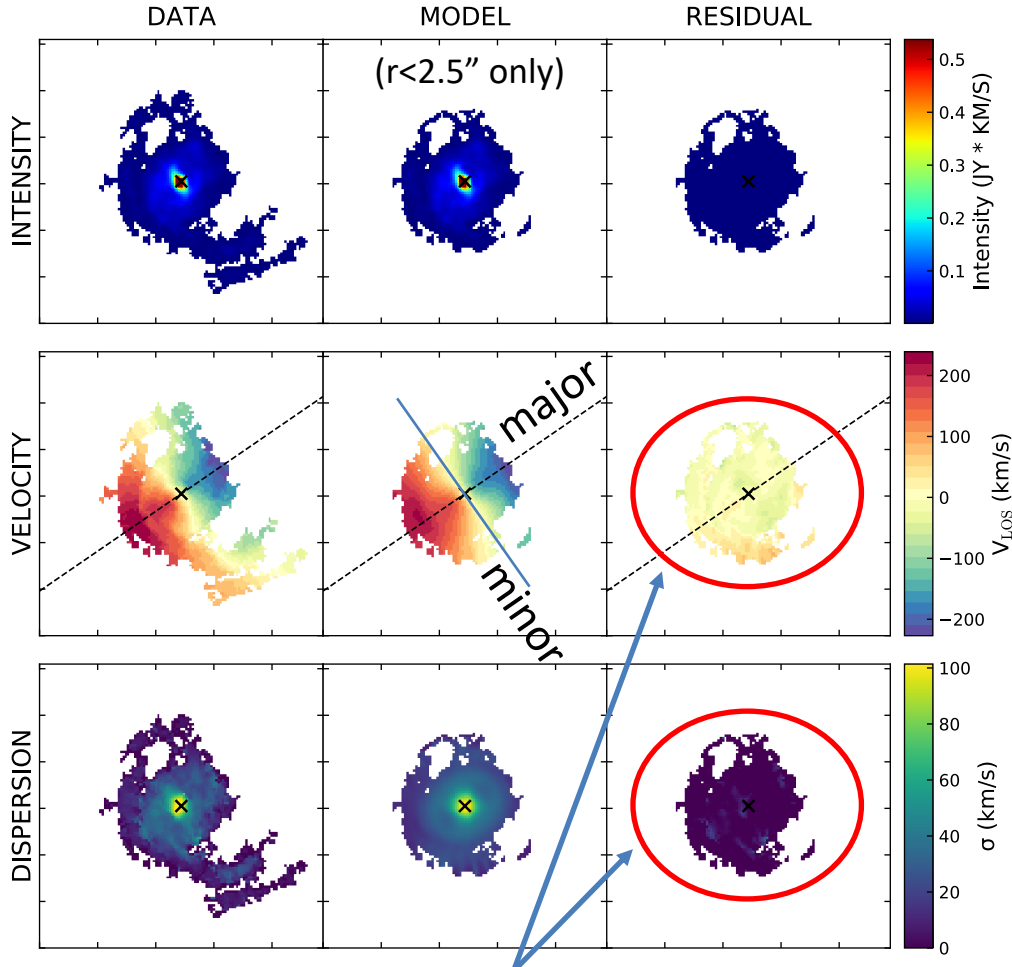
- still very ordered circular rotation
- unresolved (?) high-velocity-dispersion gas at the nucleus

K. Kohno et al. in prep.



# A possible low-velocity outflow in IZw1 ??

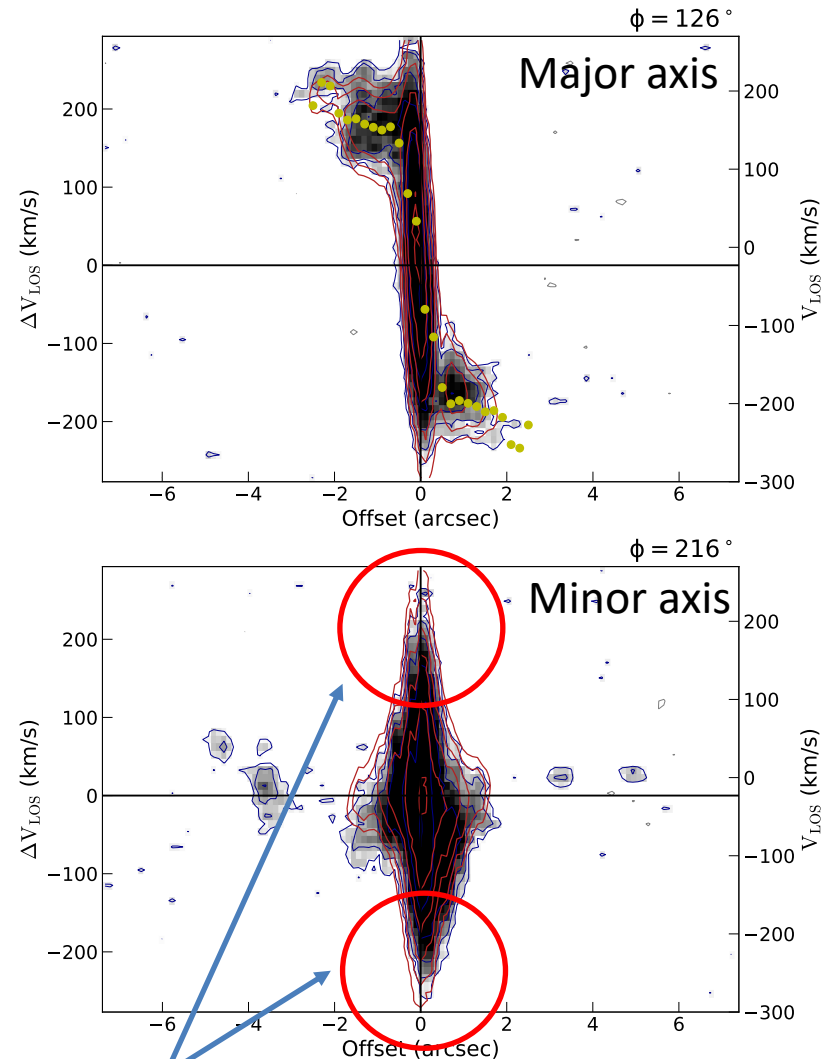
K. Kohno et al. in prep. (using 3D-Barolo code)



The fit looks reasonably good to say that there is no significant outflows..

grey-scale: observed CO(2-1)  
red contours: modeled CO(2-1)

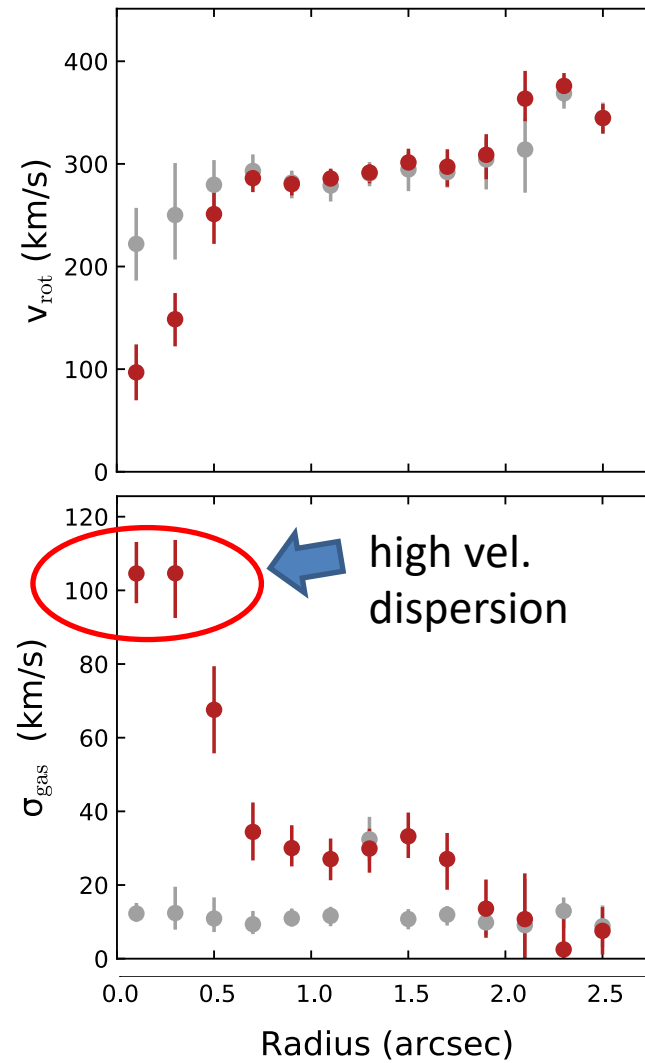
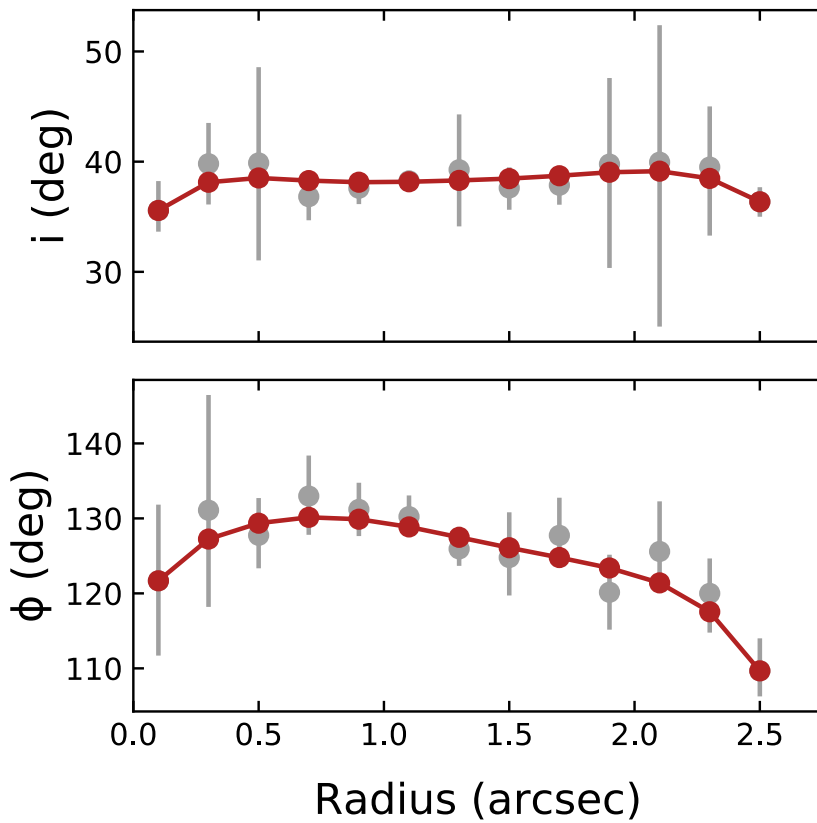
IRAS\_00509+1225



What is the origin of high velocity width ( $\pm 250$  km/s) in the PV diagram along the minor axis?

# A possible low-velocity outflow in the center of IZw1 ??

high velocity outflow in the optical [OIII], though

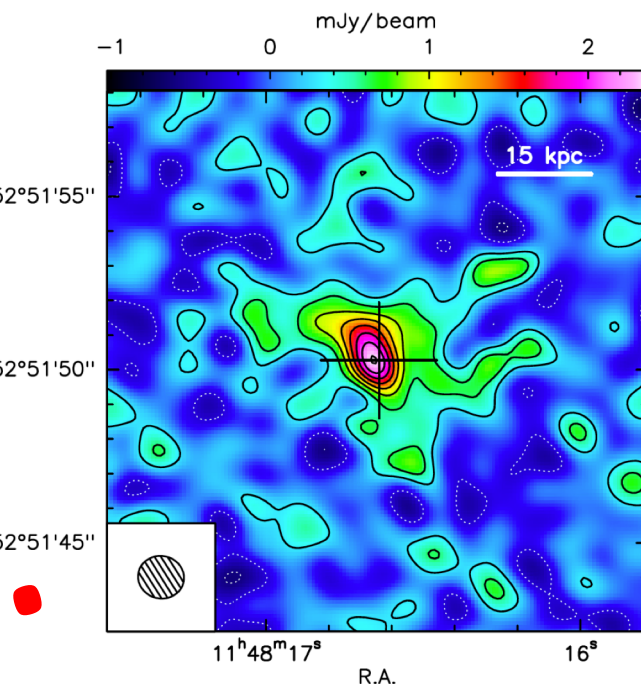
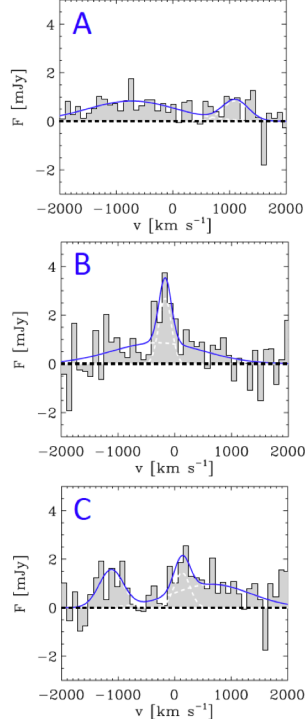
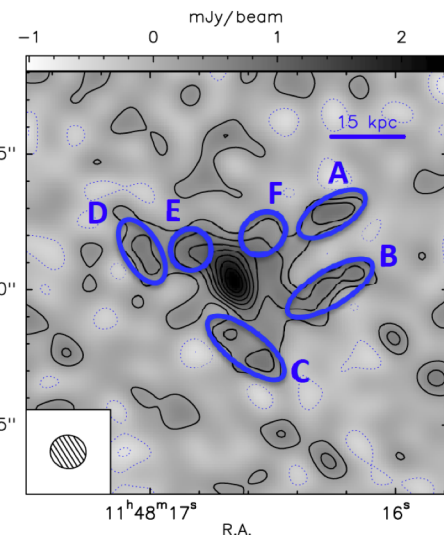
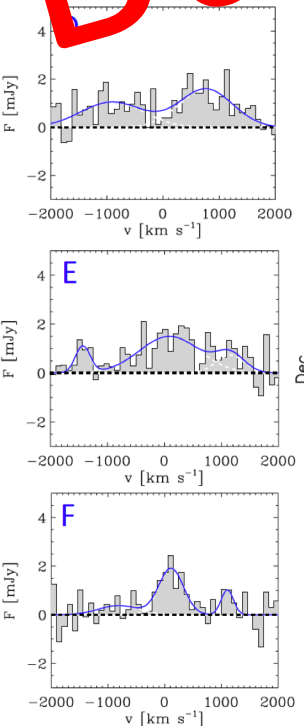


# [CII] outflows in the high-z quasar SDSS J1148+5251 (z=6.42)

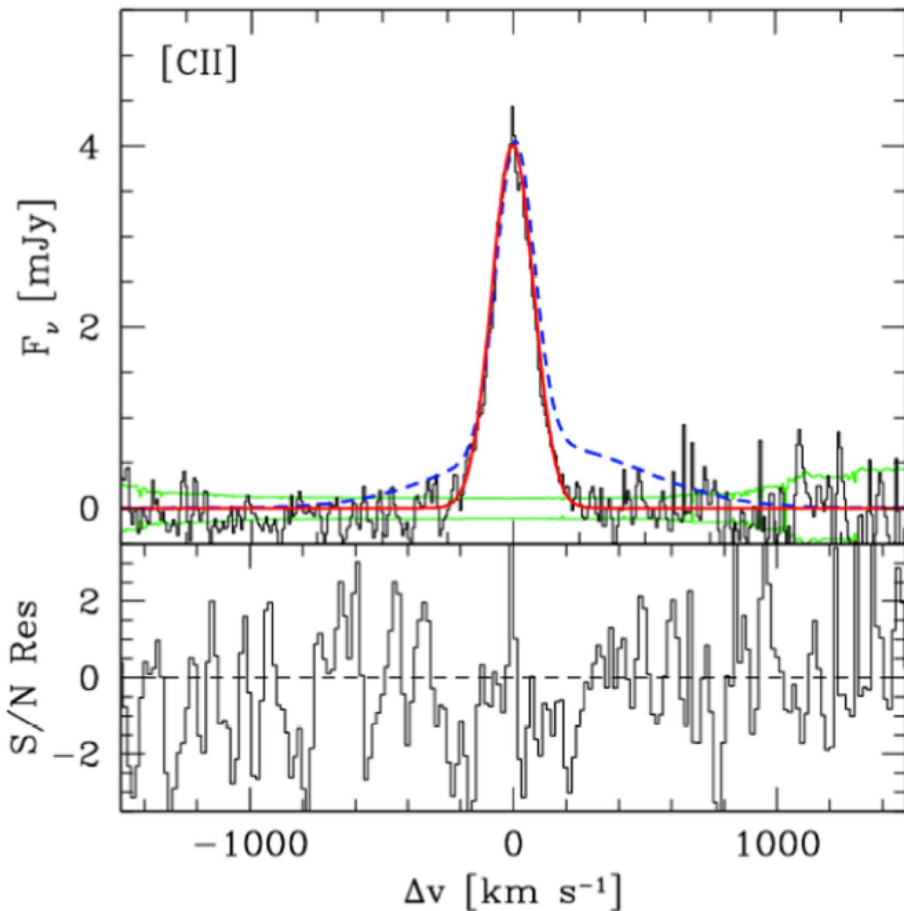
- R~30 kpc
- Dynamical timescale ~25 Myr (median)
- Mass loss rate  $1400 \pm 300 M_{\odot}/\text{yr}$
- Momentum rate  $1.0 \pm 0.14 L_{\text{AGN}}/c$
- Kinetic power  $(1.6 \pm 0.2) \times 10^{-3} L_{\text{AGN}}$

Cicone et al. 2015,  
A&A, 574, A14

**But...**



# High velocity [CII] outflows are not common in $z \sim 6$ powerful quasars?

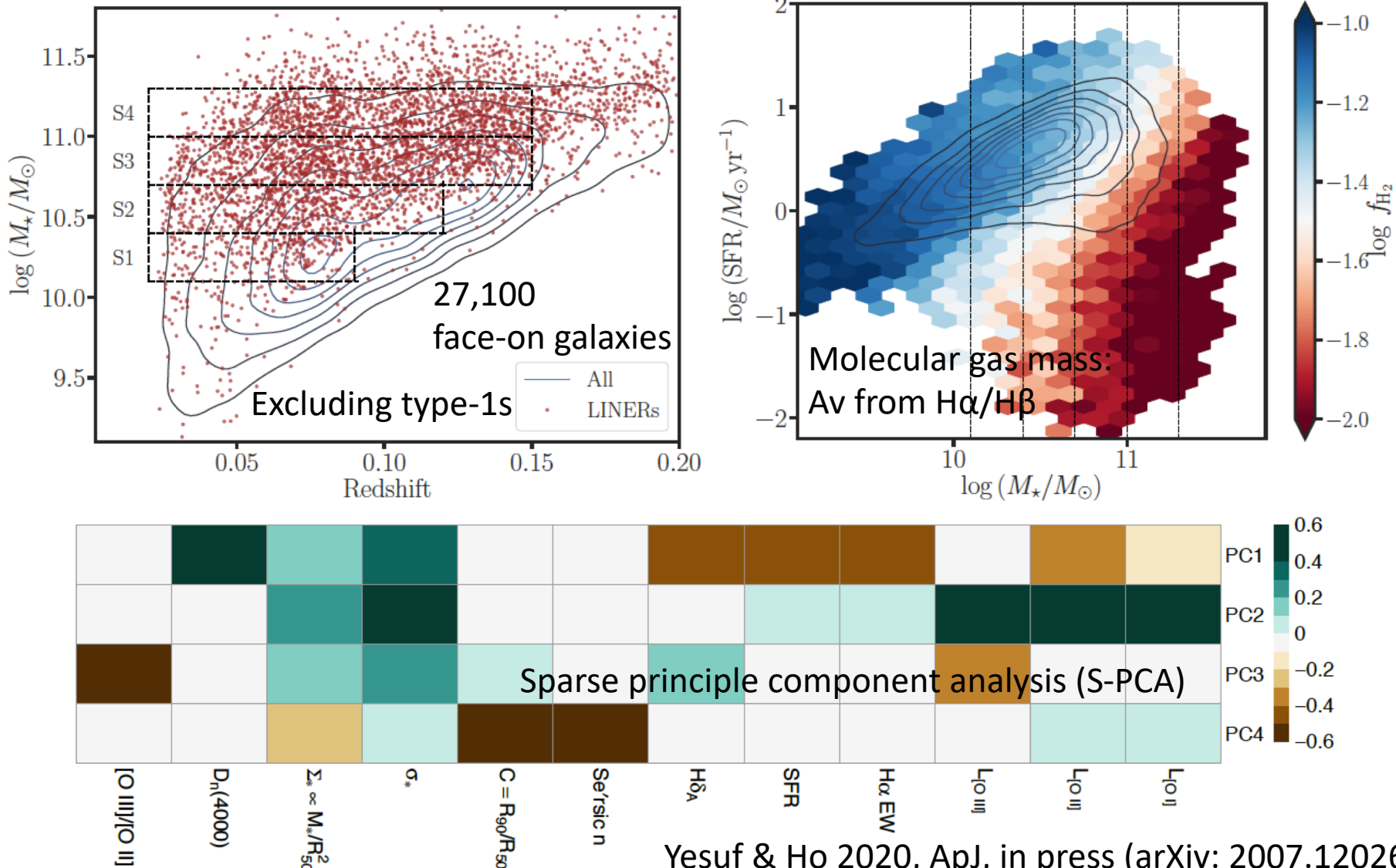


- 27 quasars at  $z > 5.94$  with ALMA [CII] observations
- In stacked ALMA [CII] spectra of individual sources, no evidence of a deviation from a single Gaussian profile (not like SDSS J1148)

Decarli et al. 2018, ApJ, 854, 97

See also Fujimoto, S., et al., 2019, ApJ, 887, 107

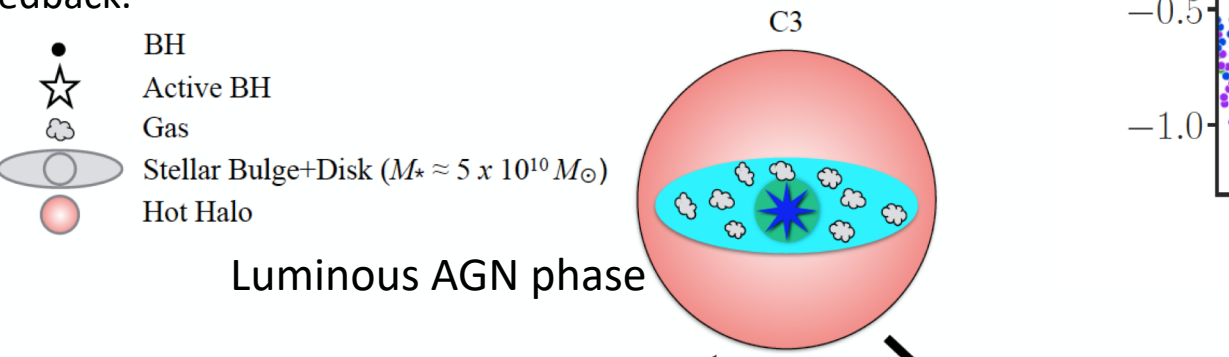
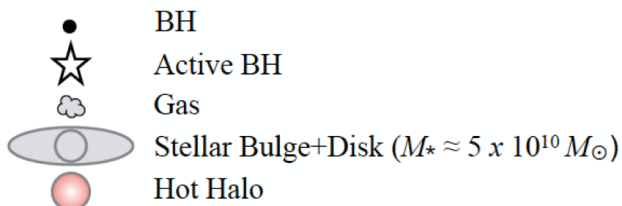
# Gas contents regulates the lifecycle of star formation and black hole accretion in galaxies



# Gas contents regulates the lifecycle of star formation and black hole accretion in galaxies

Yesuf & Ho 2020, ApJ, in press (arXiv: 2007.12026)

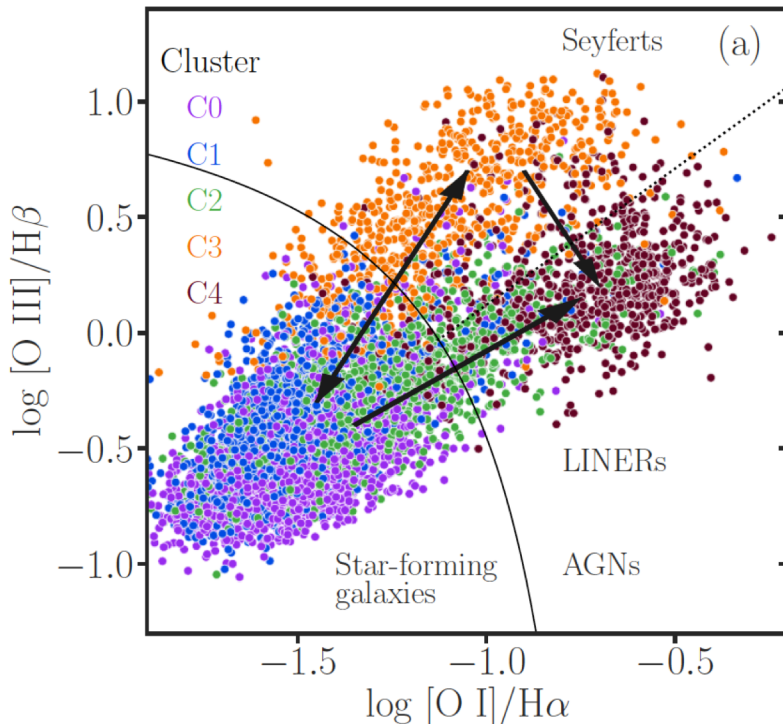
Strongly accreting BHs live in gas-rich, star-forming hosts, but neither their gas reservoir nor their ability to form stars seem to be impacted instantaneously (timescales < 0.5 Gyr) by AGN feedback.



$SFR \approx 6 M_\odot \text{ yr}^{-1}$   
 $f_{\text{H}_2} \approx 6\%$   
 $f_{\text{AGN}} \approx 2\text{-}3\%$

$SFR \approx 2 M_\odot \text{ yr}^{-1}$   
 $f_{\text{H}_2} \approx 4\%$   
 $f_{\text{AGN}} \approx 3\% \text{ (Sy)} + 11\% \text{ (L)} [\text{C2}]$   
 $f_{\text{AGN}} \approx 74\% \text{ (Sy)} + 2\% \text{ (L)} [\text{C3}]$

$SFR \approx 0.2 M_\odot \text{ yr}^{-1}$   
 $f_{\text{H}_2} \approx 2\%$   
 $f_{\text{AGN}} \approx 17\% \text{ (Sy)} + 74\% \text{ (L)}$



Our results are inconsistent with AGN feedback models predicting that central, bulge-dominated, Seyfert-like AGNs in massive galaxies have significantly lower molecular gas fractions compared to inactive galaxies of similar mass, morphology, and SFR.

# Summary 2: AGN feedback

- Necessity of negative (AGN) feedback
- Evidence for AGN feedback in cluster scales
- Molecular outflows and key physical quantities in galaxy scales
- Two modes: quasar mode vs radio mode
- Two types of conservation: energy conservation vs momentum conservation
- Recent observations of molecular outflows in AGNs
- Ultra-fast outflows (disk winds) vs galaxy-scale cold molecular outflows
- Does AGN feedback work indeed? Implications from recent measurements/estimations of cold molecular gas contents in AGNs